Lecture notes
Cosmological large-scale structure

Linear and non-linear perturbation theory

Luca Amendola
University of Heidelberg
l.amendola@thphys.uni-heidelberg.de
http://www.thphys.uni-heidelberg.de/~amendola/teaching.html
v. 1.0

November 3, 2025

UNIVERSITÄT
HEIDELBERG
ZUKUNFT
SEIT 1386

Contents

1 Linear perturbations **3**
- 1.1 The Newtonian equations . . . 3
- 1.2 Vlasov equation . . . 6
- 1.3 Evolution of linear perturbations . . . 10
- 1.4 Growth rate and growth function in ΛCDM. . . . 11

2 Correlation function and power spectrum **12**
- 2.1 Why we need correlation functions, power spectra and all that . . . 12
- 2.2 Average, variance, moments. . . . 13
- 2.3 Definition of the correlation function . . . 13
- 2.4 The n-point correlation function and the scaling hierarchy . . . 15
- 2.5 The power spectrum . . . 15
- 2.6 From the power spectrum to the moments . . . 18

3 The galaxy power spectrum **20**
- 3.1 Large scale structure . . . 20
- 3.2 The bias factor . . . 22
- 3.3 Normalization of the power spectrum . . . 22
- 3.4 The peculiar velocity field . . . 22
- 3.5 The redshift distortion . . . 24
- 3.6 Baryon acoustic oscillations . . . 28
- 3.7 Alcock-Paczyński effect[a] . . . 28
- 3.8 The BAO damping . . . 31

4 Non-linear perturbations: simplified approaches **34**
- 4.1 A first glimpse of non-linear corrections . . . 34
- 4.2 The Zel'dovich approximation . . . 35
- 4.3 Spherical collapse[b] . . . 37
- 4.4 The mass function of collapsed objects[c] . . . 39

5 Standard non-linear perturbation theory **41**
- 5.1 Second-order perturbations . . . 41
- 5.2 Spherical collapse, again . . . 42
- 5.3 Fourier space . . . 43
- 5.4 Bias and RSD . . . 49

6 Spectrum and bispectrum **55**
- 6.1 Spectrum at one loop . . . 55
- 6.2 UV correction . . . 58
- 6.3 Diagrams . . . 59

[a] Adapted from Amendola & Tsujikawa, *Dark Energy. Theory and Observations*, CUP 2010.
[b] Adapted from Amendola & Tsujikawa, *Dark Energy. Theory and Observations*, CUP 2010.
[c] Adapted from Amendola & Tsujikawa, *Dark Energy. Theory and Observations*, CUP 2010.

6.4 Bispectrum 60
6.5 Generalized kernels and symmetry conditions 61
6.6 Comparing to real data 66
6.7 Surveys 67

Chapter 1

Linear perturbations

Quick summary

- The evolution of linear matter perturbations can be studied in Newtonian gravity in a simplified case
- They coincide with full GR scalar perturbation theory in the sub-horizon, non-relativistic limit
- They can also be derived from the so-called Vlasov-Poisson equation that applies to any collisionless fluid
- After Fourier transformation, the equations can be solved analytically in various regimes: sub- and super-horizon, matter and radiation epoch
- Fluctuations grow when they are smaller than the horizon but larger than the Jeans length

1.1 The Newtonian equations

Most of the physics of cosmological perturbations is essentially Newtonian, at least as long as we consider only linear (i.e., small) pressureless perturbations at sub-horizon scales and we assume that the background evolution has already been obtained by solving the unperturbed Einstein equations. In this section we follow in part Peacock, *Cosmological Physics*. Let us consider a density field $\rho(x)$, associated to a pressure $p(x)$ and a velocity field $\mathbf{v}(x)$, under the action of a gravitational potential $\Phi(x)$ generated by the fluid itself (where x denotes the dependence on space-time coordinates). Then we have three relevant equations: a conservation equation (the fluid moves but neither disappears nor is created), the Euler equation (the fluid is accelerated under the action of pressure gradient and of gravity), and the Poisson equation (the gravitational potential depends on the fluid's density). The conservation equation in one dimension, for instance, says that the number of particles with velocity v entering in a small region dx at the border 1, equal to $(\rho dx)_1 = (\rho v dt)_1$, minus the number leaving the region at the border 2, $(\rho v dt)_2$, must be equal to the change of the number of particle in the same region, $d\rho dx$, so that $d\rho dx = [(\rho v)_1 - (\rho v)_2]dt$, or

$$\frac{\partial \rho}{\partial t} = -\frac{\partial(\rho v)}{\partial_{\epsilon} x} \tag{1.1.1}$$

This generalizes to 3D as

$$\frac{\partial \rho}{\partial t} = -\nabla(\rho \mathbf{v}) = -\rho \nabla \cdot \mathbf{v} - \mathbf{v} \cdot \nabla \rho \tag{1.1.2}$$

where $\nabla = \{\partial_x, \partial_y, \partial_z\}$ in Cartesian coordinates. Therefore, the three corresponding equations are (as usual, $G = 1$)

$$\dot{\rho} + \mathbf{v} \cdot \nabla \rho = -\rho \nabla \cdot \mathbf{v} \qquad \text{continuity} \tag{1.1.3}$$

$$\rho(\dot{\mathbf{v}} + \mathbf{v} \cdot \nabla \mathbf{v}) = -\nabla p - \rho \nabla \Phi \qquad \text{Euler} \tag{1.1.4}$$

$$\nabla^2 \Phi = 4\pi\rho \qquad \text{Poisson} \tag{1.1.5}$$

We now need to do three operations: expand the equations to first order, employ the background cosmological equations, and adopt comoving coordinates.

Let us expand the continuity equation. We put $\rho = \rho_0 + \delta\rho$, $\mathbf{v} = \mathbf{v}_0 + \delta\mathbf{v}$, where ρ_0 depends only on time (so $\nabla\rho_0 = 0$), and $\mathbf{v}_0 = H\mathbf{x}$ is the cosmological expansion. The perturbed terms $\delta\rho, \delta\mathbf{v}$ are supposed to be much smaller than the background terms. Then we have from (1.1.3)

$$\dot{\rho_0} + \dot{\delta\rho} + (\mathbf{v}_0 + \delta\mathbf{v}) \cdot \nabla\delta\rho = -(\rho_0 + \delta\rho)\nabla \cdot (\mathbf{v}_0 + \delta\mathbf{v}) \tag{1.1.6}$$

At zero-th order this gives the expected result for a pressureless fluid

$$\dot{\rho_0} = -\rho_0 H \nabla \cdot \mathbf{x} = -3H\rho_0 \tag{1.1.7}$$

We can use this equation now to simplify the perturbed one,

$$\dot{\delta\rho} + \mathbf{v}_0 \cdot \nabla\delta\rho = -\rho_0\nabla \cdot \delta\mathbf{v} - 3H\delta\rho \tag{1.1.8}$$

where we also discarded two higher order terms, $\delta\mathbf{v} \cdot \nabla\delta\rho$ and $\delta\rho\nabla \cdot \delta\mathbf{v}$. Next, we introduce the density contrast

$$\delta \equiv \frac{\delta\rho}{\rho_0} \tag{1.1.9}$$

and we notice that $\rho_0\dot{\delta} = \dot{\delta\rho} - \delta\rho\dot{\rho_0}/\rho_0 = \dot{\delta\rho} + 3H\delta\rho$. Then

$$\dot{\delta} + \mathbf{v}_0 \cdot \nabla\delta = -\nabla \cdot \delta\mathbf{v} \tag{1.1.10}$$

We notice that on the lhs we have a total derivative, $d\delta/dt \equiv \dot{\delta} + \mathbf{v}_0 \cdot \nabla\delta$.

The same operations can be applied to the Euler and Poisson equations, and we find

$$\frac{d\delta\mathbf{v}}{dt} = \dot{\delta\mathbf{v}} + \mathbf{v}_0 \cdot \nabla\delta\mathbf{v} = -\frac{\nabla\delta p}{\rho_0} - \nabla\delta\Phi - (\delta\mathbf{v} \cdot \nabla)\mathbf{v}_0 \tag{1.1.11}$$

$$\nabla^2\delta\Phi = 4\pi\rho_0\delta \tag{1.1.12}$$

The term $(\delta\mathbf{v} \cdot \nabla)\mathbf{v}_0$ can be written in explicit component form (sum over repeated indexes) as $(\delta\mathbf{v})_i\nabla_i v_{0j} = (\delta\mathbf{v})_i H\nabla_i x_j = (\delta\mathbf{v})_j H$. We have now a linearized set of equations, but we still want to put them in comoving coordinates $\mathbf{r}$,

$$\mathbf{x}(t) = a(t)\mathbf{r}(\mathbf{t}) \tag{1.1.13}$$

Then we have $\nabla = a^{-1}\nabla_r$. We now use simply $\mathbf{v}$ for $\delta\mathbf{v}$ and ϕ for $\delta\Phi$. It follows

$$a\frac{d\delta}{dt} = -\nabla_r \cdot \mathbf{v} \tag{1.1.14}$$

$$\frac{d\mathbf{v}}{dt} = -\frac{\nabla_r\delta p}{a\rho_0} - \frac{\nabla_r\phi}{a} - H\mathbf{v} \tag{1.1.15}$$

$$\nabla_r^2\phi = 4\pi a^2\rho_0\delta \tag{1.1.16}$$

This set of equations is closed by introducing the sound speed $c_s^2 \equiv \delta p/\delta\rho$. Now, with respect to the comoving observers, the background velocity v_0 is zero, and δv is the peculiar velocity, so the total derivative d/dt is identical to the partial derivative $\partial/\partial t$. More formally, moving from $\mathbf{x}$ to $a\mathbf{r}$, one has (let's consider only the $x = aX$ coordinate for simplicity) $dx = [\partial(aX)/\partial t]dt + [\partial(aX)/\partial X]dX = \dot{a}Xdt + adX$, so for any function $f(t, x)$

$$df(t,x) = \left(\frac{\partial f}{\partial t}\right)_x dt + \left(\frac{\partial f}{\partial x}\right)_t dx = \left(\frac{\partial f}{\partial t}\right)_x dt + \left(\frac{\partial f}{\partial x}\right)_t (\dot{a}Xdt + adX) \tag{1.1.17}$$

$$= \left[\left(\frac{\partial f}{\partial t}\right)_x + \left(\frac{\partial f}{\partial x}\right)_t Hx\right] dt + \left(\frac{\partial f}{\partial x}\right)_t adX = \left(\frac{\partial f}{\partial t}\right)_X dt + \left(\frac{\partial f}{\partial X}\right)_t dX \tag{1.1.18}$$

(since $\dot{a}X = Hx$) from which we see that

$$\left(\frac{\partial}{\partial t}\right)_X = \left(\frac{\partial}{\partial t}\right)_x + \left(\frac{\partial}{\partial x}\right)_t Hx \tag{1.1.19}$$

so we see that the partial derivative wrt t at fixed X is not the same as the partial derivative at fixed x. Generalizing to 3D and applying it to δ,

$$\left(\frac{\partial \delta}{\partial t}\right)_{\mathbf{r}} \equiv \dot{\delta} + \mathbf{v}_0 \cdot \nabla\delta = \left(\frac{d\delta}{dt}\right)_x \tag{1.1.20}$$

which means that, in comoving coordinates, the total derivative wrt time is actually a partial derivative. Finally, adopting the conformal time $d\tau = dt/a$ we obtain (the dot is now $\partial/\partial\tau$)

$$\dot{\delta} = -\nabla_r \cdot \mathbf{v} \tag{1.1.21}$$

$$\dot{\mathbf{v}} = -\nabla_r c_s^2 \delta - \nabla_r \phi - Ha\mathbf{v} \tag{1.1.22}$$

$$\nabla_r^2 \phi = 4\pi a^2 \rho_0 \delta \tag{1.1.23}$$

These equations can also be obtained as the $k \ll aH$ limit of the full GR treatment. In GR, for a flat space, we also can replace ρ_0 with the Friedmann relation

$$H^2 = \frac{8\pi}{3}\rho_0$$

From now on we discard the subscript r.

We define now the velocity divergence $\theta \equiv \nabla^i v_i$ and define the conformal Hubble parameter $\mathcal{H} = (da/d\tau)/a = aH$. Then, applying ∇ to the continuity and Euler equation, we get

$$\dot{\theta} = -\nabla^2 c_s^2 \delta - \nabla^2 \phi - \mathcal{H}\theta \tag{1.1.24}$$

$$\dot{\delta} = -\theta \tag{1.1.25}$$

The rotational part of the velocity field, $\omega \equiv \nabla \times v$ can be neglected in a first approximation because taking the curl of Eq. (1.1.22) one sees that ω decays away. This approximation however breaks down when collisional matter (i.e. baryons) are considered, and in the non-linear regime.

We go now to *Fourier space*. This means that all perturbation quantities will be Fourier expanded:

$$\phi = \int e^{ikr} \phi_k d^3k, \tag{1.1.26}$$

$$\delta = \int e^{ikr} \delta_k d^3k, \quad \theta = \int e^{ikr} \theta_k d^3k \tag{1.1.27}$$

but the subscript k will be dropped in the following (the Fourier normalization factors here play no role, since the equations are all in Fourier space). In other words, we assume that the perturbation variables δ, θ, ϕ etc. are the sum of plane waves $\delta_k e^{ikr}$ (I often use the short notation $kr \equiv \mathbf{k} \cdot \mathbf{r}$); since the equations are linear, each plane wave obeys the same equations with a different k. In practice, each perturbation quantity and its derivatives can be substituted as follows

$$\begin{aligned} \phi(x,\tau) &\rightarrow e^{ikr}\phi_k(\tau) \\ \nabla\phi(x,\tau) &\rightarrow ie^{ikr}\mathbf{k}\phi_k(\tau) \\ \nabla^2\phi(x,\tau) \equiv \nabla_i\nabla_i\phi(x,\tau) &\rightarrow -e^{ikr}k^2\phi_k(\tau) \end{aligned} \tag{1.1.28}$$

Furthermore, the Fourier modes e^{ikr} can be simply dropped out, since the equations are linear and therefore decoupled in the modes.

The perturbation equations in the Newtonian limit become then

$$\begin{aligned} \dot{\delta} &= -\theta \\ \dot{\theta} &= -\mathcal{H}\theta + c_s^2 k^2 \delta + k^2 \phi \\ k^2\phi &= -\frac{3}{2}\mathcal{H}^2 \Omega_m \delta \end{aligned} \tag{1.1.29}$$

i.e. the continuity, the Euler and the Poisson equations, which are as expected the Fourier transform of the equations (1.1.23) already seen in Sect. (1.1). Deriving the first equation we obtain

$$\ddot{\delta} + \mathcal{H}\dot{\delta} + \left(k^2 c_s^2 - \frac{3}{2}\mathcal{H}^2\Omega_m\right)\delta = 0 \tag{1.1.30}$$

(In the Minkowski limit, $H = 0$, this equation reduces to the fluid wave equation $\ddot{\delta} - c_s^2\nabla^2\delta = 0$, and shows that c_s is indeed the sound velocity.) This shows at once that the perturbation does not grow if

$$k^2 c_s^2 - \frac{3}{2}\mathcal{H}^2\Omega_m > 0 \tag{1.1.31}$$

i.e., if the perturbation scale $\lambda = 2\pi a/k$ is smaller than the Jeans length,

$$\lambda_J = c_s\sqrt{\frac{\pi}{\rho}} \tag{1.1.32}$$

For scales smaller than λ_J the perturbations undergo damped oscillations. For the CDM particles the velocity dispersion is always negligible. For the photons is $c/\sqrt{3}$, so that the physical scale

$$\lambda_J \simeq H^{-1} \tag{1.1.33}$$

and growth is prevented on all scales smaller than the horizon. For the baryons, finally, the sound velocity is comparable to the photon velocity before decoupling, so that baryon perturbations are damped out, but drops rapidly to a comoving scale of less than 1Mpc just after decoupling. Then the baryons are free to fall inside the dark matter potential wells, and their perturbation spectrum catches the dark matter one.

1.2 Vlasov equation

We now recover Eqs. (1.1.3,1.1.4) from a more general point of view, in order to understand which approximations have been implicitly made. Here we follow mostly [5], [4]. A general-relativistic derivation of the non-linear perturbations can be found in [3].

A flow of particles that are neither destroyed nor created ("conserved") and do not collide against each other is governed by the collisionless Boltzmann equation. Let the number dN of particles in a space volume $dV = dxdydz$ and with momenta within the volume $dp_x dp_y dp_z$ be

$$dN = f(t, \mathbf{x}, \mathbf{p})dxdydzdp_x dp_y dp_z \tag{1.2.1}$$

where f is the *distribution function* and the space-momentum volume element is called the phase-space volume. In absence of collisions, trajectories in the phase-space do not intersect, because otherwise the same initial conditions in terms of positions and momenta would give rise to two different trajectories, breaking classical determinism.

Let's first consider a 1-dimensional example. Since the particle number is conserved, the number of particles with momentum p_x entering in a space volume $dxdydz$ in direction x in the time interval dt is $\rho dxdydz = \rho v_x dtdydz$ (v_x is the x-component of the velocity and ρ is the number density of particles), minus the number exiting from the other side (see Fig. 1.2.1); if the particles move only along x, this has to be equal to the change in the number of particles inside the volume itself, $d\rho dV$. Then we have the continuity equation (the incoming velocity is taken negative)

$$d\rho dxdydz = -d(\rho v_x)dtdydz \tag{1.2.2}$$

or

$$\frac{\partial\rho}{\partial t} = -\frac{\partial(\rho v_x)}{\partial x} \tag{1.2.3}$$

This simple derivation can be extended to all six phase-space coordinates. The demonstration makes use of the following relations, valid in any number of dimensions and any choice of coordinates $\mathbf{w}$:

$$\frac{\partial}{\partial t}\int f dV = -\int_{\partial V}(f\mathbf{v})\cdot\mathbf{n}dA = -\int_V \nabla\cdot(f\mathbf{v})dV \tag{1.2.4}$$

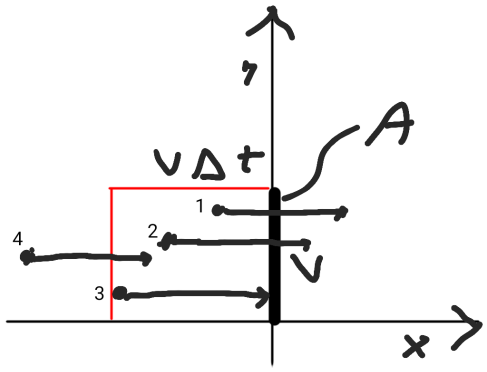

Figure 1.2.1: Flux across a surface A. Particles inside the box (for instance, particles 1,2,3) will cross the surface in Δt, particles outside (e.g., 4) will not.

where $\mathbf{v} = \dot{\mathbf{w}}$, ∇ takes derivatives wrt to $\mathbf{w}$, and $\mathbf{n}$ is the unit normal to the surface ∂V enclosing V. The first equality applies when f is a conserved quantity (mass, or number of particles, or number of microstates), the second is the divergence theorem and is always valid. Since the volume V is arbitrary, the integrands of the first and third member must be equal. For the phase-space coordinates this gives the generalized version of Eq. (1.2.3), namely the collisionless Boltzmann equation

$$\frac{\partial f}{\partial t} + \sum_{i=1}^{6} \frac{\partial (f \dot{w}_i)}{\partial w_i} = 0 \tag{1.2.5}$$

where $w = \{x, y, z, p_x, p_y, p_z\} = \{\mathbf{q}, \mathbf{p}\}$ is the phase-space vector of coordinates. Notice that if we allow for collisions, i.e. instantaneous interactions, f would not be differentiable, and an extra term taking into account this should be included.

The Boltzmann equation gives the evolution in a phase space $\mathbf{q}, \mathbf{p}$ (position and momenta) of a set of collisionless particles whose number density is $f(\mathbf{q}, \mathbf{p}, t)$. In cosmology, the velocity of a particle at position $\mathbf{x} = a\mathbf{q}$ is

$$\mathbf{v} = \frac{\partial \mathbf{x}}{\partial t} = \frac{\partial a}{\partial t}\mathbf{q} + a\frac{\partial \mathbf{q}}{\partial t} = H\mathbf{x} + \delta\mathbf{v} \tag{1.2.6}$$

where the first term is the Hubble expansion and $\delta\mathbf{v}$ defines the peculiar velocity.

Now since $\dot{\mathbf{q}} = \partial H/\partial \mathbf{p}$ and $\dot{\mathbf{p}} = -\partial H/\partial \mathbf{q}$, where H is the Hamiltonian, we have

$$\sum_{i=1}^{6} \frac{\partial (f \dot{w}_i)}{\partial w_i} = \sum_{i=1}^{6} \left(f \frac{\partial \dot{w}_i}{\partial w_i} + \dot{w}_i \frac{\partial f}{\partial w_i} \right) \tag{1.2.7}$$

$$= f\left(\frac{\partial^2 H}{\partial \mathbf{q} \partial \mathbf{p}} - \frac{\partial^2 H}{\partial \mathbf{p} \partial \mathbf{q}} \right) + \sum_{i=1}^{6} \dot{w}_i \frac{\partial f}{\partial w_i} \tag{1.2.8}$$

$$= \sum_{i=1}^{6} \dot{w}_i \frac{\partial f}{\partial w_i} \tag{1.2.9}$$

Then the Boltzmann equation says that the phase-space density f is conserved

$$\frac{df}{dt} = \frac{\partial f}{\partial t} + \sum_{n=1}^{6} \frac{\partial w_n}{\partial t}\frac{\partial f}{\partial w_n} = \frac{\partial f}{\partial t} + \frac{\partial q_i}{\partial t}\frac{\partial f}{\partial q_i} + \frac{\partial p_i}{\partial t}\frac{\partial f}{\partial p_i} = 0 \tag{1.2.10}$$

where $i = 1, 2, 3$. We need now to include the gravitational potential in this equation.

In a self-gravitating system with density $\rho(\mathbf{x})$ the potential Φ is given by

$$\Phi(\mathbf{x}) = -G \int d^3x' \frac{\rho(\mathbf{x}')}{|\mathbf{x}' - \mathbf{x}|} \tag{1.2.11}$$

However, this Newtonian potential includes also the potential induced by the homogeneous distribution, which instead in GR is shown to just source the expansion, without inducing any motion in comoving coordinates. If we write the Poisson equation as

$$\Delta\Phi = 4\pi\rho = 4\pi(\rho_0 + \delta\rho)$$

and write the operator $\Delta = x^{-2}\partial_x x^2 \partial_x$ in radial coordinates, we see that at the background level the potential is

$$\phi_0 = \frac{2\pi}{3}\rho_0 x^2 + C(t) = -\frac{1}{2}\frac{\ddot{a}}{a}x^2 + C(t) \tag{1.2.12}$$

where we used the second Friedmann equation for a pressureless component, $\ddot{a} = -4\pi a\rho_0/3$. The cosmological potential ϕ should therefore be defined by subtracting from Φ the background part:

$$\phi = \Phi - \frac{2\pi}{3}\rho_0 x^2 \tag{1.2.13}$$

Then it follows that ϕ is indeed sourced by the fluctuations,

$$\Delta\phi = 4\pi\rho_0\delta \tag{1.2.14}$$

where δ is the density contrast. Here, however, we keep using the full potential Φ. Then we can write the dynamics as

$$\frac{\partial p_i}{\partial t} = -m\nabla_i\Phi \tag{1.2.15}$$

$$\frac{\partial q_i}{\partial t} = \frac{p_i}{m} \tag{1.2.16}$$

Therefore we obtain

$$\frac{\partial f}{\partial t} + \frac{\mathbf{p}}{m}\cdot\nabla f - m\nabla\Phi\cdot\frac{\partial f}{\partial \mathbf{p}} = 0 \tag{1.2.17}$$

This is called the Vlasov-Poisson equation, and is complemented by the Poisson equation in terms of the cosmological potential

$$\nabla^2\Phi = 4\pi\rho \tag{1.2.18}$$

Notice that we are still using physical coordinates, not the comoving ones.

Instead of using the full Vlasov-Poisson equation, we can take moments. We define the particle density

$$\rho(x,t) \equiv \int f(\mathbf{q},\mathbf{p},t)d^3p \tag{1.2.19}$$

(this is of course the same quantity on the rhs on Eq. 1.2.18) and the moments (all quantities on the lhs depend on x, τ)

$$\rho\mathbf{v} \equiv \int \frac{\mathbf{p}}{m} f(\mathbf{q},\mathbf{p},t)d^3p \tag{1.2.20}$$

$$\sigma_{ij} \equiv \int (\frac{p_i}{m} - v_i)(\frac{p_j}{m} - v_j) f(\mathbf{q},\mathbf{p},t)d^3p \tag{1.2.21}$$

where $\mathbf{v}$ denotes the peculiar velocity at x averaged over the distribution of momenta, and σ_{ij} denotes the stress tensor. Note that

$$\int \frac{p_i}{m}\frac{p_j}{m} f(\mathbf{q},\mathbf{p},t) d^3p = \sigma_{ij} + \rho v_i v_j \tag{1.2.22}$$

We can now use these momenta to integrate out the Vlasov equation. Integrating over d^3p gives (since Φ does not depend on $\mathbf{p}$)

$$\frac{\partial \rho}{\partial t} + \nabla\cdot\rho\mathbf{v} - m\nabla\Phi\cdot\frac{\partial}{\partial \mathbf{p}}\int f d^3p = 0 \tag{1.2.23}$$

The last term vanishes because the momenta are integrated out, so we obtain the same continuity equation (1.1.3) we have seen in the previous section

$$\frac{\partial \rho}{\partial t} + \nabla\cdot\rho\mathbf{v} = 0 \tag{1.2.24}$$

The first order moment gives instead

$$\frac{\partial}{\partial t}\int \frac{p_i}{m} f d^3p + \int \frac{p_j}{m}\frac{p_i}{m}\nabla^j f d^3p - m\nabla_j\Phi\int \frac{p_i}{m}\frac{\partial}{\partial p_j} f d^3p = \tag{1.2.25}$$

$$\frac{\partial}{\partial t}\rho v_i + \nabla^j\int \frac{p_j}{m}\frac{p_i}{m} f d^3p + \nabla_j\Phi\int \frac{\partial p_i}{\partial p_j} f d^3p = \tag{1.2.26}$$

$$\frac{\partial}{\partial t}\rho v_i + \nabla^j(\sigma_{ij} + \rho v_i v_j) + \nabla_j\Phi\delta^j_i\int f d^3p = \tag{1.2.27}$$

$$\frac{\partial \rho}{\partial t} v_i + \rho\frac{\partial}{\partial t} v_i + \nabla^j(\sigma_{ij} + \rho v_i v_j) + \rho\nabla_i\Phi = \tag{1.2.28}$$

$$-v_i\nabla^j\rho v_j + \rho\frac{\partial}{\partial t} v_i + \nabla^j(\sigma_{ij} + \rho v_i v_j) + \rho\nabla_i\Phi = 0 \tag{1.2.29}$$

We used integration by parts in the last term of the second line and replacement with the continuity equation in the last line. Now we have

$$-v_i\nabla^j\rho v_j + \nabla^j\rho v_i v_j = \rho v_j\nabla^j v_i \tag{1.2.30}$$

and therefore

$$\frac{\partial}{\partial t} v_i + v_j\nabla^j v_i = -\nabla_i\Phi - \frac{1}{\rho}\nabla^j\sigma_{ij} \tag{1.2.31}$$

The hierarchy of moments if usually truncated at the second order (one can indeed show that for non-relativistic matter higher orders are suppressed [3]) and, to close the system of equations, some simplified assumption is taken for σ_{ij}. The most common is to assume an isotropized fluid in which the stress tensor is identified with the pressure

$$\sigma_{ij} = p\delta_{ij} \tag{1.2.32}$$

In this case we recover Eq. (1.1.4)

$$\frac{\partial}{\partial t} v_i + v_j\nabla^j v_i = -\nabla_i\Phi - \frac{1}{\rho}\nabla_i p \tag{1.2.33}$$

At the background level, there are no peculiar velocities, so $\mathbf{v} = H\mathbf{x}$, $\Phi = \phi_0 = \frac{2\pi}{3}\rho_0 x^2$. Then, since $x_j\nabla^j x_i = x_j\delta^j_i = x_i$, we have (notice that $\partial/\partial t$ has to be taken at constant x_i)

$$x_i\frac{\partial}{\partial t} H + H^2 x_i = -\frac{4\pi}{3}\rho_0 x_i - \frac{1}{\rho}\nabla^j\sigma_{ij} \tag{1.2.34}$$

For a pressureless perfect fluid $\sigma_{ij} = 0$, and therefore we recover the second Friedmann equation

$$\frac{\partial}{\partial t}H + H^2 = \frac{\ddot{a}}{a} = -\frac{4\pi}{3}\rho_0 \tag{1.2.35}$$

As promised, eqs. (1.2.24,1.2.33) coincide then with Eqs. (1.1.3,1.1.4). More in general, the stress tensor gets contributions associated to the so-called *shear* (coefficient η) and *bulk (*coefficient ζ*) viscosity*:

$$\sigma_{ij} = p\delta_{ij} - \eta(\nabla_i v_j + \nabla_j v_i - \frac{2}{3}\delta_{ij}\nabla\cdot v) - \zeta\delta_{ij}\nabla\cdot v, \tag{1.2.36}$$

In our treatment we however refer to CDM particles, which are supposed to have negligible pressure and self-interactions, so we put $\sigma_{ij} = 0$. This approximation is also called *single-stream*, meaning that particles in a given infinitesimal region all move with the same velocity. It is clear from the outset, however, that this approximation has to break down for baryonic tracers (i.e. galaxies) below a certain scale. This breaking is often called *shell-crossing* or *multi-stream*, and occurs when in the same infinitesimal region there are particles moving with different velocities. We will come back to the neglected part in Sec. 6.2.

1.3 Evolution of linear perturbations

Let's now go back to Eq. (1.1.30). For $kc_s \ll \mathcal{H}$ the perturbations grow freely: this is the phenomenon of gravitational instability. We can rewrite the Newtonian equation

$$\ddot{\delta} + \mathcal{H}\dot{\delta} - \frac{3}{2}\mathcal{H}^2\Omega_m\delta = 0 \tag{1.3.1}$$

Adopting now the time variable $\alpha = \log a$ we obtain for $\Omega_m = 1$ (Einstein-deSitter model)

$$\delta'' + (\frac{\mathcal{H}'}{\mathcal{H}} + 1)\delta' - \frac{3}{2}\delta = 0 \tag{1.3.2}$$

Putting (show this as an exercise)

$$\frac{\mathcal{H}'}{\mathcal{H}} = -\frac{1}{2} - \frac{3}{2}w \tag{1.3.3}$$

we obtain for $w = 0$

$$\delta'' + \frac{1}{2}\delta' - \frac{3}{2}\delta = 0 \tag{1.3.4}$$

which is simply solved by

$$\delta = Ae^{m\alpha} = Aa^m$$

with the two solutions

$$m_\pm = 1, -3/2 \tag{1.3.5}$$

Therefore the growth functions are

$$\delta_+ = Aa^1, \quad \delta_- = Ba^{-3/2}$$

(*growing* and *decaying* modes, respectively). The second solution becomes rapidly negligible with respect to the first one and normally is neglected. With respect to conformal time we have $\delta_+ \sim \tau^2$. Obviously the constants A, B must be fixed by the observations.

From δ_+ an important consequence follows. From the Poisson equation

$$k^2\phi = -\frac{3}{2}\mathcal{H}^2\delta$$

we see that during the matter dominated era $\mathcal{H}^2\delta_+ = a^2H^2\delta_+ = a^2a^{-3}a = cost.$ and therefore the gravitational potential remains constant.

1.4 Growth rate and growth function in ΛCDM.

In general, a good approximation for the solution of Eq. (1.3.1) is given in terms of the *growth rate* f, defined as

$$f \equiv \frac{d\log\delta_m}{d\log a} \approx \Omega_m^{\gamma}(z) \tag{1.4.1}$$

with $\gamma \approx 0.55$ (called the *growth index*) and for ΛCDM

$$\Omega_m(z) = \frac{\rho_m}{\rho_{crit}} = \frac{\Omega_{m0}a^{-3}}{\Omega_{m0}a^{-3} + 1 - \Omega_m} \tag{1.4.2}$$

The *growth function* (normalized to unity today) is given by

$$G(z) \equiv \frac{\delta_m(z)}{\delta_m(0)} = \exp\int_1^a f(z)d\log a \approx \exp\int_1^a \Omega_m^{\gamma}(z)d\log a \tag{1.4.3}$$

In this case is no longer true that $\mathcal{H}^2\delta$ is constant and therefore the gravitational potential is not a constant.

Chapter 2

Correlation function and power spectrum

Quick summary

- Here we define several measures of clustering of a distribution of points
- This chapter deal only with the mathematical properties of these statistical descriptors. In the next one we study the physical properties.
- The correlation function describes the clustering of a distribution of points in space.
- The power spectrum is the Fourier conjugate of the correlation function
- Correlation function and power spectrum are two-point descriptors. One can generalize them to n-point descriptors.
- Moments are an integral measure of clustering. The second order moment can be estimated by integrating the correlation function or the power spectrum.

2.1 Why we need correlation functions, power spectra and all that

All the perturbation variables we have studied so far, δ, Ψ, θ etc, and their Fourier transforms, are random variables. That is, we cannot know if in a given point in space-time, δ is zero, -0.01 or any other value. All we have found with GR equations is how this value will evolve in time, e.g. as $\delta \sim a$ as in MDE. If in a location δ is initially zero, it will remain so. If it is initialy negative (an underdensity) it will become more and more underdense, until the region is empty. If it is an overdensity, it will grow until it exits the regime of linearity. The perturbation variables are random fields in space and as such must be studied statistically. In practice, this means that instead of studying the field $\delta(x, y, z)$, we study its moments, in particular mean and variance. In real space, the variance $\langle \delta(x)\delta(x+r) \rangle$ as a function of separation r is called correlation function. In Fourier space, the variance $\langle \delta^2 \rangle$ as a function of wavenumber k is called power spectrum. However, the mean is trivial: $\langle \delta \rangle = 0$, since the density contrast is exactly defined as the fractional difference of the density minus its mean. Since all other perturbation variables are proportional to δ, the same applies to all of them: $\langle \Psi \rangle = \langle \Phi \rangle = \langle \theta \rangle = 0$ etc.. It is then clear that only the variance contains useful information. In principle, also higher order moments can be employed, and often they are. However, a fundamental assumption (based on the initial conditions set up by inflation) is that the initial fluctuations are Gaussian distributed, and for such a distribution only the variance is needed, since all higher order moments are either zero (the odd ones) or are function of the variance: for instance $\langle \delta^4 \rangle = 3\langle \delta^2 \rangle^2$. This is why most cosmology needs only to focus on the quadratic statistics, namely variance, correlation function, and power spectrum. However, when fluctuations grow and start becoming non-linear, their Gaussian nature will in general be lost. This is obvious if only one realizes that if in a given region δ is initially negative and keeps growing, it will at some point become a void, $\delta = -1$, and will stop there; but if it is positive, δ can grow without limit (that is, the region collapses into a structure, e.g. a galaxy, a star or even a black hole), and the final distribution of underdensities and overdensities will obviously be asymmetric

(skewed) and no longer Gaussian. The exact non-linear distribution is very difficult to obtain and generally has to be found numerically by N-body simulations.

2.2 Average, variance, moments.

Here we recall a few basic facts about random variables and statistics. If x is a random variable (e.g. δ at a point r in our case), and if $f(x)dx$ is the probability of finding x in the interval $x, x+dx$, then (integral extended in the entire domain of definition of x)

$$\int f(x)dx = 1 \tag{2.2.1}$$

$$\langle x \rangle = \int x f(x)dx \tag{2.2.2}$$

$$\langle x^2 \rangle = \int x^2 f(x)dx \tag{2.2.3}$$

and in general $\langle g(x) \rangle = \int g(x)f(x)dx$. It follows that, if a, b are constants

$$\langle a \rangle = a \tag{2.2.4}$$

$$\langle ax \rangle = a\langle x \rangle \tag{2.2.5}$$

$$\langle ag(x) + bp(x) \rangle = a\langle g(x) \rangle + b\langle p(x) \rangle \tag{2.2.6}$$

We define n-th order moments and n-th order central moments as, respectively,

$$\bar{M}_n = \int x^n f(x)dx \tag{2.2.7}$$

$$M_n = \int (x - \langle x \rangle)^n f(x)dx \tag{2.2.8}$$

The central moment M_2 is called *variance*. If x_i is a vector of several random variables, one defines multivariate moments, in particular the covariance

$$c_{ij} = \langle x_i x_i \rangle \tag{2.2.9}$$

2.3 Definition of the correlation function

Other common statistical descriptors are the $n-$point correlation functions. Let $\langle n \rangle = \rho_0 dV$ be the average number of particles in an infinitesimal volume dV, being ρ_0 the average number density. If $dN_{ab} = \langle n_a n_b \rangle$ is the average number of *pairs* in the volumes dV_a and dV_b (i.e., the product of the number of particles in one volume with the number in the other volume), separated by r_{ab}, then the 2-point correlation function $\xi(r_{ab})$ is defined as

$$dN_{ab} = \langle n_a n_b \rangle = \rho_0^2 dV_a dV_b (1 + \xi(r_{ab})) \tag{2.3.1}$$

If the distribution is uniform, then the average number of pairs is exactly equal to the product of the average number of particles in the two volumes, and the correlation ξ vanishes; if there is correlation among the volumes, on the other hand, then the correlation is different from zero. The correlation function is also defined, equivalently, as *the spatial average of the product of the density contrast* $\delta(r_a) = n_a/(\rho_0 dV) - 1$ at two different points

$$\xi(r_{ab}) = \frac{dN_{ab}}{\rho_0^2 dV_a dV_b} - 1 = \frac{\langle n_a n_b \rangle}{\rho_0^2 dV_a dV_b} - 1 = \langle (\delta_a + 1)(\delta_b + 1) \rangle - 1 = \langle \delta(r_a)\delta(r_b) \rangle \tag{2.3.2}$$

because $\langle \delta_{a,b} \rangle = 0$.

In practice it is easier to derive the correlation function as the average density of particles at a distance r from another particle. This is a *conditional* density, that is the density of particles at distance r given that

there is a particle at $r = 0$. The number of pairs is then the number of particles in both volumes divided by the number of particles $dN_a = ndV_a$ in the volume dV_a at $r = 0$:

$$dN_b = dN_{ab}/dN_a = \rho_0^2 dV_a dV_b(1 + \xi(r_{ab}))/dN_a = \rho_0 dV_b(1 + \xi(r_b)) \tag{2.3.3}$$

The correlation function can then be defined as

$$\xi(r) = \frac{dN_c(r)}{\rho_0 dV} - 1 = \frac{\langle \rho_c \rangle}{\rho_0} - 1 \tag{2.3.4}$$

(where c stands for conditional) i.e. as the average number of particles at distance r from any given particle (or number of neighbors), divided by the expected number of particles at the same distance in a uniform distribution, minus 1, or *conditional density contrast.* If the correlation is positive, there are then more particles than in a uniform distribution: the distribution is then said to be positively clustered. This definition is purely radial, and does not distinguish between isotropic and anisotropic distributions. One could generalize this definition by introducing the anisotropic correlation function as the number of pairs in volumes at distance r and a given longitude and latitude. This is useful whenever there is some reason to suspect that the distribution is indeed anisotropic, as when there is a significant distortion along the line-of-sight due to the redshift.

If the average density of particles is estimated from the sample itself, i.e. $\rho_0 = N/V$, it is clear that the integral of $dN_c(r)$ must converge to the number of particles in the sample :

$$\int_0^R dN_c(r) = \int \rho(r) dV = N \tag{2.3.5}$$

In this case the correlation function is a sample quantity, and it is subject to the integral constraint (Peebles 1980)

$$\int_0^R \xi_s(r) dV = N/\rho_0 - V = 0 \tag{2.3.6}$$

Assuming spatial isotropy this is

$$4\pi \int_0^R \xi_s(r) r^2 dr = 0 \tag{2.3.7}$$

If the sample density is different from the true density of the whole distribution, we must expect that the $\xi_s(r)$ estimated in the sample differs from the true correlation function. From Eq. (2.3.4), we see that $g(r) = 1 + \xi(r)$ scales as ρ_0^{-1}. Only if we can identify the sample density ρ_0 with the true density the estimate of $\xi(r)$ is correct. In general, the density is estimated in a survey centered on ourselves, so that what we obtain is in reality a conditional density.

The conditional density at distance r from a particle, averaged over the particles in the survey, is often denoted in the statistical literature as $\Gamma(r)$; we have therefore from Eq. (2.3.4)

$$\Gamma(r) \equiv \langle \rho_c \rangle = \rho_0(1 + \xi) \tag{2.3.8}$$

The average in spherical cells of radius R and volume V of this quantity is denoted as

$$\Gamma^*(R) \equiv \langle \rho_c \rangle_{sph} = \rho_0(1 + \widehat{\xi}) \tag{2.3.9}$$

where

$$\widehat{\xi} = V^{-1} \int \xi dV \tag{2.3.10}$$

To evaluate $\Gamma^*(R)$ one finds the average of the number of neighbors inside a distance R from any particle contained in the sample.

2.4 The n-point correlation function and the scaling hierarchy

The correlation function can be generalized to more than two points. The 3-point function for instance is defined as

$$\varsigma(r_a, r_b, r_c) = \langle \delta(r_a)\delta(r_b)\delta(r_c) \rangle \tag{2.4.1}$$

In terms of the counts in infinitesimal cells we can write

$$\begin{aligned} \varsigma(r_a, r_b, r_c) &= \langle \left(\frac{n_a}{\rho_0 dV_a} - 1 \right) \left(\frac{n_b}{\rho_0 dV_b} - 1 \right) \left(\frac{n_c}{\rho_0 dV_c} - 1 \right) \rangle \\ &= \frac{\langle n_a n_b n_c \rangle}{\rho_0^3 dV_a dV_b dV_c} - \xi_{ab} - \xi_{bc} - \xi_{ac} - 1 \end{aligned} \tag{2.4.2}$$

so that we obtain the useful relation

$$\langle n_a n_b n_c \rangle = \rho_0^3 dV_a dV_b dV_c (1 + \xi_{ab} + \xi_{bc} + \xi_{ac} + \varsigma_{abc}) \tag{2.4.3}$$

In some simple and interesting cases, the moments M_p of the counts obey the following scaling hierarchy for any box size in a certain range of scales

$$S_p = \frac{M_p}{M_2^{p-1}} = const \tag{2.4.4}$$

2.5 The power spectrum

One of the most employed statistical estimator for density fields is the power spectrum. In recent years it has been used to quantify the clustering properties in many galaxy surveys. The main reason is that almost all theories of structure formation predict a specific shape of the spectrum, because the plane waves evolve independently in the linear approximation of the gravitational equations.

Unless otherwise specified, the conventions for the 3D Fourier transforms are

$$\begin{aligned} f(x) &= \frac{V}{(2\pi)^3} \int f_k e^{ikx} d^3k \\ f_k &= \frac{1}{V} \int f(x) e^{-ikx} d^3x \end{aligned} \tag{2.5.1}$$

and it is always understood that $ikx = i\mathbf{k} \cdot \mathbf{x}$ (we'll use the bold face for vectors when there is risk of confusion). With this conventions, $f(x)$ and f_k have the same dimensions. Since $f(x)$ is real, $f^*_{\mathbf{k}} = f_{-\mathbf{k}}$. The factor of V is unnecessary but is convenient to keep f, f_k with the same dimensions. In every calculation one can however take $V = 1$ without any harm.

If we consider the Fourier transform of $f(x) \equiv 1$ we have

$$1 = \frac{V}{(2\pi)^3} \int f_k e^{ikx} d^3k \tag{2.5.2}$$

with

$$f_k = \frac{1}{V} \int e^{-ikx} d^3x \tag{2.5.3}$$

This shows that in the limit $V \to \infty$ we can take as a representation of the Dirac delta the function

$$\delta_D(\mathbf{k}) = \frac{1}{(2\pi)^3} \int e^{-i\mathbf{kx}} d^3x \tag{2.5.4}$$

(and similarly for $k \leftrightarrow x$) since indeed the oscillations cancel each other in an infinite volume and therefore $\delta_D(k) = 0$ for every $k \neq 0$, while $\delta_D(k)$ diverges for $k = 0$ and, since $(V/(2\pi)^3) f_k = \delta_D(k)$,

$$\int \delta_D(k) d^3k = \tfrac{V}{(2\pi)^3} \int f_k d^3k = f(x = 0) = 1 \tag{2.5.5}$$

The Dirac delta $\delta_D(k)$ has dimension of a volume. Analogously, the Dirac delta in real space is $\delta_D(\mathbf{x}) = (2\pi)^{-3}\int e^{i\mathbf{kx}}d^3k$. The two Dirac delta's are not the Fourier transform of each other.

Let now $\delta(x)$ be the density contrast of a density field in a survey of volume V and

$$\delta_k = \frac{1}{V}\int \delta(x)e^{-ikx}dV \tag{2.5.6}$$

its Fourier transform. The power spectrum is defined as

$$P(k) = V\langle\delta_k\delta_k^*\rangle \tag{2.5.7}$$

Notice that the power spectrum has the dimension of a volume. For a single realization (e.g. a survey or a single simulation) one has $P = V\delta_k\delta_k^*$. In this case it follows

$$P(k) = \frac{1}{V}\int \delta(x)\delta(y)e^{-ik(x-y)}dV_x dV_y \tag{2.5.8}$$

Now, putting $r = x - y$, and taking the *volume average*

$$\xi(r) = \langle\delta(y+r)\delta(y)\rangle_V = \frac{1}{V}\int \delta(y+r)\delta(y)dV_y \tag{2.5.9}$$

then,

$$P(\mathbf{k}) = \int \xi(r)e^{-i\mathbf{kr}}dV \tag{2.5.10}$$

Therefore, the power spectrum is the Fourier transform of the correlation function (Wiener-Khintchin theorem). The converse property is

$$\xi(\mathbf{r}) = (2\pi)^{-3}\int P(k)e^{i\mathbf{kr}}d^3k \tag{2.5.11}$$

(notice that here, following most literature, the Fourier volume factor is not included). Finally, assuming spatial isotropy, i.e. that the correlation function depends only on the modulus $|r|$, we obtain

$$P(k) = 4\pi\int \xi(r)\frac{\sin kr}{kr}r^2dr \tag{2.5.12}$$

A more general definition of power spectrum can also be given, but this time we have to think in terms of *ensemble averages,* rather than volume averages. Consider in fact the ensemble average of $V\delta_k\delta_{k'}^*$:

$$V\langle\delta_k\delta_{k'}^*\rangle = \frac{1}{V}\int\langle\delta(y+r)\delta(y)\rangle e^{i(k-k')y+ikr}dV_r dV_y \tag{2.5.13}$$

Performing ensemble averages, one has to think of fixing a positions and making the average over the ensemble of realizations. Then the average can enter the integration, and average only over the random variables δ. Then we obtain

$$V\langle\delta_k\delta_{k'}^*\rangle = \frac{1}{V}\int \xi(r)e^{i(k-k')y+ikr}dV_r dV_y = \frac{(2\pi)^3}{V}P(k)\delta_D(k-k') \tag{2.5.14}$$

The definition (2.5.14) states simply that modes at different wavelengths are uncorrelated if the field is statistically homogeneous (that is, if ξ does not depend on the position in which is calculated but only on the distance r; also called *translation invariance*). Notice that this property is general and not confined to the linear approximation. This will often be useful later.

One can go from Eq. (2.5.14) to Eq. (2.5.7) in this way:

$$V\langle\delta_k\delta_k^*\rangle = V\int d^3k'\langle\delta_k\delta_{k'}^*\rangle\delta_D(k-k') = \frac{(2\pi)^3}{V}\int d^3k'P(k)\delta_D(k-k')\delta_D(k-k') = \tag{2.5.15}$$

$$\frac{(2\pi)^3}{V}P(k)\int d^3k'\delta_D(k-k')\delta_D(k-k') = P(k) \tag{2.5.16}$$

where we used the identity

$$\int \delta_D(\mathbf{k}_1-\mathbf{k}_4)\delta_D(\mathbf{k}_1-\mathbf{k}_4)d^3k_1 = \int \frac{e^{-i\mathbf{x}(\mathbf{k}_1-\mathbf{k}_4)}}{(2\pi)^3}d^3x\delta_D(\mathbf{k}_1-\mathbf{k}_4)d^3k_1 = \int \frac{1}{(2\pi)^3}d^3x = \frac{V}{(2\pi)^3} \tag{2.5.17}$$

These definitions refer to infinite samples and to a continuous field. In reality, we always have a finite sample and a discrete realization of the field, i.e.. a finite number of particles. Therefore, we have to take into account the effects of both finiteness and discreteness.

To investigate the discreteness, we assume as field a collection of N particles of dimensionless masses m_i expressed in units of the average mass m_0 at positions x_i, in a volume V . In the following we will make use of the window function $W(x)$, a function which expresses the way in which the particles are selected. A typical selection procedure is to take all particles within a given region, and no particles elsewhere. In this case, the function will be a constant inside the survey, and zero outside. We will always consider such a kind of window function in the following, and normalize it so that

$$\int W(x)dV = 1 \tag{2.5.18}$$

With this normalization, $W(x) = 1/V$ inside the survey. The density contrast field we have in a specific sample is therefore the universal field times the window function (times the sample volume V because of the way we normalized W)

$$\delta_s = \delta(x)VW(x) \tag{2.5.19}$$

Let us now express the field as a sum of Dirac functions

$$\delta_s(x) = \left(\frac{\rho(x)}{\rho_0}-1\right)VW(x) = \frac{V}{N}\sum_i m_i w_i \delta_D(x-x_i) - VW(x) \tag{2.5.20}$$

where $w_i = VW(x_i)$. The Fourier transform is

$$\delta_k = \frac{1}{V}\int\left(\frac{V}{N}\sum_i m_i w_i\delta_D - VW(x)\right)e^{ikx}dV = \frac{1}{N}\sum_i m_i w_i e^{ikx_i} - W_k \tag{2.5.21}$$

where we introduced the $k-$space window function

$$W_k = \int W(x)e^{ikx}dV \tag{2.5.22}$$

normalized so that $W_0 = 1$. The most commonly used window function is the so-called top-hat function, which is the FT of the simple selection rule

$$\begin{aligned} W(x) &= 1/V \text{ inside a spherical volume } V \text{ of radius } R \\ W(x) &= 0 \text{ outside} \end{aligned} \tag{2.5.23}$$

We have then

$$\begin{aligned} W_k &= \int W(x)e^{i\mathbf{kx}}dV = V^{-1}\int e^{i\mathbf{kx}}dV \\ &= \frac{3}{4\pi}R^{-3}\int^R r^2dr\int_{-\pi}^{\pi}e^{ikr\cos\theta}d\cos\theta d\phi \\ &= \frac{3}{2}R^{-3}\int^R\left(e^{ikr}-e^{-ikr}\right)\frac{r^2}{ikr}dr \\ &= 3R^{-3}\int^R\frac{r\sin kr}{k}dr = 3\frac{\sin kR - kR\cos kR}{(kR)^3} \end{aligned} \tag{2.5.24}$$

Notice that $W_0 = 1$, and that the WF declines rapidly as $k \to \pi/R$. Now, the expected value of the power spectrum is

$$P(k) = V\langle\delta_k\delta_k^*\rangle \tag{2.5.25}$$

that is

$$P(k) = \frac{V}{N^2}\sum_{ij} m_i m_j w_i w_j e^{ik(x_i - x_j)} - VW_k^2 \tag{2.5.26}$$

Usually we do not know the masses of the galaxies, so all we can do is to use the number counts as a proxy for the density contrast: that is, we put $m_i = 1$. Then we can use the relation

$$\langle \frac{1}{N}\sum_i m_i w_i e^{ikx_i}\rangle = \frac{1}{N}\sum_i m_i \int W(x) e^{ikx} dV = W_k \tag{2.5.27}$$

Finally, if the positions x_i and x_j are uncorrelated, we can pick up only the terms with $i = j$, so that, neglecting the window function, which is important only for $k \to 0$, we obtain the pure noise spectrum

$$P_n(k) = \frac{V}{N^2}\sum_i m_i^2 w_i^2 = V/N \tag{2.5.28}$$

where the last equality holds only if $m_i = 1$ for all particles and w_i equals 0 or 1. The noise spectrum is negligible only for large densities, $\rho_0 = N/V \to \infty$. Since the galaxy distributions are often sparse, the noise is not always negligible and has to be subtracted from the estimate. For the power spectrum applies the same consideration expressed for the moments: the power spectrum does not characterize completely a distribution, unless we know the distribution has some specific property, e.g. is Gaussian, or Poisson, etc.

2.6 From the power spectrum to the moments

The power spectrum is often the basic outcome of the structure formation theories, and it is convenient to express all the other quantities in terms of it. Here we find the relation between the power spectrum and the moments of the counts in random cells.

Consider a finite cell. Divide it into infinitesimal cells with counts n_i either zero or unity. We have by definition of ξ

$$\langle n_i n_j\rangle = \rho_0^2 dV_i dV_j [1 + \xi_{ij}] \tag{2.6.1}$$

The count in the cell is $N = \sum n_i$. The variance is then

$$M_2 = \langle \frac{(N - N_0)^2}{N_0^2}\rangle = \frac{\langle N^2 + N_0^2 - 2NN_0\rangle}{N_0^2} = \frac{\langle N^2\rangle + N_0^2 - 2\langle N\rangle N_0}{N_0^2} = \frac{\langle N^2\rangle - N_0^2}{N_0^2} \tag{2.6.2}$$

where

$$\begin{aligned}\langle N^2\rangle &= \langle \sum n_i \sum n_j\rangle = \sum \langle n_i^2\rangle + \sum \langle n_i n_j\rangle = \\ &\quad N_0 + N_0^2 \int dV_i dV_j W_i W_j [1 + \xi_{ij}]\end{aligned} \tag{2.6.3}$$

where $N_0 = \rho_0 V$ is the count average, and $\xi_{ij} \equiv \xi(|\mathbf{r}_i - \mathbf{r}_j|)$. Let us simplify the notation by putting

$$W_i dV_i = dV_i^*$$

We define the integral (by definition $\int W dV = \int dV^* = 1$ for any window function)

$$\sigma^2 = \int dV_1^* dV_2^* \xi_{12} \tag{2.6.4}$$

This is clearly a dimensionless quantity. Inserting the power spectrum we have

$$\sigma^2 = (2\pi)^{-3} \int P(k) e^{i\mathbf{k}(\mathbf{r}_1 - \mathbf{r}_2)} W_1 W_2 d^3k d^3r_1 d^3r_2 \tag{2.6.5}$$

This becomes

$$\sigma_R^2 = (2\pi^2)^{-1} \int P(k) W_R^2(k) k^2 dk \tag{2.6.6}$$

where R is the size of the cells. Then we see that $\langle N^2 \rangle = N_0 + N_0^2 + N_0^2 \sigma^2$. Finally we obtain the relation between the power spectrum (or the correlation function) and the second-order moment of the counts:

$$M_2 = N_0^{-2}(\langle N^2 \rangle - N_0^2) = N_0^{-1} + \sigma^2 \tag{2.6.7}$$

The first term is the so called shot-noise, the second term is the count variance in the continuous limit. Clearly, in the limit of a high density of particles so we can neglect the noise term, σ^2 quantifies how strong the fluctuations are. If $\sigma^2 \approx M_2 \approx 1$, the numer of particles in cells have a relative variance which is as big as the average number itself. Therefore we can say that the distribution is very inhomogeneous and the linear approximation $\delta \ll 1$ fails.

For the third order moment we proceed in a similar fashion:

$$\langle N^3 \rangle = \langle \sum n_i \sum n_j \sum n_k \rangle = \sum \langle n_i^2 \rangle + 3 \sum \langle n_i^2 \rangle \sum n_i + \sum \langle n_i n_j n_k \rangle = \tag{2.6.8}$$

$$N_0 + 3N_0^2 + N_0^3 \int dV_i^* dV_j^* dV_k^* [1 + \xi_{ij} + \xi_{ik} + \xi_{jk} + \varsigma_{ijk}] \tag{2.6.9}$$

where in the last equality we used the definition of the three point correlation given in Eq. (2.4.3)

$$\langle n_i n_j n_k \rangle = \rho_0^3 dV_i dV_j dV_k [1 + \xi_{ij} + \xi_{ik} + \xi_{jk} + \varsigma_{ijk}] \tag{2.6.10}$$

The third order moment is then

$$M_3 = N_0^{-3} \langle (\Delta N)^3 \rangle = N_0^{-2} + \int dV_i^* dV_j^* dV_k^* \varsigma_{ijk} \tag{2.6.11}$$

where $\Delta N = N - N_0$. If we can assume the scaling relation $\varsigma_{ijk} = Q[\xi_{ij}\xi_{jk} + \xi_{ij}\xi_{ik} + \xi_{ik}\xi_{jk}]$ then we can express M_3 in terms of $P(k)$ and of the new parameter Q. In the limit of large N_0, a Gaussian field ($M_3 = 0$) has $Q = 0$.

Chapter 3

The galaxy power spectrum

In Ch. (1) we have seen how to derive the linear matter power spectrum as a function of scale and redshift. What we observe however is the power spectrum of the linear and non-linear galaxy distribution when distances are measured with the redshift. Its relation to the theoretical prediction is not a straightforward one, as we will see in this Chapter.

Quick summary

- The linear galaxy power spectrum expresses the clustering of galaxies in redshift space
- It is related to theoretical prediction of the matter power spectrum in real space through several corrections (the bias, the redshift distortion) and depends on the growth function
- The baryon oscillations that are prominently visible on the CMB spectrum are also visible as small wiggles on the galaxy power spectrum
- The comparison to observations can constrain several cosmological parameters, from the primordial slope n_s to Ω_m, Ω_b, to the dark energy equation of state.
- The Euclid satellite (launched in 2023) will measure the power spectrum up to redshift 2 to great precision.

3.1 Large scale structure

Let us see now how to link the primordial inflationary spectrum with the present observations of the galaxy distribution. Instead of the spectrum evaluated at horizon reenter t_H, which is different for every scale, we prefer to evaluate it at a fixed epoch t_F, for instance the decoupling epoch $z \approx 1000$. The difference is that at a fixed epoch, the perturbations that are already inside the horizon had the time to grow, contrary to those still outside. Let us consider a perturbation that reenter in MDE when the scale factor was a, and $H = (2/3)t^{-1} = a^{-3/2}H_0$ (as usual we assume the present value $a_0 = 1$) ; at that epoch, $k = aH = aa^{-3/2}H_0 = a^{-1/2}H_0$. Thus a perturbation with wavenumber k reenters when the scale factor was $a = (k/H_0)^{-2}$. This perturbation grows between a and an arbitrary instant, say a_F, as $\delta_k \sim (a_F/a) = (k/k_F)^2$ (since we are in MDE), if k_F is the scale that reenters at a_F. Therefore smaller scales reenter the horizon earlier than larger ones and have therefore more time to grow in amplitude. To conclude, the amplitude of a perturbation of size k^{-1} has the time to grow between its reenter and a_F by a factor $(k/k_F)^2$. Then the relation between δ at t_F and at t_H is

$$(\delta\rho/\rho)_k(t_F) \quad = \quad (k/k_F)^2(\delta\rho/\rho)_k(t_H)\,, \tag{3.1.1}$$

and consequently

$$P_k(t_F) = (k/k_F)^4 P_k(t_H)\,.$$

Assuming the inflationary spectrum k^{-3} with $n_s \approx 1$ it follows that for the scales reentering after equivalence

$$P_k(t_F) = Ak\,. \qquad \text{Harrison} - \text{Zeldovich spectrum} \tag{3.1.2}$$

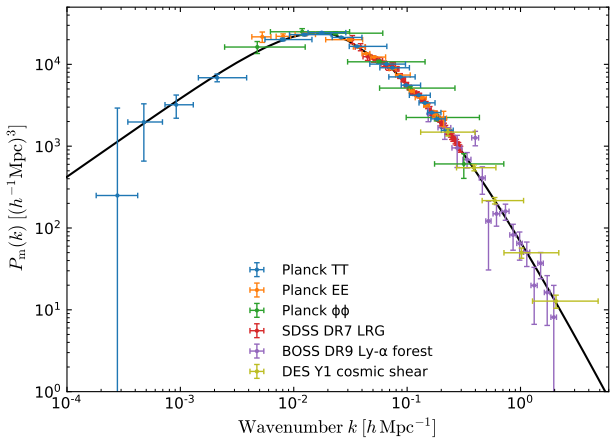

Figure 3.1.1: Power spectrum of the large scale structure (at small scales) and of the cosmic microwave background (at large scales). (ESA and the Planck Collaboration).

This scale-invariant spectrum is a remarkable prediction of inflation. During the subsequent evolution, this initial spectrum will be modified in a way that depends on the detailed components, e.g. the amount of dark matter and baryons. Note that we obtained (3.1.2) assuming exponential inflation. If inflation is a power law, the resulting spectrum becomes $P_k = Ak^{n_s}$, with $n_s \leq 1$. The Planck data of the cosmic background found $n_s = 0.96 \pm 0.01$, in complete agreement with inflation.

We can now predict the observational quantities: the power spectrum and (in the next section) the peculiar velocity field. Notice that the average of the density contrast vanishes, $< \delta >= 0$, by definition of average density. The simplest non-trivial average quantity that describe the fluctuation field is therefore the dispersion δ, that is the variance $< \delta^2 >$. In the Fourier space, the corresponding quantity is the spectrum $P(k) = \delta_k^2$. We have seen that the spectrum at horizon crossing goes like k^{-3}, modified in k^1 for the perturbations that reenter in MDE. However, those that are smaller than λ_{eq} =13 Mpc h^{-1}, reentering in RDE, do not suffer this correction since as we have seen they do not grow during RDE. In other words, for scales smaller than λ_{eq}, the spectrum at horizon crossing coincides with the one at equivalence. For these scales then the behavior remains k^{-3}. All this means that the inflationary spectrum at a fixed t, $P(k) = Ak^{n_s}$ (with n_s close to 1) is modified during RDE and MDE by a function $T^2(k)$ such that $T \sim 1$ at large scales and $T \sim k^{-4}$ at small ones. For the final spectrum we have then

$$P(k) = Ak^{n_s} T^2(k) \tag{3.1.3}$$

where $T(k)$ is called *transfer function*. This spectrum remains unvaried in slope from equivalence to now: during this epoch, in fact, perturbations grow independently of k. A simple form of T^2 that produces the requested behavior is $T^2 = 1/[1 + (k/k_{eq})^4]$. The exact transfer function can be evaluated only numerically, integrating for every k the perturbation equations. A popular approximation is (Efstathiou, Bond White 1992)

$$P(k) = Ak^{n_s} T(k)^2 \tag{3.1.4}$$

$$T(k) = \left[1 + \left[ak + (bk)^{1.5} + (ck)^2\right]^\nu\right]^{-1/\nu} \tag{3.1.5}$$

$$(a, b, c) = (6.4, 3.0, 1.7)\,\Gamma^{-1} Mpc/h, \nu = 1.13 \tag{3.1.6}$$

$$\Gamma = \Omega_{nr} h \tag{3.1.7}$$

where $T^2(k)$ has the correct limit k^{-4} . The scale at which this limit is approached is $k_t = \Gamma = \Omega_{nr} h$. In a flat model with $h = 0.5$ this is roughly $2\pi/0.5$ Mpc$/h = 12.6$ Mpc$/h$, close to the horizon scale at equivalence, as it should be.

The whole linear treatment fails naturally at very small scales, those that are non-linear and collapsed into galaxies and clusters. A rough approximation to the linearity scale is 50 Mpch^{-1}.

3.2 The bias factor

The power spectrum we observe is obtained by mapping the position of the galaxies and then performing a Fourier transform of the density contrast. However the power spectrum that is predicted by the linear perturbation theory is the mass power spectrum, not the galaxy one. The density contrast of the galaxies can be well different from the matter density contrast: for instance, galaxies could form only when the matter density is above a certain threshold. The simplest possibility is to assume that the two density contrast are proportional to each other

$$\delta_g = b\delta_m \tag{3.2.1}$$

where b is called linear *bias* factor. In this case obviously

$$P_g = b^2 P_m \tag{3.2.2}$$

Of course the real bias could be a non-linear function of δ_m, or an average of δ_m at various locations. In general, the bias factor might depend on space (i.e. on k after Fourier transformation) and time, and also on galaxy type and luminosity. In fact it is often reported that brighter galaxies have a larger bias, perhaps because they form only on density peaks. The values of b that have been reported so far are always around unity. In a later chapter we will considerably generalize the bias prescription.

3.3 Normalization of the power spectrum

Several ways to normalize the *mass* power spectrum have been employed so far: the cosmic microwave fluctuations, the cluster abundance, weak lensing.

As we have seen the CMB measures at large scales the Sachs-Wolfe effect, i.e. temperature anisotropies proportional to the gravitational potential. The amount of anisotropies is then a direct measurement of the power spectrum at large scales. If we know the shape of the transfer function, measuring the spectrum at large scales fixes its amplitude at all scales and we can estimate the normalization (see Sect. 2.5)

$$\sigma_8^2 = (2\pi^2)^{-1} \int P(k) W_{8Mpc/h}^2(k) k^2 dk \tag{3.3.1}$$

Planck (2015) result assuming ΛCDM is

$$\sigma_8 = 0.834 \pm 0.03 \tag{3.3.2}$$

Cluster abundance, along with X-ray mass-temperature relation, is another tool for estimating σ_8. In this case σ_8 is strongly degenerate with Ω_m but using also the cluster correlation function one can reduce the level of degeneracy and measure separately the two parameters. Clusters detected with the SZ effect by Planck can also give an estimate of σ_8 (see Fig. 3.3.1).

The variance σ_R increases with smaller scales R. The fact that $\sigma_8 \approx 1$ implies that fluctuations averaged over scales of 8 Mpc/h are already in the non-linear regime. As we will see later, linear approximations are valid on scales larger than roughly $R_{NL} = 60$Mpc/h, or $k_{NL} = 2\pi/R_{NL} \approx 0.1$h/Mpc.

3.4 The peculiar velocity field

The mass power spectrum can be studied also by analyzing the peculiar motion of the galaxies. It is intuitive, in fact, that a more clustered distribution of matter will induce stronger peculiar velocities. The importance of this is that the velocity field depends on the *total* mass distribution, including any unseen component. Let us start from the first of Eq. (1.1.29). In terms of the time t it becomes

$$a\frac{d\delta}{dt} = -ik^i v_i \tag{3.4.1}$$

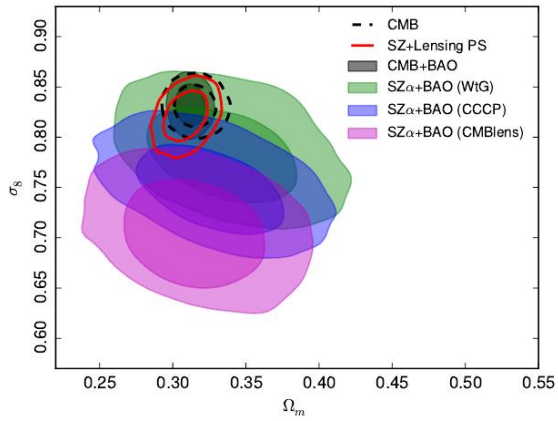

Figure 3.3.1: Planck (2015) constraints on Ω_m, σ_8 from SZ clusters and from CMB (Ade et al. A&A 594, A13, 2016; ESA and the Planck Collaboration).

Consider now the Euler Eq. (1.1.29) for $c_s = 0$:

$$\dot{v}^i = -\mathcal{H}v^i - a^2 ik^i \psi \tag{3.4.2}$$

Expressing the velocity vector by a component parallel and a component orthogonal to the potential gradient (the peculiar acceleration), we see that the orthogonal component (subscript t) obeys the equation

$$\dot{v}_t^i = -\mathcal{H}v_t^i \tag{3.4.3}$$

so that it will decay as a^{-1}. Neglecting therefore this purely rotational component, we can look for solutions of (3.4.1) in the form $v^i = F(k)k^i$. This gives immediately from (3.4.1) the relation between the peculiar velocity field and the density fluctuations in linear perturbation theory, in the Newtonian regime:

$$v^i = iHa\delta f \frac{k^i}{k^2} \tag{3.4.4}$$

where

$$f = \frac{a}{\delta}\frac{d\delta}{da} \tag{3.4.5}$$

is a function that expresses the growth rate of the fluctuations; for a flat universe in MDE we have seen that $\delta \sim a$ and $f = 1$. A good approximation for a model with matter parameter $\Omega_m(t)$, as we have seen in Sec. 1.4 , is

$$f = \Omega_m^\gamma \tag{3.4.6}$$

with $\gamma \approx 0.55$ and, for ΛCDM,

$$\Omega_m(z) = \frac{\Omega_{m0}(1+z)^3}{\Omega_{m0}(1+z)^3 + 1 - \Omega_{m0}} \tag{3.4.7}$$

The peculiar velocity at location x is

$$\mathbf{v}(x) = i\mathcal{H}f\frac{V}{(2\pi)^3}\int \delta_k \frac{\mathbf{k}}{k^2} e^{ikr} d^3k \tag{3.4.8}$$

and the average in a volume of radius R is

$$\mathbf{v}_R = \frac{1}{V_R}\int \mathbf{v} d^3r = i\mathcal{H}f\frac{V}{(2\pi)^3 V_R}\int \delta_k \frac{\mathbf{k}}{k^2} e^{ikr} W(r) d^3k d^3r = i\mathcal{H}f\frac{V}{(2\pi)^3}\int \delta_k \frac{\mathbf{k}}{k^2} W(kR) d^3k \tag{3.4.9}$$

where $W(kR)$ is the Fourier transform of the *window function*, defined as

$$W(kR) = \frac{1}{V_R}\int W(x)e^{ikx}d^3x$$

Therefore, the average of the square of the velocity is

$$\begin{aligned}\langle v^2\rangle_R &= \mathcal{H}^2f^2\frac{V^2}{(2\pi)^6}\int\langle\delta_k\delta_{k'}\rangle\frac{\mathbf{k}}{k^2}\frac{\mathbf{k}'}{k'^2}W(k'R)W(kR)d^3kd^3k' &(3.4.10)\\ &= \frac{\mathcal{H}^2f^2}{(2\pi)^3}\int P(k)\delta_D(\mathbf{k}-\mathbf{k}')\frac{\mathbf{k}}{k^2}\frac{\mathbf{k}'}{k'^2}W(k'R)W(kR)d^3kd^3k' &(3.4.11)\\ &= \frac{\mathcal{H}^2f^2}{2\pi^2}\int P(k)W^2(kR)dk &(3.4.12)\end{aligned}$$

where in the last integral we integrated over the solid angle 4π and we used the definitions (see 2.5)

$$\begin{aligned}V\langle\delta_k\delta_{k'}\rangle &= \frac{(2\pi)^3}{V}P(k)\delta_D(\mathbf{k}-\mathbf{k}')\\ \int\delta_D(\mathbf{k}-\mathbf{k}')d^3k &= 1 &(3.4.13)\end{aligned}$$

The square root of $\langle v^2\rangle_R$ is called *bulk flow*, that is the magnitude of the peculiar flow on the scale R.

3.5 The redshift distortion

The galaxy distances we measure are mostly obtained through their redshift. The redshift however includes the peculiar velocity of the galaxies themselves, so that there is an error in the distances we assign to galaxies. On very small scales the peculiar velocity of a galaxy is more or less randomly oriented, so that the error in the distance is statistical, and can be taken into account along the experimental errors. On redshift maps, the small scale peculiar velocities cause the finger-of-god effect: galaxies in a cluster acquire an additional random redshift that distorts the cluster distribution, making it appear elongated along the line of sight.

On large scales, however, the galaxies tend to fall toward concentrations, so that the velocity field is coupled to the density field. This correction is systematic, and can be accounted for in the following way.

A source at distance r with peculiar velocity along the line of sight u

$$\mathbf{v}_p = \mathbf{v}\cdot\frac{\mathbf{r}}{r} \tag{3.5.1}$$

will be assigned a distance $s = r+u(r)-u(0)$ where $\mathbf{u}\equiv\mathbf{v}_p/\mathcal{H}$ has units of distance. Consider then a coordinate transformation from real space (subscript r) to redshift space (subscript s):

$$\mathbf{s} = \mathbf{r}\left[1+\frac{u(r)-u(0)}{r}\right] \tag{3.5.2}$$

Then, if dV_s and dV_r are the volume elements in the two coordinates, we can write

$$n(r)dV_r = n(s)dV_s \tag{3.5.3}$$

where the volume element dV_s can be written in terms of the r coordinates as

$$dV_s = s^2dsd\cos\theta d\phi = r^2\left(1+\frac{\Delta u(r)}{r}\right)^2|J|drd\cos\theta d\phi = \left(1+\frac{\Delta u(r)}{r}\right)^2|J|dV_r \tag{3.5.4}$$

where the Jacobian is

$$|J| = |\frac{\partial s}{\partial r}| = 1+\frac{du}{dr} \tag{3.5.5}$$

Then we have that the density contrast in s-space is

$$\delta_s = \frac{n(s)dV_s}{n_0 dV_s} - 1 = \frac{n(r)dV_r}{n_0 dV_r \left(1 + \frac{\Delta \mathbf{u}(r)}{r}\right)^2 |J|} - 1 \tag{3.5.6}$$

where n_0 is the average density. To first order, this is

$$\begin{aligned} \delta_s &= \frac{n(r)}{n_0}(1 - 2\frac{\Delta u(r)}{r} - \frac{du}{dr}) - 1 \\ &= \left[\frac{n(r)}{n_0} - 1\right] - \frac{n(r)}{n_0}\left[2\frac{\Delta u(r)}{r} + \frac{du}{dr}\right] \\ &= \delta_r - 2\frac{\Delta u(r)}{r} - \frac{du}{dr} \end{aligned} \tag{3.5.7}$$

where in the last line we used the fact that to first order we can approximate $n(r)$ with n_0. Therefore, we see that the density contrast will be different in the two spaces. As a consequence, the correlation function and the power spectrum measured in redshift space will have to be corrected to be expressed in real space. To do so, we have to take the velocity field from the linear perturbation theory.

Eq. (3.4.8) is clearly in real space:

$$\mathbf{v} = \mathcal{H} f i \int \delta_k e^{i\mathbf{k}\cdot\mathbf{r}} \frac{\mathbf{k}}{k^2} d^3k^* \tag{3.5.8}$$

where, to simplify notation, the Fourier factor $V/(2\pi)^3$ is included in the differential d^3k^*. Its line-of-sight component is

$$u(r) = \mathcal{H}^{-1}\frac{\mathbf{r}}{r}\cdot\mathbf{v} = if\int \delta_k e^{i\mathbf{k}\cdot\mathbf{r}} \frac{\mathbf{kr}}{k^2 r} d^3k^* \tag{3.5.9}$$

while its derivative is (notice that $\mathbf{k}\cdot\mathbf{r}/(kr) = \mu$ does not depend on r)

$$\frac{du}{dr} = -f\int \delta_k e^{i\mathbf{k}\cdot\mathbf{r}} \left(\frac{\mathbf{kr}}{kr}\right)^2 d^3k^* \tag{3.5.10}$$

where we used the relation

$$\frac{d}{dr}e^{i\mathbf{k}\cdot\mathbf{r}} = i\frac{\mathbf{k}\cdot\mathbf{r}}{r}e^{i\mathbf{kr}} \tag{3.5.11}$$

Finally, we have

$$\delta_s = \delta_r - \frac{du}{dr} = \delta_r + f\int \delta_k e^{i\mathbf{kr}} \left(\frac{\mathbf{kr}}{kr}\right)^2 d^3k^* = \delta_r + f\int \delta_k e^{i\mathbf{kr}}\mu^2 d^3k^* \tag{3.5.12}$$

where $\mu = \mathbf{kr}/(kr)$ and we neglected the second term in (3.5.7) because it is negligible for large r. It is useful now to notice that the density fluctuation in the second term r.h.s. is the *mass* density fluctuation, responsible for the velocity field, while the other fluctuation terms can refer to the number density of any class of sources, e.g. galaxies. If the mass fluctuations are b times smaller that the galaxy fluctuations, we could write inside the integral at r.h.s. δ_k/b instead of δ_k. Then, the relation holds for any class of objects provided we use $\beta = f/b$ in place of f in the final result. The Fourier transform of this relation is

$$\delta_{sk} = \delta_{rk} + \beta\int \delta_{rk'} I(k,k') d^3k' \tag{3.5.13}$$

$$I(k,k') = (2\pi)^{-3}\int e^{i(k-k')r}\mu^2 d^3r \tag{3.5.14}$$

The redshift distortion then introduces a mode-mode coupling. This coupling can be broken if we can assume that the cosine

$$\mu = \frac{\mathbf{kr}}{kr} \tag{3.5.15}$$

varies much slower with r than the fast oscillating $e^{i(k-k')r}$ term, i.e. if the survey covers a small angular size and the direction of line-of-sight $\mathbf{r}/r$ is almost constant. In this case the μ^2 term goes out of the integral and we have then $I = \mu^2\delta_D(k-k')$, so finally

$$\delta_{sk} = \delta_{rk}(1+\beta\mu^2) \tag{3.5.16}$$

Notice that these are the three-dimensional Fourier coefficients. The power spectrum now is

$$P_s(k) = V\delta_{rk}^2(1+\beta\mu^2)^2 = P_r(k)(1+\beta\mu^2)^2 \tag{3.5.17}$$

If we average it over angles we get

$$P_s(k) = P_r(k)(1+2\beta\langle\mu^2\rangle+\beta^2\langle\mu^4\rangle) \tag{3.5.18}$$

where

$$\begin{aligned}\langle\mu^2\rangle &= \frac{1}{2}\int_{-1}^{1}\cos^2\theta' d\cos\theta' = 1/3\\ \langle\mu^4\rangle &= \frac{1}{2}\int\cos^4\theta' d\cos\theta' = 1/5\end{aligned} \tag{3.5.19}$$

Finally we obtain for the μ-averaged spectrum

$$P_s(k) = P_r(k)(1+2\beta/3+\beta^2/5) \tag{3.5.20}$$

The power spectrum is then boosted in redshift space, because the velocity field is directed toward mass concentrations: as a result, galaxies seem more concentrated when seen in redshift space.

At very small scales, on the other hand, the velocity orientation can be assumed to be random. The variance of $\mathbf{s}$ will be larger than the variance of $\mathbf{r}$ along the line of sight and unchanged across it: the sphere will appear pointing towards us. This is the non-linear redshift distortion, also called "fingers-of-God". The power spectrum is therefore decreased. Empirical studies have shown that a sufficiently good approximation is given by an exponential damping factor,

$$P_s(k,\mu) = P_r(k)(1+\beta\mu^2)^2 e^{-k^2\mu^2\sigma_v^2} \tag{3.5.21}$$

where σ_v is the cloud velocity dispersion along the line of sight in units of H_0; one has typically $\sigma_v \approx (300\text{km/sec})/H_0 \approx 3\text{Mpc}/h$. The exponential damping can be obtained also by considering a convolution of the correlation function with a Gaussian distribution for the redshift displacement with variance σ_v^2. An example of this procedure for a similar (but distinct) effect will be discussed in Sec. 3.8.

The final result taking into account redshift distortion (RSD), bias, growth $G(z)$ (see Eq. 1.4.3) and velocity dispersion is then rather simple:

$$P_s(k,\mu,z) = (1+\beta\mu^2)^2 b^2 G^2 P_r(k) e^{-k^2\mu^2\sigma_v^2} \tag{3.5.22}$$

where f, the growth rate and b, G all depend on z and perhaps on k, and $P_r(k)$ is today's matter power spectrum. By measuring the anisotropy combination

$$\sqrt{\frac{P_s(k,\mu=1,z)}{P_s(k,\mu=0,z)}} - 1 = \frac{f}{b} \tag{3.5.23}$$

we can then obtain information on the combination $\beta = f/b$. By measuring instead

$$\sqrt{\frac{P_s(k,1,z)-P_s(k,0,z)}{P_s(k,1,z')-P_s(k,0,z')}} = \frac{f(z)G(z)}{f(z')G(z')} \tag{3.5.24}$$

we obtain information on the combination

$$fG = \frac{\delta'}{\delta(0)} \tag{3.5.25}$$

Often the combination $f\sigma_8(z) \equiv f\sigma_8 G$ is said to be directly measurable via the redshift distortion, but this assumes one has a specific model for $P_r(k)$, e.g. ΛCDM.

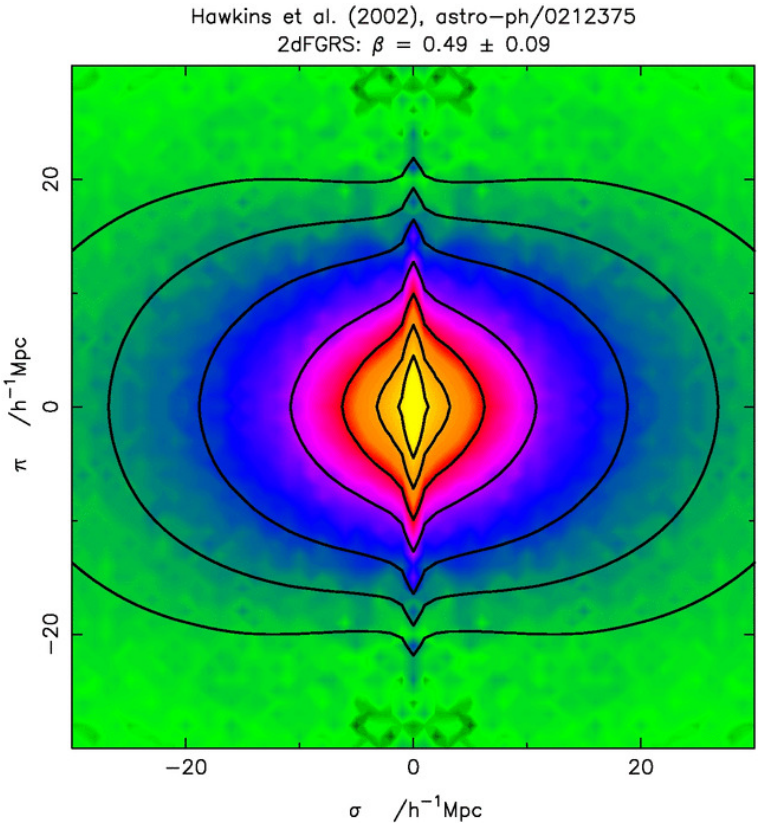

Figure 3.5.1: Correlation function versus radial (line of sight) and longitudinal (orthogonal to line of sight) coordinates π, σ, respectively. Notice the elongated "finger-of-God" feature along the radial coordinate and the squashed form along the longitudinal one (linear redshift distortion). (Hawkins et al. 2003MNRAS.346...78H).

3.6 Baryon acoustic oscillations

The spectrum of fluctuations at linear scales we observe today is a combination of the fluctuations in the dark matter and in the baryonic content. As we have seen in the CMB chapter, the baryonic component was tightly coupled to radiation before recombination and underwent Jeans oscillations on scales below the sound horizon, roughly 100 Mpc/h in comoving distance (i.e. the size they will have been expanded to by today). When the baryons finally decouple from radiation, the oscillations remain imprinted on their distribution and, in the linear regime, show up as an additional feature on the smooth power spectrum proportional to the amount of baryons, called *baryon acoustic oscillations* (BAO). Since the amount of baryons and radiation are well known, the BAO scale is essentially fixed: it constitutes then a *standard rod*.

In the correlation function, we expect therefore a local peak at roughly the same comoving scale

$$d_s^c = \frac{c_s}{c} d_H^c \approx 144\text{Mpc} \tag{3.6.1}$$

(as measured by Planck in 2015).

The correlation function is on average a isotropic function of distance. When plotted as a function of the distance along and across the line of sight the baryonic peak should then appear as a circular ring around the origin with radius d_s^c. The correlation function for galaxies in a shell around redshift z_1 is measured in redshift and angular space and the peak will therefore appear as a peak in the z, θ plane. The radius in the θ direction gives the comoving angular diameter distance $d_A^c = (1+z)d_A$ of that shell

$$d_A^c(z) = \theta d_s^c \tag{3.6.2}$$

By estimating the redshift difference Δz between the two opposite points in the ring one measures instead the difference of comoving distances along the line of sight:

$$\Delta d_A^c = \Delta r = \int_0^{z_1+\Delta z} \frac{dz}{H(z)} - \int_0^{z_1} \frac{dz}{H(z)} \approx \frac{\Delta z}{H(z)}|_{z_1} \tag{3.6.3}$$

In practice of course the entire ring is fitted by varying the cosmological parameters. Since there are two directions orthogonal to the line of sight and one along it, one can define a combined distance

$$D_V(z) \equiv [\frac{(d_A^c)^2}{H(z)} \Delta z]^{1/3} \tag{3.6.4}$$

and express the results in terms of D_V. Current measurements are however good enough to measure separately $d_A^c(z)$ and $1/H(z)$.

The peak in the correlation function manifests itself also in the power spectrum as the Fourier transform of a peak, namely oscillations at a wavenumber $k_{BAO} \approx 2\pi/d_A^c$ and multiples, appropriately called baryon acoustic oscillations (BAO), overimposed to the smooth spectrum, with an amplitude proportional to Ω_b.

The baryonic oscillations have been detected for the first time in 2005 with SDSS and 2dFGRS data, obtaining

$$\frac{r_s}{D_V(z=0.35)} \approx 0.1 \pm 0.003 \tag{3.6.5}$$

Subsequent analyses measured the BAO scale to a precision of 2-4%, with results always consistent with concordance cosmology.

To go below this precision one needs to take into account small effects that tend to "distort the ring" and smear out the oscillations: the redshift measurement error, the peculiar velocity redshift, the non-linear correction to the spectrum. Of course when estimating the cosmological parameters from the power spectrum the entire shape of the spectrum has to be taken into account, not just the BAO wiggles.

3.7 Alcock-Paczyński effect[a]

When we observe galaxies, we measures angles and redshifts, not real space distances. If we observe an angle θ subtending a transverse comoving scale λ_1 at z, then the angular diameter distance is $D_1(z) = \lambda_1/(1+z)\theta$

[a] Adapted from Amendola & Tsujikawa, *Dark Energy. Theory and Observations*, CUP 2010.

where the subscript 1 indicates a given cosmology, i.e. some values of $\Omega_m^{(0)}, \Omega_\Lambda^{(0)}$ etc. In a different cosmology (subscript 2), the relation will be $d_2(z) = \lambda_2/(1+z)\theta$, i.e. the scale has to change in order to keep the same subtending angle at the same redshift. It follows that for any cosmology the combination d/λ for each given angle is a constant. In Fourier space, the scale λ is converted into a mode k, so also the combination $k_\perp D$, where $k_\perp$ is the transverse wavenumber corresponding to that transverse scale, remains constant regardless of cosmology. Therefore, if we take a reference cosmology r, we have that for any other cosmology the *transverse* wavenumber is given by

$$k_\perp = k_{r\perp} D_r/D\,. \tag{3.7.1}$$

A similar argument can be applied to the comoving scale extending *along* the line of sight from z_1 to z_2. The scale is then $\lambda = dz/H(z)$ and in order for this scale to be seen at the same $dz = z_2 - z_1$ the product λH has to remain constant when changing cosmology. Therefore, along with (3.7.1), we have for radial modes

$$k_\parallel = k_{r\parallel} H/H_r\,. \tag{3.7.2}$$

Clearly, any wave vector $\boldsymbol{k}$ can be decomposed into $k_\parallel$ and $k_\perp$. The relations above apply therefore to any perturbation mode. Every mode $\boldsymbol{k}$ in the power spectrum can be written in terms of the reference mode $\boldsymbol{k}_r$ with an explicit dependence on the cosmological parameters inside d and H. We know then how the wavenumber changes with cosmology. This implies that if a power spectrum is isotropic for the reference cosmology, it will become anisotropic for any other cosmology, because $k_\parallel$ and $k_\perp$ change differently: this is called Alcock-Paczyński (AP) effect ([1, 2, 17]).

From the relations (3.7.1) and (3.7.2) we derive the relation between the wavenumber modulus k and the direction cosine $\mu = \boldsymbol{k}\cdot\boldsymbol{r}/k$ (here $\boldsymbol{r}$ is the unit vector parallel to the line of sight) in the reference cosmology and in the generic cosmology

$$k = (k_\parallel^2 + k_\perp^2)^{1/2} = \alpha k_r\,, \tag{3.7.3}$$

$$\mu = \frac{k_\parallel}{(k_\parallel^2 + k_\perp^2)^{1/2}} = \frac{H\mu_r}{H_r\alpha}\,, \tag{3.7.4}$$

where, putting $h = H/H_r$ and $d = D/D_r$

$$\alpha = \frac{\sqrt{\mu_r^2(h^2d^2 - 1) + 1)}}{d}\,. \tag{3.7.5}$$

Therefore the general expression for the theoretical power spectrum becomes

$$P_{gg} = P(\alpha k_r)(1 + f\mu_r^2\frac{h^2}{\alpha^2})^2 \tag{3.7.6}$$

Comparing with real data, the reference model should be the one provided by the observers. The factors α, h contains therefore additional dependence on cosmological parameters. Notice that the change in the angle μ only depends on the combination hd. If we do not know the shape of $P(k)$, at the linear level there is no way we can measure αk_r, but only the combination h/α which, as mentioned, depends only on hd. Often it is only this combination that is regarded as an AP effect.

Since the power spectrum is proportional to the volume V in which we measure the perturbations, we need to evaluate also how V depends on cosmology. If we measure the spectrum in a solid angle γ rad^2 and a shell of thickness dz, then the comoving volume is

$$V = \gamma^2 r^2 dr = \gamma^2 \frac{D^2}{(1+z)^2} r_{,z}(z) dz = \frac{D^2}{H}\frac{\gamma dz}{(1+z)^2}\,, \tag{3.7.7}$$

where $r_{,z} = dr/dz = 1/H(z)$. It follows that VH/D^2 is independent of cosmology and therefore

$$V = V_r \frac{H_r D^2}{H D_r^2} = V_r \frac{d^2}{h}\,. \tag{3.7.8}$$

The relations (3.7.3,3.7.4,3.7.8) above allow us to relate this reference power spectrum to a general power spectrum for any d, H, i.e. for any given cosmology. The theoretical power spectrum $P(k) = V\delta_k^2$ can then be compared to the real data spectrum by multiplying it by V_r/V :

$$P(k,z) = \frac{h}{d^2} P(\alpha k_r)(1 + f\mu_r^2\frac{h^2}{\alpha^2})^2\,. \tag{3.7.9}$$

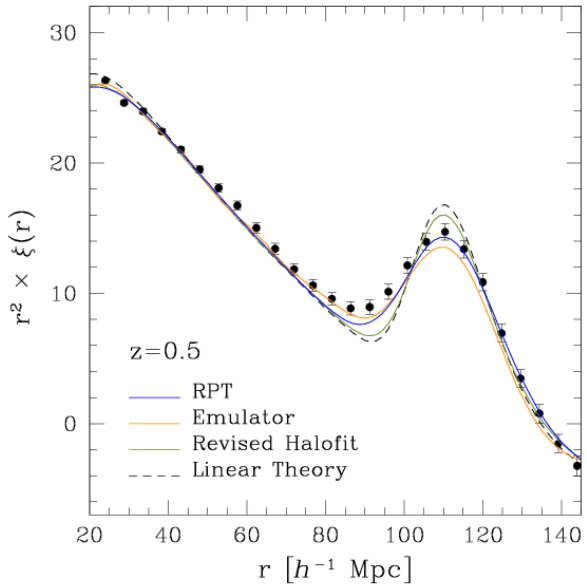

Figure 3.7.1: Baryon acoustic peak in a correlation function obtained from MICE, a very large N-body simulation. From Fosalba et al. MNRAS 448 (2015), 2987-3000 arXiv:1312.1707.

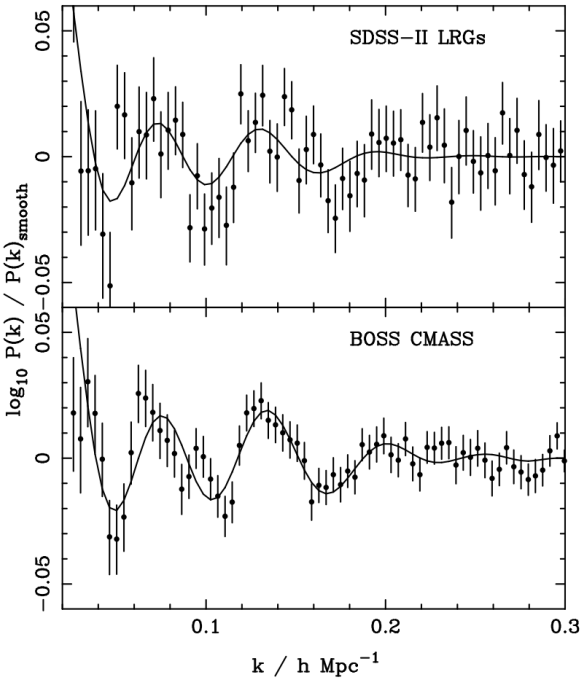

Figure 3.7.2: Baryon acoustic peak observed in the power spectrum of SDSS and BOSS galaxies. The smooth part of the spectrum has been subtracted. From Anderson et al. 2012, arXiv:1203.6594, Mon. Not. R. Astron. Soc. 427, 3435–3467 (2012).

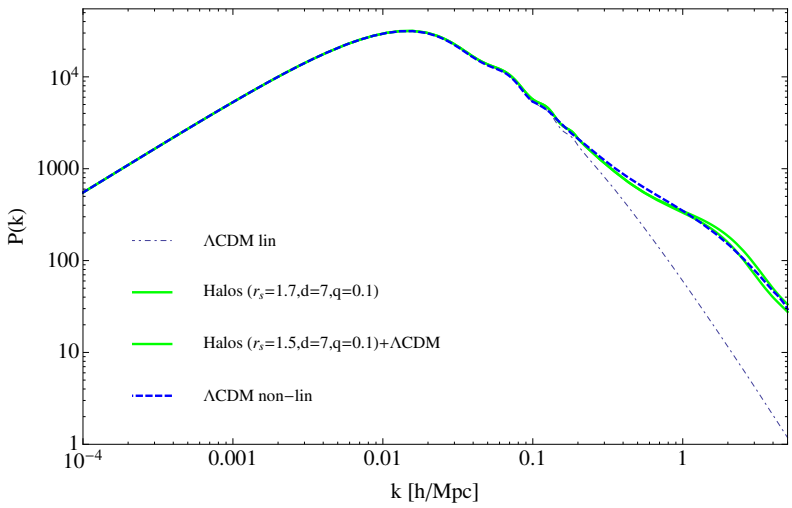

Figure 3.7.3: Matter power spectrum in linear ΛCDM (black dotted line) and including a simplified halo non-linear correction ($q = r_s/R$ and $n = d^3$, green lines), compared with a numerical non-linear spectrum (thick blue dashed line).

3.8 The BAO damping

The BAO peak is an importat probe of cosmology, and its precise estimation is therefore a crucial aspect of both theory and data analysis. In the previous section we estimated the BAO scale. That estimate, and every estimate based on numerically solving the pertrubation equations, was however an idealized one, because it assumed the galaxies did not move from their initial position so that the imprint from the baryon acoustic waves remained unchanged up to today. In reality, the initial scale imprinted on the matter distribution by the baryon-photon waves is in time slightly blurred by the random peculiar velocity of galaxies. Intuitively, one should expect therefore a damping of the BAO peaks, as we discuss below. I follow here the analysis of Ref. [10].

In order to estimate this effect, we begin by writing down the relative velocity between two galaxies (subscripts 1,2 respectively) at initial position $\mathbf{r}_1, \mathbf{r}_2$. The real-space peculiar velocity field is

$$\mathbf{v}(r) = \int \mathbf{v}_k e^{i\mathbf{kr}} \frac{d^3k}{(2\pi)^3} = i \int \dot{\delta}_k \frac{\mathbf{k}}{k^2} e^{i\mathbf{kr}} \frac{d^3k}{(2\pi)^3} \tag{3.8.1}$$

The displacement accumulated up to time t since decoupling is therefore

$$\mathbf{d}(r) = i \int \left[\int \dot{\delta}_k dt \right] \frac{\mathbf{k}}{k^2} e^{i\mathbf{kr}} \frac{d^3k}{(2\pi)^3} = iG(z) \int \delta_k \frac{\mathbf{k}}{k^2} e^{i\mathbf{kr}} \frac{d^3k}{(2\pi)^3} \tag{3.8.2}$$

where G is the growth function and δ_k the present value. Then we see that the relative displacement between the galaxies 1 and 2 is

$$\mathbf{d}_{12} = iG \int \delta_k \frac{\mathbf{k}}{k^2} [e^{i\mathbf{kr}_1} - e^{i\mathbf{kr}_2}] \frac{d^3k}{(2\pi)^3} \tag{3.8.3}$$

and

$$d_{\parallel} \equiv \mathbf{d}_{12} \cdot \frac{\mathbf{r}_{12}}{r_{12}} = iG \int \delta_k \frac{\mathbf{kr}_{12}}{k^2 r_{12}} [e^{i\mathbf{kr}_1} - e^{i\mathbf{kr}_2}] \frac{d^3k}{(2\pi)^3} \tag{3.8.4}$$

its component along the separation $\mathbf{r}_{12}$. We take as separation the scale of the BAO peak, roughly 100 Mpc/h.

The mean of the displacement vector is of course zero. The variance of the parallel displacement is

$$\langle d_\parallel d_\parallel^* \rangle = G^2 \int P(k) \left(\frac{\mathbf{k}\mathbf{r}_{12}}{k^2 r_{12}} \right)^2 \left| e^{i\mathbf{k}\mathbf{r}_{12}} - 1 \right|^2 \frac{d^3k}{(2\pi)^3} \tag{3.8.5}$$

$$= 4\pi r_{12}^2 G^2 \int P(k) W_\parallel(kr_{12}) k^2 dk \equiv s_0^2 G^2 \tag{3.8.6}$$

(there is a typo in the original expression in [10]) where we implicitly defined the total displacement today as s_0 and

$$W_\parallel(x) = \frac{2}{x^2} \left(\frac{1}{3} - \frac{\sin x}{x} - 2\frac{\cos x}{x^2} + 2\frac{\sin x}{x^3} \right) \tag{3.8.7}$$

Similarly, the displacement along the direction transverse to $\mathbf{r}_{12}$ is the same but with

$$W_\perp(x) = \frac{2}{x^2} \left(\frac{1}{3} - \frac{\sin x}{x} + \frac{\cos x}{x^2} \right) \tag{3.8.8}$$

Let us consider now the displacement of the field $d_\parallel$ parallel and transverse to the line of sight. The displacement $d_\perp$ plays a minor role since the BAO scale is affected mostly by the change in the distance of the galaxies along their separation vector. Taking into account the RSD factor $(1 + f\mu^2)$ in the power spectrum for $\mu = 0$ and $\mu = 1$, we can write therefore the r.m.s. of the displacement at any given epoch as

$$\sigma_\parallel = s_0 G(1 + f) \tag{3.8.9}$$

$$\sigma_\perp = s_0 G \tag{3.8.10}$$

where s_0 is defined above, or can be calibrated in N-body simulations; it turns out to be around 12 Mpc/h for an initial separation of 100 Mpc/h similar to the BAO scale. Therefore, the original imperturbed separation $\mathbf{r}$ between the galaxies is now moved to a new separation vector $\mathbf{y} = \mathbf{r} + \mathbf{s}$. Comparison with numerical simulation show that we can approximate the displacement distribution as a Gaussian $\Pi(\mathbf{s})$ with zero mean and standard deviation given by the σ's:

$$\Pi(\mathbf{s}) = N \exp(-\frac{1}{2}\frac{s_\parallel^2}{\sigma_\parallel^2} - \frac{1}{2}\frac{s_\perp^2}{\sigma_\perp^2}) \tag{3.8.11}$$

An imperturbed correlation function $\xi(\mathbf{r})$ will then be distorted by the convolution with the $\mathbf{s}$ field

$$\xi_s(\mathbf{r}) = \int \xi(\mathbf{r}) \Pi(\mathbf{y} - \mathbf{r}) d^3y \tag{3.8.12}$$

A convolution in real space means a product of the Fourier transformed ξ, Π in Fourier space. Therefore the unperturbed linear power spectrum P_0 becomes

$$P_s(k) = P_0(k) \exp(-\frac{1}{2}k_\parallel^2\sigma_\parallel^2 - \frac{1}{2}k_\perp^2\sigma_\perp^2) = P_0(k) e^{-k^2\sigma^2} \tag{3.8.13}$$

(there is a typo in the original expression in [10]) where, putting $k_\parallel = k\mu$ and $k_\perp^2 = k^2 - k_\parallel^2$, and $s = s_0 G/\sqrt{2}$,

$$\sigma^2 = \left[1 + f\mu^2(2 + f)\right] s^2 \tag{3.8.14}$$

This damping is similar to the FoG damping of Eq. (3.5.21). However, we are not discussing here a change in redshift space due to the peculiar velocity, but a real change in location in real space. This change in location affects only the BAO peaks, and not the smooth part of the spectrum. Therefore one should decompose the spectrum into a smooth no-wiggle component P_{nw} and a purely wiggly part P_w, and apply the BAO damping only to the latter part. In summary, the theoretical spectrum including the damping should be evaluated as

$$P_d = P_{nw} + P_w e^{-k^2\sigma^2} \tag{3.8.15}$$

The smooth spectrum for a given cosmology is usually estimated by either running a code with the same parameters as the full spectrum (without BAO damping) P but no baryons, or by using some approximate fitting function, while P_w is obtained by $P_w = P - P_{nw}$.

A more refined model for the BAO damping has been derived in Ref. [13] by a full consideration of the small-scale non-linear displacement on the BAO scale (a technique called *IR resummation*). The result is

$$P = P_{nw} + P_w e^{-k^2 \Sigma^2_{\rm tot}(\mu, k_s)} \tag{3.8.16}$$

where

$$\Sigma^2_{tot} = (1 + f\mu^2(2 + f))s^2 + f^2\mu^2(\mu^2 - 1)\delta s^2 \tag{3.8.17}$$

$$s^2 = \frac{4\pi}{3} \int_0^{k_s} P_{nw}(k)[1 - j_0(\frac{k}{k_{\rm osc}}) + 2j_2(\frac{k}{k_{\rm osc}})]dk \tag{3.8.18}$$

$$\delta s^2 = 4\pi \int_0^{k_s} P_{nw}(k) j_2(\frac{k}{k_{\rm osc}})dk \tag{3.8.19}$$

with $j_i(x)$ the spherical Bessel functions, $k_{osc} = 1/110\ h/\text{Mpc}$ the scale of the BAO oscillation, and k_s a scale of separation of long and short modes that needs to be calibrated in N-body simulations. A value $k_s = 0.2h/\text{Mpc}$ has been suggested. The expression for s coincides with $s = s_0 G/\sqrt{2}$ when s_0 is given in Eq. (3.8.6), except that here the integral extends only up to k_s, rather than infinity. The difference is however small in ΛCDM because the integral converges to a constant value for $k \gtrsim 0.2h/\text{Mpc}$. The correction proportional to δs^2 is negative and quite subdominant.

Chapter 4

Non-linear perturbations: simplified approaches

Quick summary

- Strongly non-linear fluctuations are difficult to handle and normally one has to employ powerful numerical simulations
- We first introduce a simple correction which gives a qualitative idea of the non-linear effects
- We then introduce the Zel'dovich approximation, which allows to follow in an almost analytical way the initial stages of structure formation beyond linearity
- Some more analytical results can be obtained assuming a spherical collapse. On scales of galaxies and clusters, Newtonian physics is sufficient
- Spherical collapse gives a simple but surprisingly accurate expression for the density of collapse and of virialization
- Using the so-called Press-Schechter formalism, one can approximately predict the number density of collapsed object as a function of their mass, to be compared to real data or simulations
- In this entire chapter we can safey use Newtonian gravity since we deal with scales well smaller than the horizon.

4.1 A first glimpse of non-linear corrections

All we have seen so far is only valid at linear scales where $\delta_m \ll 1$, i.e. at scales larger than 10 Mpc or so (so in fact the k^{-3} slope is never exactly reached). To measure smaller scales one has two ways: either estimate the spectrum at high redshift or find the non-linear correction.

At redshift zero the ΛCDM spectrum normalization σ equals 0.8 when averaged over spherical cells of radius $R \approx 8$ Mpc$/h$. At higher redshifts the value of σ_8 decreases proportionally to the growth function G. Since $f = d\log G/d\log a$, and putting $f \approx \Omega_m(a)^\gamma$one has $\sigma_8(z) = G(z)\sigma_8(0)$ where

$$G(z) = \exp\int_1^a f(a')\frac{da'}{a'} = \exp\int_1^a \Omega_m^\gamma(a')\frac{da'}{a'} \tag{4.1.1}$$

For instance, assuming $\Omega_{m0} = 0.3$, one has $\sigma_8(1) \approx 0.6$ and $\sigma_8(3) \approx 0.3$, and therefore the scale of non-linearity moves to smaller and smaller scales. Intergalactic lumps of neutral hydrogen called Lyman$-\alpha$ clouds along the line of sight of distant quasars absorb part of the quasar radiation and due to different redshifts appear as a "forest" of Lyman$-\alpha$ lines on the quasar's spectrum. Their power spectrum can be calculated up to redshifts of

order 4 or even more and provide a window on the linear high$-k$ tail that is otherwise hidden in non-linearities for nearby galaxies.

On smaller scales one should consider non-linear corrections that generally push the power up by even one order of magnitude. One rough way of estimating the non-linear correction is to imagine that at small scales the universe can be seen as a random collection of identical spherical halos with, for instance, the Navarro-Frenk-White (NFW) profile

$$\rho_{NFW} = \frac{\rho_0}{\frac{r}{r_s}(1+\frac{r}{r_s})^2} \tag{4.1.2}$$

where r_s is a free scale parameter that has to be fit to each halo. This functional form has been found to be a very good fit to the profiles in N-body simulations. Then one should evaluate the Fourier transform of a single halo density contrast in a radius R and volume $V = 4\pi R^3/3$,

$$\delta_1 = \frac{4\pi}{V}\int_0^R \left(\frac{\rho_{NFW}}{\bar{\rho}} - 1\right)\frac{\sin(kr)}{(kr)} r^2 dr \tag{4.1.3}$$

$$= \frac{1}{V}[\frac{4\pi}{\bar{\rho}}\int_0^R \rho_{NFW}\frac{\sin(kr)}{(kr)} r^2 dr - \frac{4\pi}{\bar{\rho}}\int_0^R \frac{\sin(kr)}{(kr)} r^2 dr] \tag{4.1.4}$$

$$= \frac{1}{V}(W_{NFW} - W_{TH}) \tag{4.1.5}$$

where $\bar{\rho}$ is the average density

$$\bar{\rho} = \frac{4\pi}{V}\int_0^R \rho_{NFW} r^2 dr \tag{4.1.6}$$

and then obtain the halo power spectrum as the sum of many random (uncorrelated) halos

$$P_h(n, R, r_s) = NV\delta_1^2 = n(W_{NFW} - W_{TH})^2 \tag{4.1.7}$$

where n is the halo number density. This can be considered a correction to be added to the linear spectrum

$$P_{NL} = P_{LIN} + P_h \tag{4.1.8}$$

Some results for P_{NL} are in Fig. (3.7.3). This particular halo correction is very naive and depends on three free parameters r_s, R, n. It can be however considerably improved by taking realistic distributions of the three parameters (see e.g. [16, 19]) and shown to be a very simple and relatively accurate description for standard cosmologies up to $k \approx 1h$/Mpc, requiring however extensive calibration with N-body simulations of many free parameters. In fact, it is still often employed to get a quick approximation under the name of *Halofit* (see App. C of [19] for a detailed implementation).

Better and more general non-linear schemes are based on fitting N-body simulations or on higher-order perturbation theory. We discuss them in the next sections.

4.2 The Zel'dovich approximation

So far we have only investigated linear perturbations, except for a brief comment on Sect. **??**. Stars, galaxies and clusters, however, are certainly not linear objects. For instance, the density contrast of a typical cluster of galaxies can be $\delta > 200$. Going from the linear treatment to the non-linear one is however generally very difficult. Even if some important step forward can be achieved by going to higher order in perturbation theory, ultimately one needs large N-body simulations.

A popular way to make progress in non-linear evolution before ressorting to numerical methods is to adopt the Zel'dovich approximation. The idea is to follow the movement of particles under the action of gravity until they hit each other and create a (fomally) infinite density. This should approximate the behavior of particles in a N-body simulation at least at some early time. Consider two sets of *comoving* coordinates. One, x_0, represents the coordinates of particles in an unperturbed Universe. Since they are comoving, they do not depend on time.

The other, $\mathbf{x}(t)$, is a perturbed one. Initially, we perturb the position of each particle by a vector field $\mathbf{s}$, called displacement. Then we assume that at some later time t the position of the particles is given by

$$\mathbf{x}(t) = \mathbf{x}_0 + g(t)\mathbf{s}(\mathbf{x}_0) \tag{4.2.1}$$

This means we assume the position at time t only depends on the initial displacement through a time (and not space) dependent function, still to be defined. The density of the particle at any given time is $\rho(x,t)$ in the perturbed Universe and $\rho_0(t)$ in the unperturbed one (which just follow the cosmic expansion, $\rho_0 \sim a^{-3}$). Since the particle number density $dn = \rho dV$ must be conserved, we have

$$\rho(x,t)d^3x = \rho_0(t)d^3x_0 \tag{4.2.2}$$

which implies

$$\rho(x,t) = \rho_0(t)\left|\frac{\partial \mathbf{x}}{\partial \mathbf{x}_0}\right|^{-1} \tag{4.2.3}$$

Let us assume now, without loss of generality, that the coordinates have been chosen along the direction of the eigenvectors of the deformation tensor

$$d_{ij} \equiv -\frac{\partial s_i}{\partial x_{0,j}} \tag{4.2.4}$$

In this case d_{ij} is diagonal and therefore

$$\left|\frac{\partial \mathbf{x}}{\partial \mathbf{x}_0}\right| = \left|I + g(t)\frac{\partial \mathbf{s}(\mathbf{x}_0)}{\partial \mathbf{x}_0}\right| = |\delta_{ij} - g(t)d_{ij}| = (1-g\lambda_1)(1-g\lambda_2)(1-g\lambda_3) \tag{4.2.5}$$

where I and δ_{ij} represent the identity matrix and λ_i are the three eigenvalues of d_{ij} (we show below that the eigenvalues are real). This means

$$\rho(x,t) = \frac{\rho_0(t)}{(1-g\lambda_1)(1-g\lambda_2)(1-g\lambda_3)} \tag{4.2.6}$$

Before we comment on this important expression, let us understand the meaning of g and s. Expanding (4.2.6) for small $g\lambda_i$, we find

$$\rho(x,t) \approx \rho_0(t)(1 + g(t)(\lambda_1+\lambda_2+\lambda_3) = \rho_0(t)(1 + g(t)\mathrm{Tr}(d_{ij})) \tag{4.2.7}$$

and therefore

$$\delta(t) \equiv \frac{\rho(x,t)-\rho_0(t)}{\rho_0(t)} = -g(t)\frac{\partial s_i}{\partial x_{0,i}} = -g(t)\nabla_{x_0}\mathbf{s}(x_0) \tag{4.2.8}$$

This expression, being a linearized one, must coincide with the growth law, $\delta(t) = G(t)\delta_0$, where $G(t)$ is the growth function we have evaluated for various cases in Chap. (1). Then we see that we should identify $g(t)$ with $G(t)$ and

$$-\nabla_{x_0}\mathbf{s}(x_0) = \delta_0 \tag{4.2.9}$$

Now, from the Poisson equation and the Friedmann equation we have

$$\nabla^2\Psi = 4\pi\rho_m\delta = \frac{3}{2}a^2H^2\Omega_m G(t)\delta_0 \tag{4.2.10}$$

where the factor a^2 arises because we are adopting comoving, rather than physical, coordinates. Then we see that

$$\delta_0 = \frac{2}{3a^2H^2\Omega_m G}\nabla^2\Psi \tag{4.2.11}$$

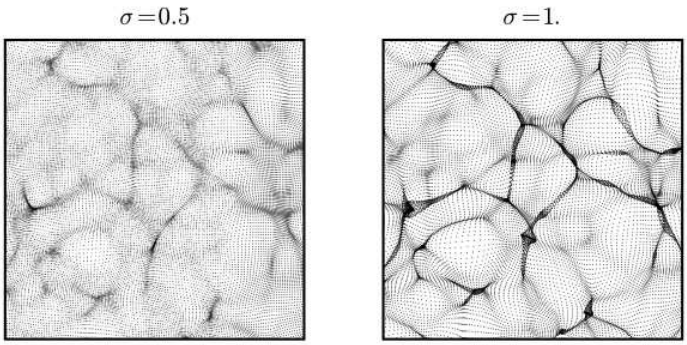

Figure 4.2.1: Formation of pancakes in a simulation based on the Zel'dovich approximation (from S. Shandarin, arXiv:0912.4520).

and therefore

$$\mathbf{s}(x_0) = -\frac{2}{3a^2H^2\Omega_m G}\nabla\Psi \tag{4.2.12}$$

With this identification of $\mathbf{s}$, the deformation tensor d_{ij} is symmetric and therefore its three eigenvalues are real. Therefore, we have completely specified the prescription (4.2.1): $g(t)$ is the growth factor, and the initial displacement field $\mathbf{s}$ is essentially the gradient of the gravitational potential, i.e. the force acting on the particles. In this way, one can run a very cheap N-body simulation: first, take the *linear* power spectrum at some early epoch for the model you want to simulate; second, convert the power spectrum for δ into a power spectrum for Ψ using Poisson equation in Fourier space; third, create a real space realization of this spectrum by overimposing sinusoidal oscillations with amplitude given by the spectrum and random phases; fourth, put particles on a regular grid; fifth, evaluate the displacement field by evaluating at every grid point (4.2.12); finally, move the particles out of their initial grid point by using (4.2.1).

To appreciate strenghts and limits of this technique, let us now come back to Eq. (4.2.6). Since $g(t)$ is a growing function (we discard the decaying mode, if any), $\rho(x,t)$ will develop a singularity as soon as one the largest λ_i is positive. This means that the particle will move primarily along the eigenvector associate to $\max\lambda_i$ and form regions of high density on the plane orthogonal to this direction: in other words, particle will tend to form planar structures, called pancakes (or *blinis* in the original Russian) by Zel'dovich, clearly visible in Fig. (4.2.1). After this singularity, the approximation will no longer be valid. In reality, is already quite surprising that the prescription (4.2.1) holds quite well beyond the linear regime!

Once the pancakes have been reached, one might assume that the particles "stick" onto, or oscillate around, the planar regions by friction or some hydrodynamic mechanism, and then continue flowing along the planes reaching the edges (called filaments) and finally slide along the filaments towards halos where, in turn, galaxies and clusters will form. This is indeed qualitatively what is seen in full N-body simulations. Most of the current codes actually exploit the Zel'dovich approximation to speed up the calculations during the earliest stages at $z \gg 1$.

Much more on this topic in [12].

4.3 Spherical collapse[a]

After the formation of pancakes, the Zel'dovich approximation is no longer viable, although it can be extended through second-order schemes or *ad hoc* prescriptions. There is however a way to get, on a first approximation which however turns out to be surprisingly accurate, an estimate of an important observable, namely how many objects form (i.e., collapse into a virialized structure) for a given mass. This approximation relies on sphericality and Gaussianity. The idea is first to find the value of the density contrast in the linear approximation at which a spherical perturbation collapse and virializes and then, find the fraction of the Gaussian distribution of

[a]Adapted from Amendola & Tsujikawa, *Dark Energy. Theory and Observations*, CUP 2010.

perturbations that are above this δ collapse value. This fraction corresponds to the fraction of perturbations that form structures for a given mass.

For scales at which Newtonian thery applies, a shell of matter at distance R from the center of a spherical overdensity with uniform density ρ moves according to the Newtonian force law

$$\frac{\mathrm{d}^2R}{\mathrm{d}t^2} = -\frac{GM(R)}{R^2} = -\frac{4}{3}\pi G\rho R\,, \tag{4.3.1}$$

where $M(R) = 4\pi\rho R^3/3$ is the *constant* mass inside the shell. Since for pressureless matter the background density scales as $\rho_0 = (3M(R_0)/4\pi)(R_0a(t))^{-3}$, where R_0 is the initial size of the perturbation, we can define the density contrast as

$$\delta = \left(\frac{a(t)R_0}{R}\right)^3 - 1\,, \tag{4.3.2}$$

inside the shell and $\delta = 0$ outside. The crucial assumption here is that δ is a step, or *top-hat*, function, which allows in fact to cancel all spatial derivatives. Replacing R with δ, the equation for δ in our time variable N is then:

$$\delta'' + \left(1 + \frac{\mathcal{H}'}{\mathcal{H}}\right)\delta' - \frac{3}{2}\Omega_m\delta = \frac{4}{3}\frac{\delta'^2}{1+\delta} + \frac{3}{2}\Omega_m\delta^2\,. \tag{4.3.3}$$

Multyiplying Eq. (4.3.1) on both sides by $2\mathrm{d}R/\mathrm{d}t$ the equation can be integrated once as

$$\left(\frac{\mathrm{d}R}{\mathrm{d}t}\right)^2 = \frac{2GM}{R} - C\,, \tag{4.3.4}$$

where C is an integration constant. This is the cycloid equation, whose solution for $C > 0$ can be given parametrically as $R = GM(1-\cos\tau)/C$ and $t = GM(\tau - \sin\tau)/C^{3/2}$ where $\tau \in (0, 2\pi)$. Substituting in δ and putting $a(t) = a_0(t/t_0)^{2/3}$ we obtain in the Einstein-de Sitter case:

$$\delta = \frac{9}{2}\frac{(\tau-\sin\tau)^2}{(1-\cos\tau)^3} - 1\,, \tag{4.3.5}$$

$$\delta_L = \frac{3}{5}\left[\frac{3}{4}(\tau-\sin\tau)\right]^{2/3}\,, \tag{4.3.6}$$

where δ_L (> 0) is the solution of the linearized equation, i.e. the left-hand-side of Eq. (4.3.3). Note that $\delta(\tau = 0) = 0$. It is convenient to use δ_L as a bookkeeping device: we express the behavior of δ as a function of δ_L instead of the parameter τ. A similar solution exists for an underdensity $\delta_L < 0$. We have assumed a constant mass $M(R)$: this implies that our analysis is valid only until shell-crossing occurs. As one expects, the radius R first increases (a small perturbation expands with the cosmological expansion), reaches a turnaround point and then decreases to zero (the perturbation collapses under its own gravity). The final singular phase is of course unphysical because the dust assumption will fail at some high density, non-radial fluctuations will develop and even the dark matter collisionless component will undergo the so-called "violent relaxation" mechanism and will set into virial equilibrium.

The main result we get from this model is the *critical* or *collapse* value $\delta_{\rm coll}$ of the *linear* fluctuation δ_L that is reached at the time of collapse. This quantity is of cosmological relevance because it is used in the Press-Schechter theory as a first approximation to the epoch of galaxy formation and to calculate the abundance of collapsed objects, as we will discuss below. It can be seen from Eq. (4.3.6) that when $\tau = 0$ the perturbations are zero, then δ reaches a turnaround at $\tau = \pi$ (for which $\delta_T \equiv \delta(\pi) = (3\pi/4)^2 - 1 \approx 4.6$ and $\delta_L \approx 1.063$) and finally for $\tau = 2\pi$ the overdensity δ (but of course not δ_L) becomes singular. This singularity occurs when

$$\delta_L = \delta_{\rm coll} = (3/5)(3\pi/2)^{2/3} \approx 1.686\,, \tag{4.3.7}$$

and it takes exactly twice as much time as for the turnaround. Notice that this value is independent of time: a spherical perturbation in the Einstein-de Sitter universe collapses to a singularity whenever the linear density

contrast equals 1.686. For other models, however, $\delta_{\rm coll}$ depends on time. An approximation for dark energy with constant $w_{\rm DE}$ in flat space is (Weinberg and Kamionkowski, MNRAS 341, 2003, 251)

$$\delta_{\rm coll}(z) = 1.686\,[1+\alpha(w_{\rm DE})\log_{10}\Omega_m(z)]\,, \tag{4.3.8}$$
$$\alpha(w_{\rm DE}) = 0.353w_{\rm DE}^4 + 1.044w_{\rm DE}^3 + 1.128w_{\rm DE}^2 + 0.555w_{\rm DE} + 0.131\,. \tag{4.3.9}$$

One can define other phenomenologically interesting epochs that are sometimes used: the epoch of non-linearity ($\delta = 1$, corresponding to $\delta_L \approx 0.57$) and the epoch of *expected* virialization. The latter is *defined* to correspond to the instant in which the kinetic energy K is related to the gravitational potential energy U by the condition

$$K = \frac{R}{2}\frac{\partial U}{\partial R}\,. \tag{4.3.10}$$

However, it is by no means obvious that this condition is enough to realize virialization, especially when dark energy is present. For an inverse-power potential ($U \propto -1/R$), the virialization implies $K = -U/2$. The radius and the density of the perturbation at virialization can be calculated by assuming conservation of energy at turnaround (when the kinetic energy vanishes; subscript T) and at a virialization epoch t_V when the kinetic energy satisfies $K_V = -U_V/2$, i.e.

$$U_T = U_V + K_V = U_V/2\,. \tag{4.3.11}$$

Since for a uniform sphere $U = -3GM/5R$ (and remembering once again we are assuming $M =$ constant), we obtain the relation $R_V = R_T/2$. Hence the virialized radius is half the turnaround radius. The density inside this radius turns out to be $\delta_V \approx 178$ and the epoch of this occurrence is very close to the final collapse time. A numerical fit for $w_{\rm DE} =$ constant models in flat space gives (Weinberg and Kamionkowski, MNRAS 341, 2003, 251)

$$\delta_V \approx 178[1+b_1\theta^{b_2}(z)]\,, \tag{4.3.12}$$
$$\theta = \frac{1-\Omega_m(z)}{\Omega_m(z)}\,, \tag{4.3.13}$$
$$b_1 = 0.399 - 1.309(|w_{\rm DE}|^{0.426}-1)\,, \tag{4.3.14}$$
$$b_2 = 0.941 - 0.205(|w_{\rm DE}|^{0.938}-1)\,, \tag{4.3.15}$$

if z is the collapse redshift.

It is difficult to go much beyond this kind of phenomenological parametrization. A full understanding of non-linear physics in dark energy would require extensive N-body simulations coupled to lattice simulations of scalar fields, a technical feat which is still largely to be explored.

4.4 The mass function of collapsed objects[b]

The main reason why it is worthwhile to discuss the abstract phenomenon as a "spherical collapse" is that the critical value $\delta_{\rm coll}$ and the virial radius R_V (or rather the mass contained within that radius) enter the Press-Schecther (PS) formula for the abundance of virialized objects. The main idea behind the PS formula is that we can estimate the number of collapsed objects formed in a random Gaussian field by simply counting at any given time how many regions have an overdensity above the collapse threshold given by $\delta_{\rm coll}$.

Suppose at some redshift z we smooth a random Gaussian field of density fluctuations over cells of radius R, each containing on average the mass $M = 4\pi R^3\rho/3$ with $\rho(z)$ the background density. Since the smoothing is a linear operation, if the field is Gaussian then also the density contrast δ in the cells will be distributed as a Gaussian probability distribution function with variance $\sigma_M^2(z)$. Suppose that *all* the cells with $\delta > \delta_{\rm coll}$ undergo collapse and virialization. The fraction of collapsed regions (i.e. the fraction of space containing objects of mass *larger* than M) will be then

$$p(M,z)|_{\delta>\delta_{\rm coll}} = \frac{1}{\sigma_M(z)\sqrt{2\pi}}\int_{\delta_{\rm coll}}^{\infty}\exp\left(-\frac{\delta_M^2}{2\sigma_M^2(z)}\right)\,{\rm d}\delta_M = \frac{1}{2}\,{\rm erfc}\left(\frac{\delta_{\rm coll}}{\sqrt{2}\sigma_M(z)}\right)\,, \tag{4.4.1}$$

[b] Adapted from Amendola & Tsujikawa, *Dark Energy. Theory and Observations*, CUP 2010.

where erfc(x) is the error function. The fraction containing objects of mass within the range $[M, M + \mathrm{d}M]$ is given by

$$\mathrm{d}p(M,z) = \left| \frac{\partial p(M,z)|_{\delta>\delta_{\rm coll}}}{\partial M} \right| \mathrm{d}M \,. \tag{4.4.2}$$

Remember that in general the threshold $\delta_{\rm coll}$ depends on z. Although the boxes with $\delta > \delta_{\rm coll}$ are certainly not in the linear regime, the idea is to use the linear regime to estimate the fraction of collapsed regions. We are then implicitly assuming that the variance $\sigma_M(z)$ is in the linear regime ($\sigma_M \ll 1$) and therefore that it can be calculated from Eq. (2.6.6) with the linear spectrum at any redshift. By using the growth function $D(z)$ we have $\sigma_M(z) = D(z)\sigma_M(0)$.

Now, suppose in a volume V we find N collapsed objects, each occupying a volume $V_M = M/\rho$. Then by definition the volume occupied collectively by the N objects is the fraction $\mathrm{d}p$ of V, i.e.

$$NV_M = V\mathrm{d}p \,, \tag{4.4.3}$$

and therefore the number density $\mathrm{d}n$ of collapsed halos with mass in the $\mathrm{d}M$ range (the *mass function*) will be

$$\mathrm{d}n = \frac{N}{V} = \frac{\mathrm{d}p}{V_M} = \frac{\rho}{M} \left| \frac{\partial p(M,z)|_{\delta>\delta_{\rm coll}}}{\partial M} \right| \mathrm{d}M = \sqrt{\frac{2}{\pi}} \frac{\rho}{M^2} \frac{\delta_{\rm coll}}{\sigma_M} \left| \frac{\mathrm{d}\,\ln\sigma_M}{\mathrm{d}\,\ln M} \right| e^{-\delta^2_{\rm coll}/(2\sigma^2_M)} \mathrm{d}M \,. \tag{4.4.4}$$

The extra factor of two that we have inserted in the last step is required because we want all the masses to end up in some object, so that we impose the condition

$$V \int_0^\infty \left(\frac{\mathrm{d}n}{\mathrm{d}M} \right) \mathrm{d}M = 1 \,. \tag{4.4.5}$$

This factor-of-2 adjustment can be justified with a random walk analysis of fluctuations. In any case, one finds it necessary to fit N-body simulations. Sometimes the number density $n(M,z)$ is taken to be the comoving number density (i.e. is multiplied by a^3): in this case also ρ should be identified with the comoving background density.

Equivalently, Eq. (4.4.4) is sometimes written as

$$\frac{M}{\rho} \left| \frac{\mathrm{d}n}{\mathrm{d}\,\ln\sigma_M} \right| = f(\sigma_M, z) \,, \tag{4.4.6}$$

where all the cosmological information is contained in the function

$$f(\sigma_M, z) = \sqrt{\frac{2}{\pi}} \frac{\delta_{\rm coll}}{\sigma_M} e^{-\delta^2_{\rm coll}/(2\sigma^2_M)} \,. \tag{4.4.7}$$

The number density $\mathrm{d}n(M,z)$ can then be "directly" confronted with the observed densities of objects (clusters, galaxies, quasars) at any redshift. The mass M is often taken to be the virial mass of that class of objects. Because of the exponential dependence on $\delta_{\rm coll}/\sigma_M$, the PS formula is quite sensitive to the cosmological model.

The simplicity of the PS approach must not hide the fact that it relies on a dangerous extrapolation of the linear theory, on the critical assumption of spherical collapse with top-hat filter, on a dubious definition of virialization, and on the absence of processes like merging, dissipation, shell crossing. Surprisingly, this shaky foundation did not prevent the PS formula to prove itself a valuable first approximation to the abundances obtained through numerical simulations. Not surprisingly, many works have been dedicated to improving the original PS formula by including corrections due to departure from sphericity or merging or by directly fitting to large N-body simulations. A remarkably successful fit is given by (Jenkins et al. MNRAS 321 (2001) 372)

$$f(\sigma_M, z) = 0.315 \exp(-|0.61 - \ \ln\sigma_M(z)|^{3.8}) \,. \tag{4.4.8}$$

This fit has been found to hold for a large range of masses, redshifts, and cosmological parameters, including dark energy with constant or varying $w_{\rm DE}$.

Chapter 5

Standard non-linear perturbation theory

In this chapter we introduce a systematic way to estimate the effect of non-linearities on the power spectrum. We work entirely in Newtonian gravity since we refer to scales much smaller than the horizon, and neglect radiation since we refer to the late-time universe. A useful review for this section is Bernardeau et al. 2002 [4]. For redshift distortions and biased tracers, I followed [18] **[7]** [11].

Quick summary

1. The Newtonian fluidodynamics equation are non-linear; this non-linearity is expected to be important at small scales (large k's)
2. In Fourier space, the non-linear terms becomes convolutions of the perturbation variables δ, θ, with some kernels
3. Finding the correct kernels is the main problem of non-linear perturbation theory
4. We derive here the standard perturbation theory (Eulerian SPT) kernels; they are analytical in the Einstein-deSitter (EdS) limit $\Omega_m = 1$, which however is a decent approximation also for ΛCDM and similar cosmologies
5. What we observe however are galaxies in redshift space, so the kernels must be improved to take this into account

5.1 Second-order perturbations

We now go back to the general non-linear Newtonian fluidodynamical equations

$$\dot{\rho} + \mathbf{v} \cdot \nabla \rho = -\rho \nabla \cdot \mathbf{v} \qquad \text{continuity} \tag{5.1.1}$$

$$\rho(\dot{\mathbf{v}} + \mathbf{v} \cdot \nabla \mathbf{v}) = -\nabla p - \rho \nabla \Phi \qquad \text{Euler} \tag{5.1.2}$$

$$\nabla^2 \Phi = 4\pi\rho \qquad \text{Poisson} \tag{5.1.3}$$

where the dot is here a derivative wrt cosmic time, $\mathbf{v} = \mathbf{v}_p + H\mathbf{x}$ is the total velocity, including the Hubble expansion $\mathbf{v}_H = H\mathbf{x}$, and $\mathbf{v}_p$ the peculiar velocity. We now perform the same steps as in Chap. 1 but keep the second-order terms. By introducing the density contrast $\delta = (\rho(x,t) - \rho_0(t))/\rho_0(t)$ the first one can be written as ($\dot{\rho} = (\dot{\rho_0 \delta}) + \dot{\rho}_0 = \dot{\rho_0}(1+\delta) + \rho_0 \dot{\delta}$)

$$\dot{\rho_0}(1+\delta) + \rho_0 \dot{\delta} + \rho_0 (\mathbf{v_p} + H\mathbf{x}) \cdot \nabla \delta = -\rho_0 (1+\delta)(\nabla \cdot \mathbf{v_p} + 3H) \tag{5.1.4}$$

Since at the background level $\dot{\rho}_0 + 3H\rho_0 = 0$, this becomes (we suppress the subscript p from now on)

$$\frac{d\delta}{dt} \equiv \dot{\delta} + H\mathbf{x} \cdot \nabla \delta = -\nabla \cdot (1+\delta)\mathbf{v} \tag{5.1.5}$$

On the rhs a nabla operator wrt physical coordinates $\mathbf{x} = a\mathbf{r}$, which becomes $a^{-1}\nabla_r$ converting to comoving coordinates. On the lhs, as already demonstrated,

$$\left(\frac{d\delta}{dt}\right)_x \equiv \dot{\delta} + \mathbf{v}_0 \cdot \nabla\delta = \left(\frac{\partial\delta}{\partial t}\right)_{\mathbf{r}} \tag{5.1.6}$$

Finally, therefore, the continuity equation is (dot is from now on the derivative wrt conformal time, so the a^{-1} factors cancel out)

$$\dot{\delta} = -\nabla(1+\delta)\mathbf{v} \tag{5.1.7}$$

where the nabla is now wrt comoving coordinates and we suppressed the subscript r.

The same steps as above lead to the following form of the Euler equation

$$\dot{\mathbf{v}} + \mathcal{H}\mathbf{v} = -\nabla(\mathbf{v}\cdot\nabla\mathbf{v}) - \nabla\phi \tag{5.1.8}$$

where$\mathcal{H} = aH$, ϕ is the cosmological potential defined in Eq. (1.2.13), and now $\mathbf{v}$ is the peculiar velocity. Taking the gradient and employing the Poisson equation for the cosmological potential ϕ, i.e. $\nabla^2\phi = 4\pi a^2\rho_0\delta$ (see Eq. 1.1.23), we obtain

$$\dot{\theta} + \mathcal{H}\theta + \frac{3}{2}\mathcal{H}^2\delta = -\nabla(\mathbf{v}\cdot\nabla\mathbf{v}) \tag{5.1.9}$$

where $\theta \equiv \nabla\mathbf{v}$, and we employed the Friedmann equation $3\mathcal{H}^2 = 8\pi a^2\rho_0$.

The two equations (5.1.7),(5.1.9) are the basic starting point for the non-linear perturbation theory. They can be combined into a single non-linear second order equation if we assume that $\mathbf{v}$ is irrotational also at second order, i.e. $\mathbf{v} = \nabla w$, where w is a velocity potential and of course $\theta = \nabla^2 w$. Let us first rewrite the equations using $N \equiv \log a$ as independent variable and redefining $\theta_{new} = \theta_{old}/\mathcal{H}$:

$$\frac{d\delta}{dN} \equiv \delta' + \mathbf{v}\nabla\delta = -(1+\delta)\theta \tag{5.1.10}$$

$$\theta' = -(1+\frac{\mathcal{H}'}{\mathcal{H}})\theta - \frac{3}{2}\delta - \nabla_i(v_j\nabla^j v^i) \tag{5.1.11}$$

The last term is

$$\nabla_i(v_j\nabla^j v^i) = \nabla_i\left[(\nabla_j w)\nabla^j\nabla^i w)\right] = (\nabla_i\nabla_j w)(\nabla^j\nabla^i w) + \left[(\nabla_j w)\nabla_i\nabla^j\nabla^i w\right] \tag{5.1.12}$$

$$= (\nabla_i\nabla_j w)(\nabla^j\nabla^i w) + \left[(\nabla_j w)\nabla^j\nabla^2 w)\right] = (\nabla_i\nabla_j w)^2 + v_i\nabla^i\theta \tag{5.1.13}$$

so

$$\frac{d\theta}{dN} \equiv \theta' + v_i\nabla^i\theta = -(1+\frac{\mathcal{H}'}{\mathcal{H}})\theta - \frac{3}{2}\delta - (\nabla_i\nabla_j w)^2 \tag{5.1.14}$$

5.2 Spherical collapse, again

We now solve the equations in a special case, the spherical collapse. That is, we study how the density contrast evolve when the dominant component of the velocity is purely radial, i.e. the non-linear collapse is approximately spherical. This gives an estimate of the growth in the non-linear regime.

Here and in the next section we will often refer to the Einstein-de Sitter (EdS) model due to its simplicity that allows for analytical solutions. This is a cosmological model with zero spatial curvature and only pressureless matter, so that $\Omega_m = 1$. Therefore, the Hubble expansion function as a function of redshift is simply $H = H_0(1+z)^{3/2}$. Moreover, the linear growth of perturbations if $\delta \sim a$ and therefore the rate is $f = 1$. Although today's best-fit model is considerably different, the EdS is a good approximation for the past history at redshifts higher that a few, and overall not a terrible approximation even today.

If the fluid moves spherically, one can write $\mathbf{v} = v\{1,1,1\}/\sqrt{3}$ and

$$(\nabla_i\nabla_j w)^2 = (\nabla_i v_j)(\nabla^i v^j) = \frac{1}{3}\theta^2 \tag{5.2.1}$$

so finally

$$\frac{d\theta}{dN} \equiv \theta' + v_i \nabla^i \theta = -(1 + \frac{\mathcal{H}'}{\mathcal{H}})\theta - \frac{3}{2}\delta - \frac{1}{3}\theta^2 \tag{5.2.2}$$

Now, differentiating (5.1.10) and inserting (5.2.2), and neglecting the gradient terms $\nabla\delta, \nabla\theta$ because near the center of a spherical perturbations they must indeed vanish, we obtain the same spherical collapse equation already encountered in Eq. (4.3.3):

$$\delta'' + \left(1 + \frac{\mathcal{H}'}{\mathcal{H}}\right)\delta' - \frac{3}{2}\Omega_m \delta = \frac{4}{3}\frac{\delta'^2}{1+\delta} + \frac{3}{2}\Omega_m \delta^2 \,. \tag{5.2.3}$$

where now δ depends only on time. In a Einstein-de Sitter (EdS) Universe in which $\Omega_m = 1$, one has $\frac{\mathcal{H}'}{\mathcal{H}} = -\frac{1}{2}$ and, as we know already, one finds at first order $G^{(1)} = G^{(1)\prime} = G^{(1)\prime\prime} = a$ and the growth function $f = 1$. At second order, we can neglect the denominator $1 + \delta$ at rhs, and write

$$\frac{4}{3}\frac{\delta'^2}{1+\delta} + \frac{3}{2}\Omega_m \delta^2 \approx \left(\frac{4}{3}f^2 + \frac{3}{2}\Omega_m\right)\delta^2 = \frac{17}{6}\delta^2 \tag{5.2.4}$$

We now expand $\delta = G^{(1)}\delta^{(1)} + G^{(2)}(\delta^{(1)})^2 + ...$ Therefore at second order we get in EdS

$$G^{(2)\prime\prime} + \frac{1}{2}G^{(2)\prime} - \frac{3}{2}G^{(2)} = \frac{17}{6}G^{(1)2} \,. \tag{5.2.5}$$

Under the Ansatz $G^{(2)} = \alpha G^{(1)2}$ we find

$$G^{(2)} = \frac{17}{21}G^{(1)2} \,. \tag{5.2.6}$$

One sees therefore that the second-order perturbations grow as $G^{(1)2}$ in a EdS model. Although this result has been derived in the spherical collapse case, in the following we will assume that the second order perturbations grow as $G^{(1)2}$ even outside this assumption. Later on we will write down the general equations for the second-order growth, and show that $G^{(1)2}$ is a good approximation.

5.3 Fourier space

We now consider in detail the *space* dependence of the second-order perturbations, in order to derive a correction to the power spectrum. This approach is called Eulerian perturbation theory (because the observer is supposed to stay at fixed coordinates), or simply standard perturbation theory (SPT). There are other approaches in literature, for instance Lagrangian Perturbation Theory, in which the main concept is to follow the particle's trajectories through the evolution of a displacement field, and Kinetic Field Theory [15], a non-perturbative approach in which the main idea is to build a partition function for the ensemble of particles. We will not discuss them here.

In the linear regime, Eq. (5.1.7) gives $\dot{\delta} = -\nabla\mathbf{v}$, which can be immediately Fourier-transformed as $\dot{\delta} = -i\mathbf{k}\mathbf{v} = -\theta$. Now we put $\dot{\delta} = \mathcal{H}\delta' = \mathcal{H}f\delta$, and notice that at the linear level the velocity vector $\mathbf{v}$ is sourced by the gravitational gradient, and therefore $\mathbf{v} \propto \mathbf{k}$ (provided the rotational part has decayed away). Then putting $\mathbf{v} = A\mathbf{k}$ we find

$$\mathbf{v} = i\mathcal{H}\delta_k f \frac{\mathbf{k}}{k^2} \tag{5.3.1}$$

where δ_k is the total matter field. This can also be written as

$$\mathbf{v} = -i\theta\frac{\mathbf{k}}{k^2} \tag{5.3.2}$$

so we can convert $\mathbf{v}, \delta, \theta$ at linear level one onto another. It is also to be noticed that the linear equation (1.3.2) can be written in general

$$f' + f^2 + Ff - S = 0 \tag{5.3.3}$$

introducing a "friction" coefficient $F = 1 + \mathcal{H}'/\mathcal{H} = \frac{1}{2}(1 - 3w_{DE}\Omega_{DE})$ and a "source" term $S = 3\Omega_m/2$.

Expanding in Fourier modes, we have $\delta(x) = (2\pi)^{-3}\int \delta_k e^{i\mathbf{kx}} d^3k$, and the analog for $\mathbf{v}$. The Fourier decomposition gives for Eq. (5.1.7)

$$\int \dot{\delta}_k e^{i\mathbf{kx}} \frac{d^3k}{(2\pi)^3} = -\nabla(1 + \int \delta_k e^{i\mathbf{kx}} \frac{d^3k}{(2\pi)^3})(\int \mathbf{v}_{k'} e^{i\mathbf{k'x}} \frac{d^3k'}{(2\pi)^3}) \tag{5.3.4}$$

or

$$\int \dot{\delta}_k e^{i\mathbf{kx}} \frac{d^3k}{(2\pi)^3} = -i\int \mathbf{v}_k \mathbf{k} e^{i\mathbf{kx}} d^3k - i\int \delta_k \mathbf{v}_{k'}(\mathbf{k}+\mathbf{k}') e^{i(\mathbf{k}+\mathbf{k}')\mathbf{x}} \frac{d^3k}{(2\pi)^3}\frac{d^3k'}{(2\pi)^3} \tag{5.3.5}$$

Integrating over $(2\pi)^{-3}e^{-i\mathbf{k''x}}d^3x$ one gets on the lhs

$$\int \frac{\dot{\delta}_k}{(2\pi)^3} e^{i(\mathbf{k}-\mathbf{k''})\mathbf{x}} \frac{d^3k}{(2\pi)^3} d^3x = \int \dot{\delta}_k \frac{d^3k}{(2\pi)^3}\delta_D(\mathbf{k}-\mathbf{k''}) = \frac{\dot{\delta}_{k''}}{(2\pi)^3} \tag{5.3.6}$$

and on the rhs

$$-\frac{i\mathbf{v}_{k''}\mathbf{k''}}{(2\pi)^3} - i\int \delta_k \mathbf{v}_{k'}(\mathbf{k}+\mathbf{k}')\delta_D(\mathbf{k}+\mathbf{k}'-\mathbf{k''})\frac{d^3k}{(2\pi)^3}\frac{d^3k'}{(2\pi)^3} \tag{5.3.7}$$

So we have (switching some k labeling)

$$\dot{\delta}_k + i\mathbf{v}_k\mathbf{k} = -i\int \delta_{k_1}\mathbf{v}_{k_2}(\mathbf{k}_1+\mathbf{k}_2)(2\pi)^3\delta_D(\mathbf{k}_1+\mathbf{k}_2-\mathbf{k})\frac{d^3k_1}{(2\pi)^3}\frac{d^3k_2}{(2\pi)^3} \tag{5.3.8}$$

We now expand the perturbation variables as

$$\delta = \varepsilon\delta^{(1)} + \varepsilon^2\delta^{(2)} + ... \tag{5.3.9}$$

and similarly for θ and $\mathbf{v}$, where the small parameter ε is temporarily inserted to keep track of the order. Inserting these expansions, one immediately sees that at order ε the $\delta^{(1)}, \theta^{(1)}$ cancel out since they obey the first order equation $\dot{\delta}^{(1)} = -\theta^{(1)}$. At order ε^2, the lhs remains formally the same (but now the quanities are second order), while at rhs we get products of first order terms, so we can use first order equations as e.g. $\delta_{k_1} = -i\mathbf{k}_1\mathbf{v}_1/(\mathcal{H}f) = -\theta/(\mathcal{H}f)$. In the following calculations we simplify the notation by defining $d^3k/(2\pi)^3 \to d^3k$, i.e. the factor of $(2\pi)^3$ will be understood, and put back at the very end. Then, using Eq. (5.3.2), at order ε^2 one has

$$\varepsilon^2\dot{\delta}^{(2)}_{\mathbf{k}} + \varepsilon^2\theta^{(2)}_{\mathbf{k}} = \varepsilon^2\mathcal{H}f\int \delta^{(1)}_{k_1}\delta^{(1)}_{k_2}\frac{\mathbf{k}_2}{k_2^2}\cdot(\mathbf{k}_1+\mathbf{k}_2)(2\pi)^3\delta_D(\mathbf{k}_1+\mathbf{k}_2-\mathbf{k})d^3k_1d^3k_2 \tag{5.3.10}$$

(Clearly, here and often below, we could immediately do one of the 3D integrals on the rhs thanks to the Dirac delta, but it is convenient to keep the expression in this more symmetric form.) The terms on the rhs couple different $\mathbf{k}$ modes, whereas they are uncoupled at the linear level. From now on, we delete the ε and also suppress the superscripts $(1), (2)$ when not needed, since it is clear that wherever there is a single perturbation variable, it has to be second order, and wherever there is a product of two perturbation variables, they have to be first order. Also, the perturbation variables at the lhs of the equations are understood to be functions of $\mathbf{k}$ and we suppress the subscript $\mathbf{k}$, so that $\delta_i \equiv \delta^{(1)}(\mathbf{k}_i)$.

As already seen, we define the linear growth factor G (dropping the superscript (1)) such that $G(z=0) = 1$ and

$$\delta = G(z)\delta_0 \tag{5.3.11}$$

and the growth rate $f \equiv G'/G$ (we assume G, f are k-independent). It is again useful to define a new divergence:

$$\theta_{new} = \frac{\theta_{old}}{\mathcal{H}} \tag{5.3.12}$$

Then Eq. (5.3.10) can be written as

$$\mathcal{H}\delta' + \mathcal{H}\theta = \mathcal{H}G^2 f \int \delta_1\delta_2 \frac{\mathbf{k}_2\mathbf{k}_1 + \mathbf{k}_2\mathbf{k}_2}{k_2^2}(2\pi)^3\delta_D(\mathbf{k}_1+\mathbf{k}_2-\mathbf{k})d^3k_1 d^3k_2 \tag{5.3.13}$$

where the prime is $d/d\log a$ and where δ_i are evaluated at the present time (so they are independent of time). All δ, θ inside the integrals from now on are the present values. We rewrite this as

$$\theta + \delta' = G^2 f \int \delta_1\delta_2\alpha(\mathbf{k}_1,\mathbf{k}_2)(2\pi)^3\delta_D(\mathbf{k}_1+\mathbf{k}_2-\mathbf{k})d^3k_1 d^3k_2 \equiv C \tag{5.3.14}$$

In this and the following equations, we observe that the homogenous part of the equation (i.e., the l.h.s) is identical to the first order equations, and therefore the homogenous solution coincides with the first order solution, which we already included in the expansion (5.3.9). Therefore, in the following we only need to identify particular solutions of the inhomogeneous equations.

Since we can switch the labels $1, 2$ inside the integral, the kernel $\alpha(\mathbf{k}_1,\mathbf{k}_2)$ can be symmetrized

$$\alpha(\mathbf{k}_1,\mathbf{k}_2) = \frac{1}{2}\left[\frac{\mathbf{k}_2\cdot(\mathbf{k}_1+\mathbf{k}_2)}{k_2^2} + \frac{\mathbf{k}_1\cdot(\mathbf{k}_1+\mathbf{k}_2)}{k_1^2}\right] \tag{5.3.15}$$

$$= \frac{1}{2}\left(\frac{\mathbf{k}_2}{k_1^2} + \frac{\mathbf{k}_1}{k_2^2}\right)\cdot(\mathbf{k}_1+\mathbf{k}_2) \tag{5.3.16}$$

This symmetrization is always possible and sometimes used explicitly, sometimes understood. Similarly, the general Euler equation (5.1.9) in real space can be written as

$$\theta' + F\theta + S\delta = -\nabla\left[(\int \mathbf{v}_k e^{i\mathbf{k}\mathbf{x}}d^3k)\cdot\nabla\int \mathbf{v}_{k'}e^{i\mathbf{k}'\mathbf{x}}d^3k'\right] \tag{5.3.17}$$

$$= -i\nabla\left[\int(\mathbf{v}_k\cdot\mathbf{k}')\mathbf{v}_{k'}e^{i\mathbf{k}\mathbf{x}}e^{i\mathbf{k}'\mathbf{x}}d^3k d^3k'\right] \tag{5.3.18}$$

$$= \int(\mathbf{v}_k\cdot\mathbf{k}')(\mathbf{v}_{k'}\cdot(\mathbf{k}+\mathbf{k}'))e^{i(\mathbf{k}'+\mathbf{k})\mathbf{x}}d^3k' d^3k \tag{5.3.19}$$

From now on we put ourselves in an Einstein-de Sitter model (i.e. $\Omega_m = 1$). In this case, $G = G' = G'' = a$. Moreover, $F = 1/2, S = 3/2$. Although in EdS $f = 1$, we keep explicitly f in some expressions. Notice that we always assume that G and f only depend on time and not on k. Then we see that

$$\theta' + F\theta + S\delta = -G^2\int\theta_k\theta_{k'}(\frac{\mathbf{k}}{k^2}\cdot\mathbf{k}')(\frac{\mathbf{k}'}{k'^2}\cdot(\mathbf{k}+\mathbf{k}'))e^{i(\mathbf{k}'+\mathbf{k})\mathbf{x}}d^3k' d^3k \tag{5.3.20}$$

$$= -G^2\int\theta_k\theta_{k'}(\frac{\mathbf{k}\cdot\mathbf{k}'}{k^2k'^2}\mathbf{k}'\cdot(\mathbf{k}+\mathbf{k}'))e^{i(\mathbf{k}'+\mathbf{k})\mathbf{x}}d^3k' d^3k \tag{5.3.21}$$

The kernel can be symmetrized:

$$\beta(\mathbf{k}_1,\mathbf{k}_2) = \frac{1}{2}[(\frac{\mathbf{k}\cdot\mathbf{k}'}{k^2k'^2}\mathbf{k}'\cdot(\mathbf{k}+\mathbf{k}')) + (\mathbf{k}\leftrightarrow\mathbf{k}')] = \frac{1}{2k^2k'^2}[\mathbf{k}\cdot\mathbf{k}'(\mathbf{k}'+\mathbf{k})\cdot(\mathbf{k}+\mathbf{k}')] = \frac{\mathbf{k}\cdot\mathbf{k}'(\mathbf{k}'+\mathbf{k})^2}{2k^2k'^2} \tag{5.3.22}$$

Integrating again over $(2\pi)^{-3}e^{-i\mathbf{k}''\mathbf{x}}d^3x$ one gets

$$\theta' + F\theta + S\delta = -G^2\int\theta_1\theta_2\beta(\mathbf{k}_1,\mathbf{k}_2)(2\pi)^3\delta_D(\mathbf{k_1}+\mathbf{k}_2-\mathbf{k})d^3k_1 d^3k_2 \tag{5.3.23}$$

$$= -G^2f^2\int\delta_1\delta_2\beta(\mathbf{k}_1,\mathbf{k}_2)(2\pi)^3\delta_D(\mathbf{k}_1+\mathbf{k}_2-\mathbf{k})d^3k_1 d^3k_2 \equiv E \tag{5.3.24}$$

where now all perturbation variables are in Fourier space, where (after symmetrization)

$$\alpha = \frac{(\mathbf{k}_1+\mathbf{k}_2)}{2}(\frac{\mathbf{k}_1}{k_1^2}+\frac{\mathbf{k}_2}{k_2^2}) = 1 + \frac{1}{2}\mathbf{k}_1\mathbf{k}_2(\frac{1}{k_1^2}+\frac{1}{k_2^2}) \tag{5.3.25}$$

$$\beta = \frac{(\mathbf{k}_1+\mathbf{k}_2)^2(\mathbf{k}_1\mathbf{k}_2)}{2k_1^2k_2^2} \tag{5.3.26}$$

We can now differentiate the θ equation (5.3.14) and obtain

$$\theta' + \delta'' = 2G^2(f^2 + \frac{1}{2}f') \int \delta_1\delta_2\alpha(\mathbf{k}_1,\mathbf{k}_2)(2\pi)^3\delta_D(\mathbf{k}_1+\mathbf{k}_2-\mathbf{k})d^3k_1d^3k_2 = C' \tag{5.3.27}$$

Then we insert the θ' equation, replace again $\theta = C - \delta'$ and obtain an equation for the second order δ alone on the lhs

$$\delta'' + (-F(C-\delta') - S\delta + E) = C'$$

or

$$\delta'' + F\delta' - S\delta = C' - E + FC \tag{5.3.28}$$

Putting $\delta^{(2)} = G^{(2)}\delta_k^{(2)}$, where $\delta_k^{(2)}$ depends only on $\mathbf{k}$, and, as shown in Eq. (5.2.6), $G^{(2)} = AG^2$, we see that

$$G^{(2)'} = 2AG^2f; \quad G^{(2)''} = 4AG^2f^2 + 2AG^2f' \tag{5.3.29}$$

and thus

$$\delta'' + F\delta' - S\delta = [(G^{(2)})'' + FG^{(2)\prime} - SG^{(2)}]\delta = (4(f^2+\frac{1}{2}f') + 2Ff - S)AG^2\delta_k^{(2)} = (4(f^2+\frac{1}{2}f') + 2Ff - S)\delta^{(2)} \tag{5.3.30}$$

In EdS, putting $f = 1$, the last expression equals $7\delta^{(2)}/2$ and then one has from (5.3.28)

$$\delta^{(2)} = \frac{2}{7}(\delta'' + F\delta' - S\delta) = 2\frac{C' - E + FC}{7} \tag{5.3.31}$$

$$= \frac{2G^2}{7}\int \delta_1\delta_2[2\alpha + \beta + \frac{1}{2}\alpha](2\pi)^3\delta_D(\mathbf{k}_1+\mathbf{k}_2-\mathbf{k})d^3k_1d^3k_2 \tag{5.3.32}$$

Notice that we do not need the value of A, but just that $G^{(2)} \propto G^2$. So we obtain

$$\delta^{(2)} = \frac{G^2}{7}\int \delta_1\delta_2[5\alpha + 2\beta](2\pi)^3\delta_D(\mathbf{k}_1+\mathbf{k}_2-\mathbf{k})d^3k_1d^3k_2 \tag{5.3.33}$$

$$= \frac{2G^2}{7}\int \delta_1\delta_2[5\frac{\mathbf{k}}{4}(\frac{\mathbf{k}_1}{k_1^2}+\frac{\mathbf{k}_2}{k_2^2}) + \frac{(\mathbf{k}_1+\mathbf{k}_2)^2(\mathbf{k}_1\mathbf{k}_2)}{2k_1^2k_2^2}](2\pi)^3\delta_D(\mathbf{k}_1+\mathbf{k}_2-\mathbf{k})d^3k_1d^3k_2 \tag{5.3.34}$$

$$= G^2\int \delta_1\delta_2F_2(\mathbf{k}_1,\mathbf{k}_2)(2\pi)^3\delta_D(\mathbf{k}_1+\mathbf{k}_2-\mathbf{k})d^3k_1d^3k_2 \tag{5.3.35}$$

where

$$F_2 = \frac{5\alpha+2\beta}{7} = \frac{2}{7}\left[5\frac{\mathbf{k}}{4}(\frac{\mathbf{k}_1}{k_1^2}+\frac{\mathbf{k}_2}{k_2^2}) + \frac{(\mathbf{k}_1+\mathbf{k}_2)^2(\mathbf{k}_1\mathbf{k}_2)}{2k_1^2k_2^2}\right] \tag{5.3.36}$$

$$= \frac{2}{7}\left[\frac{5}{4}(2 + \mathbf{k}_1\mathbf{k}_2(\frac{1}{k_1^2}+\frac{1}{k_2^2}) + \frac{(k_1^2+k_2^2+2\mathbf{k}_1\mathbf{k}_2)(\mathbf{k}_1\mathbf{k}_2)}{2k_1^2k_2^2}\right] \tag{5.3.37}$$

$$= \frac{2}{7}\left[\frac{5}{2} + \frac{7}{4}\mathbf{k}_1\mathbf{k}_2(\frac{1}{k_1^2}+\frac{1}{k_2^2}) + \frac{(\mathbf{k}_1\mathbf{k}_2)^2}{k_1^2k_2^2}\right] \tag{5.3.38}$$

$$= \frac{5}{7} + \frac{1}{2}\mathbf{k}_1\mathbf{k}_2(\frac{1}{k_1^2}+\frac{1}{k_2^2}) + \frac{2}{7}\frac{(\mathbf{k}_1\mathbf{k}_2)^2}{k_1^2k_2^2} \tag{5.3.39}$$

Similarly, one can write an equation for $\theta^{(2)}$ alone

$$\theta^{(2)} + \delta'^{(2)} = \theta^{(2)} + 2G^2f\delta^{(2)} = G^2f\int \delta_1\delta_2\alpha(\mathbf{k}_1,\mathbf{k}_2)(2\pi)^3\delta_D(\mathbf{k}_1+\mathbf{k}_2-\mathbf{k})d^3k_1d^3k_2 \tag{5.3.40}$$

from which, since $GG' = G^2$ in EdS,

$$\theta^{(2)} = -2G^2 f \int \delta_1\delta_2 F_2(\mathbf{k}_1,\mathbf{k}_2)(2\pi)^3\delta_D(\mathbf{k}_1+\mathbf{k}_2-\mathbf{k})d^3k_1d^3k_2 \tag{5.3.41}$$

$$+ G^2 f \int \delta_1\delta_2 \alpha(\mathbf{k}_1,\mathbf{k}_2)(2\pi)^3\delta_D(\mathbf{k}_1+\mathbf{k}_2-\mathbf{k})d^3k_1d^3k_2 \tag{5.3.42}$$

or

$$\theta^{(2)} = -G^2 f \int \delta_1\delta_2 G_2(2\pi)^3\delta_D(\mathbf{k}_1+\mathbf{k}_2-\mathbf{k})d^3k_1d^3k_2 \tag{5.3.43}$$

with

$$G_2 = 2F_2 - \alpha = \frac{3\alpha+4\beta}{7} = \frac{10}{7} + \mathbf{k}_1\mathbf{k}_2(\frac{1}{k_1^2}+\frac{1}{k_2^2}) + \frac{4}{7}\frac{(\mathbf{k}_1\mathbf{k}_2)^2}{k_1^2k_2^2} - \frac{\mathbf{k}_1+\mathbf{k}_2}{2}(\frac{\mathbf{k}_1}{k_1^2}+\frac{\mathbf{k}_2}{k_2^2}) \tag{5.3.44}$$

$$= \frac{10}{7} + \mathbf{k}_1\mathbf{k}_2(\frac{1}{k_1^2}+\frac{1}{k_2^2}) + \frac{4}{7}\frac{(\mathbf{k}_1\mathbf{k}_2)^2}{k_1^2k_2^2} - 1 - \frac{1}{2}(\frac{\mathbf{k}_2\mathbf{k}_1}{k_1^2}+\frac{\mathbf{k}_1\mathbf{k}_2}{k_2^2}) \tag{5.3.45}$$

$$= \frac{3}{7} + \mathbf{k}_1\mathbf{k}_2(\frac{1}{k_1^2}+\frac{1}{k_2^2}) + \frac{4}{7}\frac{(\mathbf{k}_1\mathbf{k}_2)^2}{k_1^2k_2^2} - \frac{1}{2}\mathbf{k}_2\mathbf{k}_1(\frac{1}{k_1^2}+\frac{1}{k_2^2}) \tag{5.3.46}$$

$$= \frac{3}{7} + \frac{1}{2}\mathbf{k}_2\mathbf{k}_1(\frac{1}{k_1^2}+\frac{1}{k_2^2}) + \frac{4}{7}\frac{(\mathbf{k}_1\mathbf{k}_2)^2}{k_1^2k_2^2} \tag{5.3.47}$$

In general, it happens that $G^{(2)} \approx AG^2$ even for non EdS models.

Whatever the cosmology, therefore, one always has, to a good approximation, the forms

$$\theta^{(2)} = -G^2 f \int \delta_1\delta_2 G_2(\mathbf{k}_1,\mathbf{k}_2)(2\pi)^3\delta_D(\mathbf{k}_1+\mathbf{k}_2-\mathbf{k})\frac{d^3k_1}{(2\pi)^3}\frac{d^3k_2}{(2\pi)^3} \tag{5.3.48}$$

$$\delta^{(2)} = G^2 \int \delta_1\delta_2 F_2(\mathbf{k}_1,\mathbf{k}_2)(2\pi)^3\delta_D(\mathbf{k}_1+\mathbf{k}_2-\mathbf{k})\frac{d^3k_1}{(2\pi)^3}\frac{d^3k_2}{(2\pi)^3} \tag{5.3.49}$$

(we inserted back the $(2\pi)^3$ factors) where G is the linear growth function and

$$F_2 = \frac{5}{7} + \frac{\mathbf{k}_1\mathbf{k}_2}{2k_1k_2}(\frac{k_1}{k_2}+\frac{k_2}{k_1}) + \frac{2}{7}(\frac{\mathbf{k}_1\mathbf{k}_2}{k_1k_2})^2 \tag{5.3.50}$$

$$G_2 = \frac{3}{7} + \frac{\mathbf{k}_1\mathbf{k}_2}{2k_1k_2}(\frac{k_1}{k_2}+\frac{k_2}{k_1}) + \frac{4}{7}(\frac{\mathbf{k}_1\mathbf{k}_2}{k_1k_2})^2 \tag{5.3.51}$$

(Notice that although is a good approximation to take $f = 1$ in (5.3.30), the factor f is $\theta^{(2)}$ is necessary). Note that

$$F_2(\mathbf{k}_1,-\mathbf{k}_1) = 0 \tag{5.3.52}$$

$$G_2(\mathbf{k}_1,-\mathbf{k}_1) = 0 \tag{5.3.53}$$

This property is a consequence of the fact that at any order we have $\delta_{\mathbf{k}=0} = V^{-1}\int\delta(x)d^3x = 0$, i.e. mass conservation, and the same for all perturbation variables.

The procedure can be extended to all orders by a recursive process for $n \geq 2$, see e.g. [4]:

$$F_n(\mathbf{k}_1,...\mathbf{k}_n) = \sum_{m=1}^{n-1}\frac{G_m(\mathbf{k}_1,...\mathbf{k}_m)}{(2n+3)(n-1)}\left[(2n+1)\alpha(\mathbf{q}_1,\mathbf{q}_2)F_{n-m}(\mathbf{k}_{m+1},...\mathbf{k}_n) + 2\beta(\mathbf{q}_1,\mathbf{q}_2)G_{n-m}(\mathbf{k}_{m+1},...\mathbf{k}_n)\right] \tag{5.3.54}$$

$$G_n(\mathbf{k}_1,...\mathbf{k}_n) = \sum_{m=1}^{n-1}\frac{G_m(\mathbf{k}_1,...\mathbf{k}_m)}{(2n+3)(n-1)}\left[3\alpha(\mathbf{q}_1,\mathbf{q}_2)F_{n-m}(\mathbf{k}_{m+1},...\mathbf{k}_n) + 2n\beta(\mathbf{q}_1,\mathbf{q}_2)G_{n-m}(\mathbf{k}_{m+1},...\mathbf{k}_n)\right] \tag{5.3.55}$$

where $\mathbf{q}_1 \equiv \mathbf{k}_1 + ... + \mathbf{k}_m$, $\mathbf{q}_2 \equiv \mathbf{k}_{m+1} + ... + \mathbf{k}_n$ and $F_1 = G_1 = 1$. So one gets for instance (see Appendix for a detailed calculation of F_3)

$$\theta^{(3)} = G^3 \int \theta_1\theta_2\theta_3 G_3(\mathbf{k}_1,\mathbf{k}_2,\mathbf{k}_3)(2\pi)^3\delta_D(\mathbf{k}_1+\mathbf{k}_2+\mathbf{k}_3-\mathbf{k})\frac{d^3k_1}{(2\pi)^3}\frac{d^3k_2}{(2\pi)^3}\frac{d^3k_3}{(2\pi)^3} \tag{5.3.56}$$

$$= -G^3 \int \delta_1\delta_2\delta_3 G_3(\mathbf{k}_1,\mathbf{k}_2,\mathbf{k}_3)(2\pi)^3\delta_D(\mathbf{k}_1+\mathbf{k}_2+\mathbf{k}_3-\mathbf{k})\frac{d^3k_1}{(2\pi)^3}\frac{d^3k_2}{(2\pi)^3}\frac{d^3k_3}{(2\pi)^3} \tag{5.3.57}$$

$$\delta^{(3)} = G^3 \int \delta_1\delta_2\delta_3 F_3(\mathbf{k}_1,\mathbf{k}_2,\mathbf{k}_3)(2\pi)^3\delta_D(\mathbf{k}_1+\mathbf{k}_2+\mathbf{k}_3-\mathbf{k})\frac{d^3k_1}{(2\pi)^3}\frac{d^3k_2}{(2\pi)^3}\frac{d^3k_3}{(2\pi)^3} \tag{5.3.58}$$

where

$$F_3 = \frac{1}{18}[7\alpha(k_1,k_2+k_3)F_2(k_2,k_3) + 2\beta(k_1,k_2+k_3)G_2(k_2,k_3) + G_2(k_1,k_2)(7\alpha(k_1+k_2,k_3)+2\beta(k_1+k_2,k_3))] \tag{5.3.59}$$

$$G_3 = \frac{1}{18}[3\alpha(k_1,k_2+k_3)F_2(k_2,k_3) + 6\beta(k_1,k_2+k_3)G_2(k_2,k_3) + G_2(k_1,k_2)(3\alpha(k_1+k_2,k_3)+6\beta(k_1+k_2,k_3))] \tag{5.3.60}$$

(to be symmetrized). As will be shown shortly, we need also the third order for δ to derive the corrected power spectrum.

The approximation $G^{(2)} \propto G^2$ can be easily lifted. Let us restart with Eq. (5.3.28)

$$\delta'' + F\delta' - S\delta = C' - E + FC = 2G^2(f^2 + \frac{1}{2}f')\int \delta_1\delta_2\alpha(\mathbf{k}_1,\mathbf{k}_2)(2\pi)^3\delta_D(\mathbf{k}_1+\mathbf{k}_2-\mathbf{k})\frac{d^3k_1}{(2\pi)^3}\frac{d^3k_2}{(2\pi)^3} \tag{5.3.61}$$

$$- G^2f^2\int \delta_1\delta_2\beta(\mathbf{k}_1,\mathbf{k}_2)(2\pi)^3\delta_D(\mathbf{k}_1+\mathbf{k}_2-\mathbf{k})d^3k_1d^3k_2 \tag{5.3.62}$$

$$+ FG^2f\int \delta_1\delta_2\alpha(\mathbf{k}_1,\mathbf{k}_2)(2\pi)^3\delta_D(\mathbf{k}_1+\mathbf{k}_2-\mathbf{k})\frac{d^3k_1}{(2\pi)^3}\frac{d^3k_2}{(2\pi)^3} \tag{5.3.63}$$

$$= G^2(2f^2+f'+Ff)\int \delta_1\delta_2\alpha(\mathbf{k}_1,\mathbf{k}_2)(2\pi)^3\delta_D(\mathbf{k}_1+\mathbf{k}_2-\mathbf{k})\frac{d^3k_1}{(2\pi)^3}\frac{d^3k_2}{(2\pi)^3} \tag{5.3.64}$$

$$+ G^2f^2\int \delta_1\delta_2\beta(\mathbf{k}_1,\mathbf{k}_2)(2\pi)^3\delta_D(\mathbf{k}_1+\mathbf{k}_2-\mathbf{k})\frac{d^3k_1}{(2\pi)^3}\frac{d^3k_2}{(2\pi)^3} \tag{5.3.65}$$

Then we write the general solution as a linear combination of separable terms

$$\delta^{(2)} = G^2[g_A(a)A(\mathbf{k}) + g_B(a)B(\mathbf{k})] \tag{5.3.66}$$

with

$$A(k) = \int \delta_1\delta_2\alpha(\mathbf{k}_1,\mathbf{k}_2)(2\pi)^3\delta_D(\mathbf{k}_1+\mathbf{k}_2-\mathbf{k})\frac{d^3k_1}{(2\pi)^3}\frac{d^3k_2}{(2\pi)^3} \tag{5.3.67}$$

$$B(k) = \int \delta_1\delta_2\beta(\mathbf{k}_1,\mathbf{k}_2)(2\pi)^3\delta_D(\mathbf{k}_1+\mathbf{k}_2-\mathbf{k})\frac{d^3k_1}{(2\pi)^3}\frac{d^3k_2}{(2\pi)^3} \tag{5.3.68}$$

By identifying separately on both sides of (5.3.65) the terms with α and those with β, we obtain two equations, one for g_A and one for g_B

$$\begin{aligned} &g_A'' + (4f+F)g_A' + g_A\left(2f^2+S\right) = f^2+S \\ &g_B'' + (4f+F)g_B' + g_B\left(2f^2+S\right) = f^2 \end{aligned} \tag{5.3.69}$$

(we used Eq. 5.3.3). Now one can see that the combination $D = g_A + g_B$ obeys the equation

$$D'' + (4f+F)D' + D\left(2f^2+S\right) = 2f^2+S \tag{5.3.70}$$

which has particular solution $D = 1$. Therefore $g_B = 1 - g_A$. Then the new time-dependent kernel is

$$F_2(\mathbf{k}_1, \mathbf{k}_2, a) = g_A(a)\alpha(\mathbf{k}_1, \mathbf{k}_2) + (1 - g_A(a))\beta(\mathbf{k}_1, \mathbf{k}_2) = g_A(a)(\alpha(\mathbf{k}_1, \mathbf{k}_2) - \beta(\mathbf{k}_1, \mathbf{k}_2)) + \beta(\mathbf{k}_1, \mathbf{k}_2) \quad (5.3.71)$$

The initial conditions can be taken to be standard pure EdS (i.e. dominated by CDM), so that $g_A = 1$ and $g'_A = 0$. A similar set of equations gives the third order growth. In EdS, with $F = \frac{1}{2}, S = \frac{3}{2}, f = 1$, the equations become

$$g''_A + \frac{9}{2}g'_A + \frac{7}{2}g_A = \frac{5}{2} \quad (5.3.72)$$

$$g''_B + \frac{9}{2}g'_B + \frac{7}{2}g_B = 1 \quad (5.3.73)$$

solved by $g_A = 5/7$ and $g_B = 2/7$ (we consider only the growing solution as usual), recovering the EdS solutions.

For $\theta^{(2)}$ we can proceed as above, starting from Eq. (5.3.40), that we rewrite as

$$\theta^{(2)} + \delta'^{(2)} = \theta^{(2)} + (G^2 g_A)' A(\mathbf{k}) + (G^2 g_B)' B(\mathbf{k}) = f G^2 A(\mathbf{k}) \quad (5.3.74)$$

from which

$$\theta^{(2)} = G^2\{[-g'_A - 2f g_A + f]A(\mathbf{k}) - (g'_B + f g_B)B(\mathbf{k})\} \quad (5.3.75)$$

In EdS, $f = 1$ and $g_A = 5/7, g_B = 2/7$, so we get $\theta^{(2)} = -G^2[\frac{3}{7}A(\mathbf{k}) + \frac{2}{7}B(\mathbf{k})]$ which agrees with Eq. (5.3.48).

The solution of (5.3.69) can in general only be obtained numerically; an accurate fit for wCDM is provided in [20]. As already mentioned, however, the approximation $G^{(2)} \propto G^2$ is usually good to within a few percent at most.

Since $f \approx \Omega_m^{0.54}$ and therefore $\Omega_m \approx f^2$, one has $S \approx 3f^2/2$, and then the rhs of both equations (5.3.69) is $7G^2 f^2/2$. This means that as long as $\Omega_m \approx f^2$, as in this more general case, $\delta^{(2)}$ is separable in a function that depends only on time and one that depends only on $\mathbf{k}$. This occurs at all orders. This is the fundamental reason why $G^{(2)} \propto G^2$ is a good approximation.

5.4 Bias and RSD

To see the effect of the redshift distortion on the kernels, we go back to the real space-redshift space mapping[a]

$$\mathbf{s} = \mathbf{r}\left[1 + \frac{u(r)}{r}\right] \quad (5.4.1)$$

(we assume that the velocity $u(0)$ of the observer has been subtracted out) in Eq. (3.5.6)

$$\delta_s = \frac{n(s)dV_s}{n_0 dV_s} - 1 = \frac{n(r)dV_r}{n_0 dV_r \left(1 + \frac{\Delta\mathbf{u}(r)}{r}\right)^2 |J|} - 1 \quad (5.4.2)$$

where $|J| = 1 + \frac{du}{dr}$ and

$$u = \mathcal{H}^{-1}\mathbf{v} \cdot \frac{\mathbf{r}}{r} \quad (5.4.3)$$

This relation is exact at all orders. The term $\Delta u/r$ can be neglected because we assume the galaxies are very distant. So we have

$$\delta_s = \frac{n(r)dV_r}{n_0 dV_r |J|} - 1 = \frac{1 + \delta(r)}{1 + \frac{du}{dr}} - 1 = \frac{\delta(r) - \frac{du}{dr}}{1 + \frac{du}{dr}} \quad (5.4.4)$$

In Fourier space, this equation becomes

$$\delta_s(k) = \int d^3s[\frac{\delta(r) - \frac{du}{dr}}{1 + \frac{du}{dr}}]e^{i\mathbf{ks}} = \int \frac{d^3s}{1 + \frac{du}{dr}}[\delta(r) - \frac{du}{dr}]e^{i\mathbf{kr} + i\mathbf{k}\frac{\mathbf{r}}{r}u} = \int d^3r[\delta(r) - \frac{du}{dr}]e^{i\mathbf{kr} + i\mathbf{k}\frac{\mathbf{r}}{r}u} \quad (5.4.5)$$

[a] For this section, we follow in part Refs. [18, 11].

(since $d^3s = |J|d^3r$). The term inside the square brackets is usually called redshift space distortion, RSD; the additional term in the exponent instead is responsible for the excess of clustering along the line of sight, and is called fingers-of-God (FOG) effect.

Now we write $\mathbf{v} \cdot \frac{\mathbf{r}}{r} = v\mu_\theta$ and define $\theta = ik_\theta v/\mathcal{H}$, so that

$$e^{i\mathbf{k}\frac{\mathbf{r}}{r}u} = e^{i\mathbf{k}\frac{\mathbf{r}}{r}\frac{v}{\mathcal{H}}\mu_\theta} = e^{ik\mu\frac{v}{\mathcal{H}}\mu_\theta} = e^{\frac{k}{k_\theta}\theta\mu\mu_\theta} \tag{5.4.6}$$

The term $\theta\mu_\theta/k_\theta$ is a field in real space. We can write it as a Fourier integral and expand the exponential in a series of Fourier integrals

$$e^{k\mu\theta\frac{\mu_\theta}{k_\theta}} = \sum_{n=0} \frac{(k\mu)^n}{n!}[\frac{\mu_\theta}{k_\theta}\theta(\mathbf{r})]^n = 1+ \tag{5.4.7}$$

$$\sum_{n=1} \frac{(k\mu)^n}{n!} \int \frac{d^3q_1}{(2\pi)^3}\frac{\mu_1}{q_1}\theta(\mathbf{q}_1)e^{-i\mathbf{q}_1\mathbf{r}} \int \frac{d^3q_2}{(2\pi)^3}\frac{\mu_2}{q_2}\theta(\mathbf{q}_2)e^{-i\mathbf{q}_2\mathbf{r}}.. \int \frac{d^3q_n}{(2\pi)^3}\frac{\mu_n}{q_n}\theta(\mathbf{q}_n)e^{-i\mathbf{q}_n\mathbf{r}} \tag{5.4.8}$$

$$= 1 + \sum_{n=1} \frac{(k\mu)^n}{n!} \int \frac{d^3q_1}{(2\pi)^3}\frac{\mu_1}{q_1}\theta(\mathbf{q}_1) \int \frac{d^3q_2}{(2\pi)^3}\frac{\mu_2}{q_2}\theta(\mathbf{q}_2).. \int \frac{d^3q_n}{(2\pi)^3}\frac{\mu_n}{q_n}\theta(\mathbf{q}_n)e^{-i\sum_i^n \mathbf{q}_i\mathbf{r}} \tag{5.4.9}$$

so that

$$\delta_s(\mathbf{k}) = \int d^3r[\delta(\mathbf{r}) - \frac{du}{dr}]\{e^{i\mathbf{kr}} + \sum_{n=1} \frac{(k\mu)^n}{n!} \int \frac{d^3q_1}{(2\pi)^3}\frac{\mu_1}{q_1}\theta(\mathbf{q}_1) \int \frac{d^3q_2}{(2\pi)^3}\frac{\mu_2}{q_2}\theta(\mathbf{q}_2).. \int \frac{d^3q_n}{(2\pi)^3}\frac{\mu_n}{q_n}\theta(\mathbf{q}_n)e^{i(\mathbf{k}-\sum_i^n \mathbf{q}_i)\mathbf{r}}\} \tag{5.4.10}$$

We assumed that the angle μ is a constant. This is called *flat-field* approximation: the galaxies are so far, and the field of view is so small in angular extension and in depth, that the angles between the vectors $\mathbf{k}$ and the line of sight r, is constant.

Before proceding further, we need now to consider the bias between galaxies δ_g and dark matter δ. A reasonable model, called *local deterministic bias*, for the non-linear bias is the expansion

$$\delta_g(\mathbf{r}) = b_1\delta(\mathbf{r}) + \frac{1}{2}b_2\delta(\mathbf{r})^2 + ... \tag{5.4.11}$$

where the parameters b_i are supposed to depend only on time and not on space. A constant b_0 is absent because we require $\langle\delta_g\rangle = 0$. It is generally assumed that there is no velocity bias, so $\theta_g = \theta$. The reason is that, if the equivalence principle is satisfied, baryons and dark matter respond to the same gravitational potential and therefore acquire the same velocity if the initial conditions are the same. Here we refer explicitly to galaxies but a similar treatment can be applied to any *tracer* of the underlying mass distribution: Lyman-α clouds, standard candles, 21cm, etc. At the end, each tracer field will be characterized by a set of bias functions, of which $b_1, b_2, ..$ are just a first simplified example.

In Fourier space this δ_g expansion becomes at second order

$$\delta_g(\mathbf{k}) = b_1\delta^{(1)}(\mathbf{k}) + \frac{1}{2}b_2 \int \frac{d^3q_1}{(2\pi)^3}\frac{d^3q_2}{(2\pi)^3}(2\pi)^3\delta_D(\mathbf{k}-\mathbf{q}_1-\mathbf{q}_2)\delta^{(1)}(\mathbf{q}_1)\delta^{(1)}(\mathbf{q}_2) + ... \tag{5.4.12}$$

Let us consider now the first terms of the expansion (5.4.10). The first term reproduces the linear theory:

$$\delta_g^{(1)}(\mathbf{k}) = \int d^3r[b_1\delta(\mathbf{r}) - \frac{du}{dr}]e^{i\mathbf{kr}} = \int d^3r b_1\delta(\mathbf{r})e^{i\mathbf{kr}} - \int d^3r\frac{du}{dr}e^{i\mathbf{kr}} \tag{5.4.13}$$

$$= \delta^{(1)}(\mathbf{k})(b_1 + f\mu^2) \tag{5.4.14}$$

(the subscript g stands now for galaxies in redshift space) where we used the linear theory relation (Eq. 5.3.1)

$$\mathbf{v}(\mathbf{k}) = i\mathcal{H}\delta_k f\frac{\mathbf{k}}{k^2} \tag{5.4.15}$$

from which

$$u(r) = \frac{\mathbf{r}}{r}\cdot\frac{\mathbf{v}}{\mathcal{H}}(\mathbf{r}) = if\int \frac{d^3k'}{(2\pi)^3}\delta(\mathbf{k}')\frac{\mathbf{k'r}}{k'^2r}e^{-i\mathbf{k}'\cdot\mathbf{r}} \tag{5.4.16}$$

while its derivative is (notice that $\mathbf{k}\cdot\mathbf{r}/(kr)=\mu$ is assumed constant)

$$\frac{du}{dr}=-f\int\delta(\mathbf{k'})e^{-i\mathbf{k'}\cdot\mathbf{r}}\left(\frac{\mathbf{k'r}}{k'r}\right)^2\frac{d^3k'}{(2\pi)^3}=-f\int\delta(\mathbf{k'})e^{-i\mathbf{k'}\cdot\mathbf{r}}\mu^2\frac{d^3k'}{(2\pi)^3} \tag{5.4.17}$$

so that

$$\int d^3r\frac{du}{dr}e^{i\mathbf{kr}}=-f\int d^3r\frac{d^3k}{(2\pi)^3}\delta(\mathbf{k'})e^{i(\mathbf{k}-\mathbf{k'})\cdot\mathbf{r}}\mu^2=-f\int\frac{d^3k}{(2\pi)^3}\delta_D(\mathbf{k}-\mathbf{k'})\delta(\mathbf{k'})\mu^2=-f\mu^2\delta(\mathbf{k})=\mu^2\theta(\mathbf{k}) \tag{5.4.18}$$

This is the usual linear Kaiser effect, and no FOG effect is present.

The second term gives

$$\delta_g(\mathbf{k})=\int d^3r[\delta(\mathbf{r})-\frac{du}{dr}]e^{i(\mathbf{k}-\mathbf{q_1})\mathbf{r}}k\mu\frac{d^3q_1}{(2\pi)^3}\frac{\mu_1}{q_1}\theta(\mathbf{q}_1) \tag{5.4.19}$$

$$=\int d^3r\int\frac{d^3q_0}{(2\pi)^3}[\delta(\mathbf{q}_0)-\theta(\mathbf{q}_0)\mu_0^2]e^{i(\mathbf{k}-\mathbf{q}_0-\mathbf{q}_1)\mathbf{r}}k\mu\frac{d^3q_1}{(2\pi)^3}\frac{\mu_1}{q_1}\theta(\mathbf{q}_1) \tag{5.4.20}$$

$$=\int\frac{d^3q_0}{(2\pi)^3}\frac{d^3q_1}{(2\pi)^3}[\delta(\mathbf{q}_0)-\theta(\mathbf{q}_0)\mu_0^2](2\pi)^3\delta_D(\mathbf{k}-\mathbf{q}_0-\mathbf{q}_1)k\mu\frac{\mu_1}{q_1}\theta(\mathbf{q}_1) \tag{5.4.21}$$

Relabeling $0,1,...$ into 1,2,..., it is then not difficult to see that the entire series can be recast in the more symmetric form

$$\delta_g(\mathbf{k})=\sum_{n=1}\int\frac{d^3q_1}{(2\pi)^3}\int\frac{d^3q_2}{(2\pi)^3}...\int\frac{d^3q_n}{(2\pi)^3}[\delta(\mathbf{q_1})-\theta(\mathbf{q_1})\mu_1^2](2\pi)^3\delta_D(\mathbf{k}-\sum_{i=1}^n\mathbf{q}_i)\frac{(k\mu)^{n-1}}{(n-1)!}\frac{\mu_2}{q_2}\theta(\mathbf{q}_2)\frac{\mu_3}{q_3}\theta(\mathbf{q}_3)..\frac{\mu_n}{q_n}\theta(\mathbf{q}_n) \tag{5.4.22}$$

(with the understanding that for $n=1$ the product of $\mu_i q_i^{-1}\theta_i$ factors reduces to unity). Notice that, in several references, θ is defined with the opposite sign.

This expansion is valid at all orders. Now we can use for δ,θ the expansion (5.3.9) and the results 5.3.48-5.3.49 of the previous section, plus the bias expansion (5.4.12), systematically collecting terms that contribute with the same power of ε. At second order the terms that contribute are as follows

$$\delta_g^{(2)}(\mathbf{k})=b_1\delta^{(2)}(\mathbf{k})-\theta^{(2)}(\mathbf{k})\mu^2+\int\frac{d^3q_1}{(2\pi)^3}\frac{d^3q_2}{(2\pi)^3}(2\pi)^3\delta_D(\mathbf{k}-\mathbf{q}_1-\mathbf{q}_2)\frac{b_2}{2}\delta^{(1)}(\mathbf{q}_1)\delta^{(1)}(\mathbf{q}_2) \tag{5.4.23}$$

$$+\int\frac{d^3q_1}{(2\pi)^3}\frac{d^3q_2}{(2\pi)^3}[b_1\delta^{(1)}(\mathbf{q}_1)-\theta^{(1)}(\mathbf{q}_1)\mu_1^2](2\pi)^3\delta_D(\mathbf{k}-\mathbf{q}_1-\mathbf{q}_2)k\mu\frac{\mu_2}{q_2}\theta^{(1)}(\mathbf{q}_2) \tag{5.4.24}$$

$$=\int\frac{d^3q_1}{(2\pi)^3}\frac{d^3q_2}{(2\pi)^3}\delta^{(1)}(\mathbf{q}_1)\delta^{(1)}(\mathbf{q}_2)[b_1F_2+G_2f\mu^2+\frac{b_2}{2}+fk\mu b_1\frac{\mu_2}{q_2}+f^2\mu_1^2\mu k\frac{\mu_2}{q_2}](2\pi)^3\delta_D(\mathbf{k}-\mathbf{q}_1-\mathbf{q}_2) \tag{5.4.25}$$

$$=\int\frac{d^3q_1}{(2\pi)^3}\frac{d^3q_2}{(2\pi)^3}\delta^{(1)}(\mathbf{q}_1)\delta^{(1)}(\mathbf{q}_2)[b_1F_2+G_2f\mu^2+\frac{b_2}{2}+fk\mu[\frac{\mu_2}{q_2}(b_1+f\mu_1^2)](2\pi)^3\delta_D(\mathbf{k}-\mathbf{q}_1-\mathbf{q}_2) \tag{5.4.26}$$

$$=\int\frac{d^3q_1}{(2\pi)^3}\frac{d^3q_2}{(2\pi)^3}\delta^{(1)}(\mathbf{q}_1)\delta^{(1)}(\mathbf{q}_2)[b_1F_2+G_2f\mu^2+\frac{b_2}{2}+\frac{fk\mu}{2}[\frac{\mu_1}{q_1}(b_1+f\mu_2^2)+\frac{\mu_2}{q_2}(b_1+f\mu_1^2)](2\pi)^3\delta_D(\mathbf{k}-\mathbf{q}_1-\mathbf{q}_2 \tag{5.4.27}$$

$$=\int\frac{d^3q_1}{(2\pi)^3}\frac{d^3q_2}{(2\pi)^3}\delta^{(1)}(\mathbf{q}_1)\delta^{(1)}(\mathbf{q}_2)Z_2(\mathbf{q}_1,\mathbf{q}_2)(2\pi)^3\delta_D(\mathbf{k}-\mathbf{q}_1-\mathbf{q}_2) \tag{5.4.28}$$

where in the fifth line we symmetrized the new kernel, which now can be read as

$$Z_2(\mathbf{q}_1,\mathbf{q}_2)=b_1F_2+G_2f\mu^2+\frac{fk\mu}{2}[\frac{\mu_1}{q_1}(b_1+f\mu_2^2)+\frac{\mu_2}{q_2}(b_1+f\mu_1^2)]+\frac{b_2}{2} \tag{5.4.29}$$

A similar calculations leads to the third order kernel. Before we do that, however, we need to observe that the bias scheme above is incomplete. Various tentative schemes have been introduced in the literature, since we know very little about the exact mechanism of bias. In general one can expect δ_g to depend not only on the matter δ but also on other variables that influence the assembly of galaxies from the underlying distribution. In particular, one should expect a dependence on the gravitational force. The density contrast is proportional to $\Delta\Phi$ due to the Poisson equation, so we expect that a generic expansion for δ_g will include second derivatives of the potential, i.e. the tensor $\partial_i\partial_j\Phi$. Notice that there could not be a dependence on Φ and on $\partial_i\Phi$ without further derivatives, because the Equivalence Principle tells us that one can always find a local frame in which there is no gravitational potential nor force. Similarly, one should also expect a dependence on the second derivatives of the peculiar velocity field (tidal field).

A traceless stress tensor (or *tidal* tensor) of gravitational forces can be defined as

$$K_{ij} = (\partial_i\partial_j\Phi) - \frac{1}{3}\delta_{ij}\Delta\Phi \tag{5.4.30}$$

The tensor K_{ij} is defined to be traceless because the trace part of $(\partial_i\partial_j\Phi)$ would correspond to $\Delta\Phi$, which by Poisson equation is simply proportional to δ and therefore degenerate with the other terms. With the tidal tensor, one can form the scalar

$$\mathcal{G}_2 = K_{ij}K^{ij} = (\partial_i\partial_j\Phi)^2 + \frac{1}{9}\delta_{ij}\delta^{ij}(\Delta\Phi)^2 - \frac{2}{3}(\partial_i\partial_j\Phi)\delta^{ij}(\Delta\Phi) \tag{5.4.31}$$

$$= (\partial_i\partial_j\Phi)^2 - \frac{1}{3}(\Delta\Phi)^2 \tag{5.4.32}$$

In Fourier space K_{ij} becomes

$$K_{ij}(\mathbf{k}) = (\frac{k_ik_j}{k^2} - \frac{1}{3}\delta_{ij})\delta(\mathbf{k}) \tag{5.4.33}$$

The scalar $\mathcal{G}_2$ is then of the same order as $\delta^{(2)}$. We need however to go to third order. A very general form of the bias to third order can then be taken as [9, 7]

$$\delta_g = b_1\delta + \underbrace{\frac{b_2}{2}\delta^2 + b_G\mathcal{G}_2}_{2nd} + \underbrace{\frac{b_3}{3!}\delta^3 + b_\Gamma\Gamma_3 + b_{\delta\mathcal{G}}\mathcal{G}_2\delta + b_{\mathcal{G}_3}\mathcal{G}_3}_{3rd} + ... \tag{5.4.34}$$

where all the parameters are functions of time only, and now we added yet another contribution from a similarly defined velocity stress tensor

$$\Gamma_3 = \mathcal{G}_2(\Phi_g) - \mathcal{G}_2(\Phi_v) \tag{5.4.35}$$

where Φ_g is the gravitational potential and Φ_v the velocity potential, and finally

$$\mathcal{G}_3 = K_{ij}K^{jm}K^i_m \tag{5.4.36}$$

Additional stochastic, i.e. non-deterministic, terms can also be considered, that are generally to be expected since the initial conditions are themselves random variables. In the simplest formulation in which the stochastic term is Poissonian noise, this adds to (5.4.34) a term ε whose power spectrum is just a constant, and therefore can be absorbed into the shot noise we already considered.

It turns out that the $b_3, b_{\delta\mathcal{G}}, b_{\mathcal{G}_3}$ terms are degenerate with other terms after taking into account the UV correction (see next chapter). Also a higher-derivative term $R_*\partial^2\delta$ should be added to (5.4.34), but again it can be absorbed into the UV correction. There are then overall four free bias parameters, $b = b_1, b_2, b_G, b_\Gamma$ that are only time-dependent. Adopting $\beta = f/b_1$, the generalized kernels Z_2, Z_3 can be written as

$$Z_2(\mathbf{q}_a, \mathbf{q}_b) = b_1\{F_2(\mathbf{q}_a, \mathbf{q}_b) + \beta\mu^2 G_2(\mathbf{q}_a, \mathbf{q}_b) + \frac{\beta b\mu k}{2}\left[\frac{\mu_{az}}{q_a}(1+\beta\mu_{bz}^2) + \frac{\mu_{bz}}{q_b}(1+\beta\mu_{az}^2)\right]\} + \frac{b_2}{2} + b_G S_1(\mathbf{q}_a, \mathbf{q}_b) \tag{5.4.37}$$

(already symmetrized) and

$$Z_3(\mathbf{q}_1,\mathbf{q}_2,\mathbf{q}_3) = b_1\{F_3(\mathbf{q}_1,\mathbf{q}_2,\mathbf{q}_3) + \beta\mu^2 G_3(\mathbf{q}_1,\mathbf{q}_2,\mathbf{q}_3) + \beta\mu kb[F_2(\mathbf{q}_1,\mathbf{q}_2) + \beta\mu_{12z}^2 G_2(\mathbf{q}_1,\mathbf{q}_2)]\frac{\mu_{3z}}{q_3}$$
$$+ \beta\mu kb(1+\beta\mu_{1z}^2)\frac{\mu_{23z}}{q_{23}}G_2(\mathbf{q}_2,\mathbf{q}_3) + \frac{(\beta\mu k)^2}{2}b_1^2(1+\beta\mu_{1z}^2)\frac{\mu_{2z}}{q_2}\frac{\mu_{3z}}{q_3}\}$$
$$+ 2b_G S_1(\mathbf{q}_1,\mathbf{q}_2+\mathbf{q}_3)F_2(\mathbf{q}_2,\mathbf{q}_3) + b_G b_1\beta\mu k\frac{\mu_{1z}}{q_1}S_1(\mathbf{q}_2,\mathbf{q}_3)$$
$$+ 2b_\Gamma S_1(\mathbf{q}_1,\mathbf{q}_1+\mathbf{q}_3)(F_2(\mathbf{q}_2,\mathbf{q}_3) - G_2(\mathbf{q}_2,\mathbf{q}_3)) \tag{5.4.38}$$

(to be symmetrized), where in Z_3 terms in b_2 have been discarded because degenerate with other terms, and

$$S_1(\mathbf{q}_1,\mathbf{q}_2) = \frac{(\mathbf{q}_1\cdot\mathbf{q}_2)^2}{q_1^2 q_2^2} - 1 \tag{5.4.39}$$

Double subscripts, e.g. 12, refer to $\mathbf{k}_1+\mathbf{k}_2$. All μ's are the angles wrt the line of sight $\hat{z}$, except μ_1 , which is the angle between k and k_1. All angles can be expressed in terms of μ,μ_1,ϕ_1 by the relations

$$\mu_{2z} = \frac{\mathbf{q}_2\mathbf{z}}{k_2} = \frac{(\mathbf{k}-\mathbf{q}_1)\mathbf{z}}{|\mathbf{k}-\mathbf{q}_1|} = \frac{-k\mu + q_1\mu\mu_1 + q_1(1-\mu^2)^{1/2}(1-\mu_1^2)^{1/2}\cos\phi_1}{(q_1^2+k^2-2kq_1\mu_1)^{1/2}} \tag{5.4.40}$$
$$\mu_{1z} = \frac{\mathbf{q}_1\mathbf{z}}{k_1} = \mu\mu_1 + (1-\mu^2)^{1/2}(1-\mu_1^2)^{1/2}\cos\phi_1 \tag{5.4.41}$$

and μ_{12z},μ_{23z} denote the angles between $\mathbf{k}_1+\mathbf{k}_2$ and $\hat{z}$ etc. The ϕ_1 integration is always analytical and can be included in the definition of the kernels.

Appendix: Third order kernels

At order ε^3we have (here I absorb the factors of G inside the perturbation variables and take the EdS value $f=1$; moreover, for shortness, every term d^3k etc. is meant to include $(2\pi)^3$at denominator)

$$\delta'^{(3)}_{\mathbf{k}} + \theta^{(3)}_{\mathbf{k}} = -\int(\delta^{(1)}_{k_1}\theta^{(2)}_{k_2} + \delta^{(2)}_{k_1}\theta^{(1)}_{k_2})\alpha(\mathbf{k}_1,\mathbf{k}_2)(2\pi)^3\delta_D(\mathbf{k}_1+\mathbf{k}_2-\mathbf{k})d^3k_1d^3k_2 \tag{5.4.42}$$
$$= \int\delta_{k_1}\delta_{q_2}\delta_{q_3}G_2(\mathbf{q}_2,\mathbf{q}_3)(2\pi)^3\delta_D(\mathbf{k}_1+\mathbf{q}_2+\mathbf{q}_3-\mathbf{k})\alpha(\mathbf{k}_1,\mathbf{q}_{23})d^3k_1d^3q_2d^3q_3 \tag{5.4.43}$$
$$+ \int\delta_{k_2}\delta_{q_1}\delta_{q_3}F_2(\mathbf{q}_1,\mathbf{q}_3)(2\pi)^3\delta_D(\mathbf{q}_1+\mathbf{q}_3+\mathbf{k}_2-\mathbf{k})\alpha(\mathbf{q}_{13},\mathbf{k}_2)d^3q_1d^3k_2d^3q_3 \tag{5.4.44}$$
$$= \int\delta_{k_1}\delta_{k_2}\delta_{k_3}G_2(\mathbf{k}_2,\mathbf{k}_3)(2\pi)^3\delta_D(\mathbf{k}_1+\mathbf{k}_2+\mathbf{k}_3-\mathbf{k})\alpha(\mathbf{k}_1,\mathbf{k}_{23})d^3k_1d^3k_2d^3k_3 \tag{5.4.45}$$
$$+ \int\delta_{k_1}\delta_{k_2}\delta_{k_3}F_2(\mathbf{k}_1,\mathbf{k}_3)(2\pi)^3\delta_D(\mathbf{k}_1+\mathbf{k}_2+\mathbf{k}_3-\mathbf{k})\alpha(\mathbf{k}_{13},\mathbf{k}_2)d^3k_1d^3k_2d^3k_3 \tag{5.4.46}$$
$$= \int\delta_{k_1}\delta_{k_2}\delta_{k_3}[G_2(\mathbf{k}_2,\mathbf{k}_3)\alpha(\mathbf{k}_1,\mathbf{k}_{23}) + F_2(\mathbf{k}_1,\mathbf{k}_3)\alpha(\mathbf{k}_{13},\mathbf{k}_1)](2\pi)^3\delta_D(\mathbf{k}_1+\mathbf{k}_2+\mathbf{k}_3-\mathbf{k})d^3k_1d^3k_2d^3k_3 \tag{5.4.47}$$
$$= \int\delta_{k_1}\delta_{k_2}\delta_{k_3}\alpha_3(\mathbf{k}_1,\mathbf{k}_2,\mathbf{k}_3)(2\pi)^3\delta_D(\mathbf{k}_1+\mathbf{k}_2+\mathbf{k}_3-\mathbf{k})d^3k_1d^3k_2d^3k_3 \tag{5.4.48}$$

where we defined $\mathbf{k}_{ij} = \mathbf{k}_i + \mathbf{k}_j$ and

$$\alpha_3(\mathbf{k}_1,\mathbf{k}_2,\mathbf{k}_3) = G_2(\mathbf{k}_2,\mathbf{k}_3)\alpha(\mathbf{k}_1,\mathbf{k}_{23}) + F_2(\mathbf{k}_1,\mathbf{k}_3)\alpha(\mathbf{k}_{13},\mathbf{k}_1) \tag{5.4.49}$$

For the Euler equation at 3rd order we get

$$\theta' + F\theta + S\delta = -\int [\theta_1^{(1)}\theta_2^{(2)} + \theta_1^{(2)}\theta_2^{(1)}]\beta(\mathbf{k}_1,\mathbf{k}_2)(2\pi)^3\delta_D(\mathbf{k_1}+\mathbf{k}_2-\mathbf{k})d^3k_1d^3k_2 \tag{5.4.50}$$

$$= -\int \delta_{k_1}\delta_{q_2}\delta_{q_3}G_2(\mathbf{q}_2,\mathbf{q}_3)\delta_D(\mathbf{q}_2+\mathbf{q}_3-\mathbf{k}_2)\beta(\mathbf{k}_1,\mathbf{k}_2)(2\pi)^3\delta_D(\mathbf{k_1}+\mathbf{k}_2-\mathbf{k})d^3k_1d^3k_2d^3q_2d^3q_3 \tag{5.4.51}$$

$$-\int \delta_{q_1}\delta_{q_3}\delta_{k_2}G_2(\mathbf{q}_1,\mathbf{q}_3)\delta_D(\mathbf{q}_1+\mathbf{q}_3-\mathbf{k}_1)\beta(\mathbf{k}_1,\mathbf{k}_2)(2\pi)^3\delta_D(\mathbf{k_1}+\mathbf{k}_2-\mathbf{k})d^3k_1d^3k_2d^3q_1d^3q_3 \tag{5.4.52}$$

$$= -\int \delta_{k_1}\delta_{q_2}\delta_{q_3}G_2(\mathbf{q}_2,\mathbf{q}_3)\beta(\mathbf{k}_1,\mathbf{q}_{23})(2\pi)^3\delta_D(\mathbf{k_1}+\mathbf{q}_2+\mathbf{q}_3-\mathbf{k})d^3k_1d^3q_2d^3q_3 \tag{5.4.53}$$

$$-\int \delta_{q_1}\delta_{q_3}\delta_{k_2}G_2(\mathbf{q}_1,\mathbf{q}_3)\beta(\mathbf{q}_{13},\mathbf{k}_2)(2\pi)^3\delta_D(\mathbf{q}_1+\mathbf{q}_3+\mathbf{k}_2-\mathbf{k})d^3q_1d^3k_2d^3q_3 \tag{5.4.54}$$

$$= -\int \delta_{k_1}\delta_{k_2}\delta_{k_3}G_2(\mathbf{k}_2,\mathbf{k}_3)\beta(\mathbf{k}_1,\mathbf{k}_{23})(2\pi)^3\delta_D(\mathbf{k_1}+\mathbf{k}_2+\mathbf{k}_3-\mathbf{k})d^3k_1d^3k_2d^3k_3 \tag{5.4.55}$$

$$-\int \delta_{k_1}\delta_{k_3}\delta_{k_2}G_2(\mathbf{k}_1,\mathbf{k}_3)\beta(\mathbf{k}_{13},\mathbf{k}_2)(2\pi)^3\delta_D(\mathbf{k}_1+\mathbf{k}_3+\mathbf{k}_2-\mathbf{k})d^3k_1d^3k_2d^3k_3 \tag{5.4.56}$$

$$= -\int \delta_{k_1}\delta_{k_2}\delta_{k_3}\beta_3(\mathbf{k}_1,\mathbf{k}_2,\mathbf{k}_3)(2\pi)^3\delta_D(\mathbf{k_1}+\mathbf{k}_2+\mathbf{k}_3-\mathbf{k})d^3k_1d^3k_2d^3k_3 \tag{5.4.57}$$

where

$$\beta_3(\mathbf{k}_1,\mathbf{k}_2,\mathbf{k}_3) = G_2(\mathbf{k}_2,\mathbf{k}_3)\beta(\mathbf{k}_1,\mathbf{k}_{23}) + G_2(\mathbf{k}_1,\mathbf{k}_3)\beta(\mathbf{k}_{13},\mathbf{k}_2) \tag{5.4.58}$$

We can then repeat the same steps as for the second order. We only have to change

$$G^{(3)'} = 3AG^3; \quad G^{(3)''} = 9AG^3 \tag{5.4.59}$$

so that now

$$\delta'' + F\delta' - S\delta = [(G^{(3)})'' + FG^{(3)\prime} - SG^{(3)}]\delta = (9+3F-S)AG^3\delta_k^{(3)} = 9\delta^{(3)} \tag{5.4.60}$$

and obtain

$$F_3 = \frac{7\alpha_3+2\beta_3}{18} = \frac{7[G_2(\mathbf{k}_2,\mathbf{k}_3)\alpha(\mathbf{k}_1,\mathbf{k}_{23}) + F_2(\mathbf{k}_1,\mathbf{k}_3)\alpha(\mathbf{k}_{13},\mathbf{k}_1)] + 2[G_2(\mathbf{k}_2,\mathbf{k}_3)\beta(\mathbf{k}_1,\mathbf{k}_{23}) + G_2(\mathbf{k}_1,\mathbf{k}_3)\beta(\mathbf{k}_{13},\mathbf{k}_2)]}{18} \tag{5.4.61}$$

$$= \frac{7F_2(\mathbf{k}_1,\mathbf{k}_3)\alpha(\mathbf{k}_{13},\mathbf{k}_1) + 2G_2(\mathbf{k}_1,\mathbf{k}_3)\beta(\mathbf{k}_{13},\mathbf{k}_2) + G_2(\mathbf{k}_2,\mathbf{k}_3)[7\alpha(\mathbf{k}_1,\mathbf{k}_{23}) + 2\beta(\mathbf{k}_1,\mathbf{k}_{23})]}{18} \tag{5.4.62}$$

which coincides with Eq. (5.3.59) up to a reshuffling of indexes. A similar calculation produces G_3.

Chapter 6

Spectrum and bispectrum

Quick summary

1. We can now combine the results of the previous section into the correlators: spectra and bispectra
2. Suitable "counterterms" should be added to take into account shear and viscosity of tracers
3. We show that the rules for building higher order terms can be described using "Feynman" diagrams
4. We also generalize further the kernels beyond EdS and ΛCDM by invoking general symmetry principles
5. Finally, we see how to compare the theoretical spectra to observational data

6.1 Spectrum at one loop

Let's collect the first three terms of the δ_g expansion obtained so far: (check factors of 2π in this section!)

$$\delta_g^{(1)}(\mathbf{k}) = \delta^{(1)}(\mathbf{k}) Z_1(\mathbf{k}) \tag{6.1.1}$$

$$\delta_g^{(2)}(\mathbf{k}) = \int \frac{d^3q_1}{(2\pi)^3}\frac{d^3q_2}{(2\pi)^3}\delta^{(1)}(\mathbf{q}_1)\delta^{(1)}(\mathbf{q}_2) Z_2(\mathbf{q}_1,\mathbf{q}_2)(2\pi)^3\delta_D(\mathbf{k}-\mathbf{q}_1-\mathbf{q}_2) \tag{6.1.2}$$

$$\delta_g^{(3)}(\mathbf{k}) = \int \frac{d^3q_1}{(2\pi)^3}\frac{d^3q_2}{(2\pi)^3}\frac{d^3q_3}{(2\pi)^3}\delta^{(1)}(\mathbf{q}_1)\delta^{(1)}(\mathbf{q}_2)\delta^{(1)}(\mathbf{q}_3) Z_3(\mathbf{q}_1,\mathbf{q}_2,\mathbf{q}_3)(2\pi)^3\delta_D(\mathbf{k}-\mathbf{q}_1-\mathbf{q}_2-\mathbf{q}_3) \tag{6.1.3}$$

where

$$Z_1(\mathbf{k}) = b_1 + f\mu^2 \tag{6.1.4}$$

In the rest of this section the internal momenta $\mathbf{q}_i$ will be denoted as $\mathbf{k}_i$.

In this and the next section we need to make use of Wick's theorem. This applies to correlation of Gaussian fields, i.e. to the linear density contrast $\delta^{(1)}$ (notice that $\delta^{(2)}$ and all higher order terms are of course non-Gaussian, being formed out of product of Gaussial variables). The theorem says that all odd moments vanish and all even moments can be written in terms of a sum of products of second-order ones. Schematically

$$\langle \delta_1 ... \delta_{2p+1}\rangle = 0 \tag{6.1.5}$$

$$\langle \delta_1 ... \delta_{2p}\rangle = \sum_{\text{all pairs}} \prod_{p \text{ pairs}} \langle \delta_i \delta_j\rangle \tag{6.1.6}$$

where $\delta_i = \delta^{(1)}(\mathbf{k}_i)$. For instance

$$\langle \delta_1\delta_2\delta_3\delta_4\rangle = \langle\delta_1\delta_2\rangle\langle\delta_3\delta_4\rangle + \langle\delta_1\delta_3\rangle\langle\delta_2\delta_4\rangle + \langle\delta_1\delta_4\rangle\langle\delta_2\delta_3\rangle \tag{6.1.7}$$

As we have already mentioned, the linear power spectrum including bias and redshift distortion is

$$P_{gg,L} = \langle \delta_g^{(1)} \delta_g^{(1)*} \rangle = b^2 (1 + \beta \mu^2)^2 P_L \tag{6.1.8}$$

where P_L is the matter power spectrum at any z, so the factors of G are now included in its definition (the factor of V appearing in (2.5.7) can be conveniently put to unity; they would anyway cancel out in the final result). Analogously, the power spectrum up to fourth order in the linear δ (the third cancels out because the linear δ are Gaussian and all odd moments of Gaussian variables vanish) is then

$$\begin{aligned} P_{gg}(k) &= \langle \delta_g(\mathbf{k}) \delta_g(\mathbf{k}) \rangle = \langle (\delta^{(1)} + \delta^{(2)} + \delta^{(3)})_g (\delta^{(1)*} + \delta^{(2)*} + \delta^{(3)*})_g \rangle \\ &= \langle \delta_g^{(1)} \delta_g^{(1)*} \rangle + \langle \delta_g^{(2)} \delta_g^{(2)*} \rangle + \langle \delta_g^{(1)} \delta_g^{(3)*} \rangle + \langle \delta_g^{(3)} \delta_g^{(1)*} \rangle = (b + f\mu^2)^2 P_L \qquad (6.1.9) \\ &+ \int \langle \delta_{k_1}^{*(1)} \delta_{k_2}^{*(1)} \delta_{k_3}^{(1)} \delta_{k_4}^{(1)} \rangle Z_2(\mathbf{k}_1, \mathbf{k}_2) Z_2(\mathbf{k}_3, \mathbf{k}_4) (2\pi)^3 \delta_D(\mathbf{k}_1 + \mathbf{k}_2 - \mathbf{k}) (2\pi)^3 \delta_D(\mathbf{k}_3 + \mathbf{k}_4 - \mathbf{k}) \frac{d^3k_1}{(2\pi)^3} \frac{d^3k_2}{(2\pi)^3} \frac{d^3k_3}{(2\pi)^3} \frac{d^3k_4}{(2\pi)^3} \\ &+ 2(b + f\mu^2) \int \langle \delta_k^{*(1)} \delta_{k_1}^{(1)} \delta_{k_2}^{(1)} \delta_{k_3}^{(1)} \rangle Z_3(\mathbf{k}_1, \mathbf{k}_2, \mathbf{k}_3) (2\pi)^3 \delta_D(\mathbf{k}_1 + \mathbf{k}_2 + \mathbf{k}_3 - \mathbf{k}) \frac{d^3k_1}{(2\pi)^3} \frac{d^3k_2}{(2\pi)^3} \frac{d^3k_3}{(2\pi)^3} \qquad (6.1.10) \end{aligned}$$

Now since the linear $\delta^{(1)}$'s are supposed to be Gaussian variables, one has due to Wick's theorem that (the superscript (1) is understood)

$$\langle \delta_{k_1}^* \delta_{k_2}^* \delta_{k_3} \delta_{k_4} \rangle = \langle \delta_{k_1}^* \delta_{k_2}^* \rangle \langle \delta_{k_3} \delta_{k_4} \rangle + \langle \delta_{k_1}^* \delta_{k_3} \rangle \langle \delta_{k_2}^* \delta_{k_4} \rangle + \langle \delta_{k_1}^* \delta_{k_4} \rangle \langle \delta_{k_2}^* \delta_{k_3} \rangle \tag{6.1.11}$$

where

$$\langle \delta_{k_1} \delta_{k_2}^* \rangle = \langle \delta_{k_1} \delta_{-k_2} \rangle = (2\pi)^3 P_L(k_1) \delta_D(\mathbf{k}_1 - \mathbf{k}_2) \tag{6.1.12}$$

So we have, e.g. for the first term, $\langle \delta_{k_1}^* \delta_{k_2}^* \rangle = (2\pi)^3 P_L(k_1) \delta_D(\mathbf{k}_1 + \mathbf{k}_2)$ and therefore

$$\begin{aligned} &\int \langle \delta_{k_1}^* \delta_{k_2}^* \rangle \langle \delta_{k_3} \delta_{k_4} \rangle Z_2(\mathbf{k}_1, \mathbf{k}_2) Z_2(\mathbf{k}_3, \mathbf{k}_4) (2\pi)^3 \delta_D(\mathbf{k}_1 + \mathbf{k}_2 - \mathbf{k}) (2\pi)^3 \delta_D(\mathbf{k}_3 + \mathbf{k}_4 - \mathbf{k}) \frac{d^3k_1}{(2\pi)^3} \frac{d^3k_2}{(2\pi)^3} \frac{d^3k_3}{(2\pi)^3} \frac{d^3k_4}{(2\pi)^3} = \\ &\int P_L(k_1) \delta_D(\mathbf{k}_1 + \mathbf{k}_2) P_L(k_3) \delta_D(\mathbf{k}_3 + \mathbf{k}_4) Z_2(\mathbf{k}_1, \mathbf{k}_2) Z_2(\mathbf{k}_3, \mathbf{k}_4) \delta_D(\mathbf{k}_1 + \mathbf{k}_2 - \mathbf{k}) \delta_D(\mathbf{k}_3 + \mathbf{k}_4 - \mathbf{k}) d^3k_1 d^3k_2 d^3k_3 d^3k_4 = \\ &\int P_L(k_1) P_L(k_3) Z_2(\mathbf{k}_1, -\mathbf{k}_1) Z_2(\mathbf{k}_3, -\mathbf{k}_3) \delta_D(-\mathbf{k}) \delta_D(-\mathbf{k}) d^3k_1 d^3k_3 = 0 \end{aligned} \tag{6.1.13}$$

since $\delta_D(-\mathbf{k})$ vanish for all $\mathbf{k}$ except $\mathbf{k} = 0$. The other two terms instead do not vanish and give two identical contributions of this form (considering the last one):

$$\int P_L(k_1) \delta_D(\mathbf{k}_1 - \mathbf{k}_4) P_L(k_2) \delta_D(\mathbf{k}_2 - \mathbf{k}_3) Z_2(\mathbf{k}_1, \mathbf{k}_2) Z_2(\mathbf{k}_3, \mathbf{k}_4) \delta_D(\mathbf{k}_1 + \mathbf{k}_2 - \mathbf{k}) \delta_D(\mathbf{k}_3 + \mathbf{k}_4 - \mathbf{k}) d^3k_1 d^3k_2 d^3k_3 d^3k_4 = \tag{6.1.14}$$

$$\int P_L(k_1) \delta_D(\mathbf{k}_1 - \mathbf{k}_4) P_L(|\mathbf{k} - \mathbf{k}_1|) \delta_D(\mathbf{k} - \mathbf{k}_1 - \mathbf{k}_3) Z_2(\mathbf{k}_1, \mathbf{k} - \mathbf{k}_1) Z_2(\mathbf{k}_3, \mathbf{k}_4) \delta_D(\mathbf{k}_3 + \mathbf{k}_4 - \mathbf{k}) d^3k_1 d^3k_3 d^3k_4 = \tag{6.1.15}$$

$$\int P_L(k_1) \delta_D(\mathbf{k}_1 - \mathbf{k}_4) P_L(|\mathbf{k} - \mathbf{k}_1|) \delta_D(\mathbf{k} - \mathbf{k}_1 - \mathbf{k} + \mathbf{k}_4) Z_2(\mathbf{k}_1, \mathbf{k} - \mathbf{k}_1) Z_2(\mathbf{k} - \mathbf{k}_4, \mathbf{k}_4) d^3k_1 d^3k_4 = \tag{6.1.16}$$

$$\int P_L(k_1) \delta_D(\mathbf{k}_1 - \mathbf{k}_4) P_L(|\mathbf{k} - \mathbf{k}_1|) \delta_D(-\mathbf{k}_1 + \mathbf{k}_4) Z_2(\mathbf{k}_1, \mathbf{k} - \mathbf{k}_1) Z_2(-\mathbf{k} + \mathbf{k}_1, \mathbf{k}_1) d^3k_1 d^3k_4 \tag{6.1.17}$$

Here we estimated the product of Dirac deltas as follows (already introduced in Eq. (2.5.17)):

$$\int \delta_D(\mathbf{k}_1 - \mathbf{k}_4) \delta_D(\mathbf{k}_1 - \mathbf{k}_4) d^3k_1 = \int \frac{e^{-i\mathbf{x}(\mathbf{k}_1 - \mathbf{k}_4)}}{(2\pi)^3} d^3x \delta_D(\mathbf{k}_1 - \mathbf{k}_4) d^3k_1 = \int \frac{1}{(2\pi)^3} d^3x = \frac{V}{(2\pi)^3} \tag{6.1.18}$$

Then we get (putting again $V = 1$)

$$\int P_L(k_1)P_L(|\mathbf{k}-\mathbf{k}_1|)Z_2^2(\mathbf{k}_1,\mathbf{k}-\mathbf{k}_1)\frac{d^3k_1}{(2\pi)^3} \equiv P_{22} \tag{6.1.19}$$

Similarly, for the last term in Eq. (6.1.10)

$$\langle\delta_k^*\delta_{k_1}\delta_{k_2}\delta_{k_3}\rangle = \langle\delta_k^*\delta_{k_1}\rangle\langle\delta_{k_2}\delta_{-k_3}^*\rangle + (1\leftrightarrow 2) + (2\leftrightarrow 3) \tag{6.1.20}$$

and each of the three term equals

$$\int \langle\delta_k^*\delta_{k_1}\rangle\langle\delta_{k_2}\delta_{-k_3}^*\rangle Z_3(\mathbf{k}_1,\mathbf{k}_2,\mathbf{k}_3)(2\pi)^3\delta_D(\mathbf{k}_1+\mathbf{k}_2+\mathbf{k}_3-\mathbf{k})\frac{d^3k_1}{(2\pi)^3}\frac{d^3k_2}{(2\pi)^3}\frac{d^3k_3}{(2\pi)^3} = \tag{6.1.21}$$

$$(2\pi)^6\int P_L(k)\delta_D(\mathbf{k}-\mathbf{k}_1)P_L(k_2)\delta_D(\mathbf{k}_2+\mathbf{k}_3)Z_3(\mathbf{k}_1,\mathbf{k}_2,\mathbf{k}_3)(2\pi)^3\delta_D(\mathbf{k}_1+\mathbf{k}_2+\mathbf{k}_3-\mathbf{k})\frac{d^3k_1}{(2\pi)^3}\frac{d^3k_2}{(2\pi)^3}\frac{d^3k_3}{(2\pi)^3} = \tag{6.1.22}$$

$$(2\pi)^6\int P_L(k)\delta_D(\mathbf{k}-\mathbf{k}_1)P_L(k_2)\delta_D(\mathbf{k}-\mathbf{k}_1)Z_3(\mathbf{k}_1,\mathbf{k}_2,\mathbf{k}-\mathbf{k}_1-\mathbf{k}_2)\frac{d^3k_1}{(2\pi)^3}\frac{d^3k_2}{(2\pi)^3} = \tag{6.1.23}$$

$$\int P_L(k)P_L(k_2)Z_3(\mathbf{k}_1,\mathbf{k}_2,-\mathbf{k}_2)\frac{d^3k_2}{(2\pi)^3} = \tag{6.1.24}$$

$$P_L(k)\int P_L(k_1)Z_3(\mathbf{k},\mathbf{k}_1,-\mathbf{k}_1)\frac{d^3k_1}{(2\pi)^3} \equiv P_{13} \tag{6.1.25}$$

(renaming $\mathbf{k}_2$ into $\mathbf{k}_1$ in the last step). So finally the one-loop spectrum for galaxies in redshift space is

$$P_{gg}(\mathbf{k},z) = (b+f\mu^2)^2P_L(\mathbf{k},z) + 2P_{22}(\mathbf{k},z) + 6(b+f\mu^2)P_{13}(\mathbf{k},z) \tag{6.1.26}$$

The shot noise spectrum Eq. (2.5.28) should also be added when comparing to obervations. It is convenient to discard from P_{gg} a constant term that arises in the limit $k\to 0$, since it can be absorbed into the constant shot noise.

Notice that an additive constant in Z_3 would produce a term $const\times P_L\int P_L(k_1)d^3k_1/(2\pi)^3 \sim const\times P_L$ which can be absorbed into the power spectrum normalization. This is the reason why the b_3 term in the bias expansion Eq. (5.4.34) can be neglected.

The integrations in P_{22}, P_{13} can be best performed by taking the z-axis in the $\mathbf{k}$-direction, and then using spherical coordinates

$$\mathbf{k}_1 = k_1\left\{\sqrt{1-\mu_1^2}\cos\phi_1, \sqrt{1-\mu_1^2}\sin\phi_1, \mu_1\right\} \tag{6.1.27}$$

$$\mathbf{k} = k\{0,0,1\} \tag{6.1.28}$$

The ϕ_1 integral is analytical, so we are left with at most double integrals. For instance we have in EdS

$$\int Z_2^2(\mathbf{k}_1,\mathbf{k}-\mathbf{k}_1)d\phi_1 = \tag{6.1.29}$$

$$[98r^2\left(r^2-2\mu_1 r+1\right)^2]^{-1}\pi\left\{r\left(\mu_1^2(2b_1(7f+5)-14b_G+f(7f+6))-7b_1f-3b_1-7b_2+14b_G+f\right)\right. \tag{6.1.30}$$

$$\left.-7(f+1)\mu_1(b_1+f)-7b_2r^3+14b_2\mu_1r^2\right\}^2 \tag{6.1.31}$$

and

$$\int Z_3(\mathbf{k},\mathbf{k}_1,-\mathbf{k}_1)d\phi_1 d\mu_1 = \tag{6.1.32}$$

$$(10584r^5)^{-1}\pi[-6\left(r^2-1\right)^3\tanh^{-1}\left(\frac{2r}{r^2+1}\right)\left(b_1\left(101r^2-164\right)+21\left(r^2-1\right)(4b_\Gamma-5c_2)\right) \tag{6.1.33}$$

$$++4b_1r\left(303r^6-1300r^4-2203r^2+492\right)+84r\left(r^2+1\right)\left(3r^4-14r^2+3\right)(4b_\Gamma-5c_2)] \tag{6.1.34}$$

where $r = k_1/k$ and $c_2 = \frac{10}{7}b_1 - 2b_G$.

6.2 UV correction

This non-linear power spectrum, also called one-loop $P(k)$, is however still not a good approximation to N-body simulations even for relatively small $k < 0.2h$/Mpc. What is still missing from the picture is the stress tensor defined in Eq. (1.2.36) for the tracers

$$\sigma_{ij} = p\delta_{ij} - \eta(\partial_i v_j + \partial_j v_i - \frac{2}{3}\delta_{ij}\partial_k v^k) - \zeta\delta_{ij}\partial_k v^k \tag{6.2.1}$$

As already discussed, this tensor goes beyond the single-stream approximation so far employed. The stress tensor can be generalized and expanded to first order as follows [6]

$$\sigma^{ij} = p_b\delta^{ij} + \rho_b[c_s^2\delta\delta^{ij} - \frac{3}{4}\frac{c_{sv}^2}{\mathcal{H}}(\partial^i v^j + \partial^j v^i - \frac{2}{3}\delta^{ij}\partial_k v^k) - \frac{c_{bv}^2}{\mathcal{H}}\delta^{ij}\partial_k v^k] + ... \tag{6.2.2}$$

(do not confound the Kronocker symbol δ^{ij} with the density contrast δ) where the subscript b stands for background values. In practice, we redefined

$$\eta = \frac{3}{4}\rho_b\frac{c_{sv}^2}{\mathcal{H}} \tag{6.2.3}$$

$$\zeta = \rho_b\frac{c_{bv}^2}{\mathcal{H}} \tag{6.2.4}$$

and introduced the perturbed pressure $p = p_b + c_s^2\rho_b\delta$. The three time-dependent velocity factors, c_s, c_{sv}, c_{bv}, are new free parameters, that can be measured in N-body simulations or used as free parameter to fit the data. Notwithstanding the notation, they are not supposed to be positive definite. This stress tensor happens to be roughly of the same order as the one-loop corrections [6], so we can ignore the "..." in Eq. (6.2.2), even if we take δ, v^i at first order. Intuitively, we can consider the pressure and viscosity coefficients $c_{s,sv,bv}$ as first-order entities themselves, i.e. carrying a factor of ε.

The term in Eq. (1.2.31) is

$$\frac{1}{\rho_b}\partial_j\sigma^{ij} = c_s^2\partial^i\delta - \frac{3}{4}\frac{c_{sv}^2}{\mathcal{H}}(\partial^i\partial_j v^j + \Delta v^i - \frac{2}{3}\partial^i\partial_k v^k) - \frac{c_{bv}^2}{\mathcal{H}}\partial^i\partial_k v^k \tag{6.2.5}$$

In terms of $\theta = ik_i v^i/\mathcal{H}$ and in Fourier space this is

$$\frac{1}{\rho_b}\partial_j\sigma^{ij}(\mathbf{k}) = i[c_s^2 k^i\delta - \frac{3}{4}c_{sv}^2(k^i\theta + k^i\theta - \frac{2}{3}k^i\theta) - c_{bv}^2 k^i\theta] = ik^i[c_s^2\delta(\mathbf{k}) - c_v^2\theta(\mathbf{k})] = ik^i[c_s^2 + c_v^2 f]\delta(\mathbf{k}) \tag{6.2.6}$$

with $c_v^2 = c_{sv}^2 + c_{bv}^2$ and where we also replaced $c_v^2\theta = -c_v^2 f\delta$. Assuming now that c_v^2 is of order ε^2, and δ of order ε^1, implies that the expression on the rhs of the previous equation is effectively third order. Now, if we add this term to the Euler equation (5.3.24), we get at third order

$$\theta'^{(3)} + F\theta^{(3)} + S\delta^{(3)} - (c_s^2 + c_v^2 f)k^2\delta^{(1)} = -G^3 f^3\int \delta_1^{(1)}\delta_2^{(1)}\delta_3^{(1)}\beta_3(\mathbf{k}_1,\mathbf{k}_2,\mathbf{k}_3)\delta_D(\mathbf{k}_1+\mathbf{k}_2+\mathbf{k}_3-\mathbf{k})\frac{d^3k_1}{(2\pi)^3}\frac{d^3k_2}{(2\pi)^3}\frac{d^3k_3}{(2\pi)^3} \tag{6.2.7}$$

Carrying the perturbation theory with the extra pressure and viscosity terms we obtain that $\delta^{(3)}$ acquires a correction

$$\delta_{s,v}^{(3)} \sim (c_s^2 + c_v^2 f)k^2\delta^{(1)} \tag{6.2.8}$$

In the power spectrum, this will produce an additional *negative* term, often called a *counterterm*, that at the lowest non-trivial order is proportional to

$$P_{\rm ctr} \equiv \langle\delta^{(1)}\delta_{s,v}^{(3)}\rangle \sim (c_s^2 + c_v^2 f)k^2\langle\delta^{(1)}\delta^{(1)}\rangle = -2c_0 P_L(k)k^2 \tag{6.2.9}$$

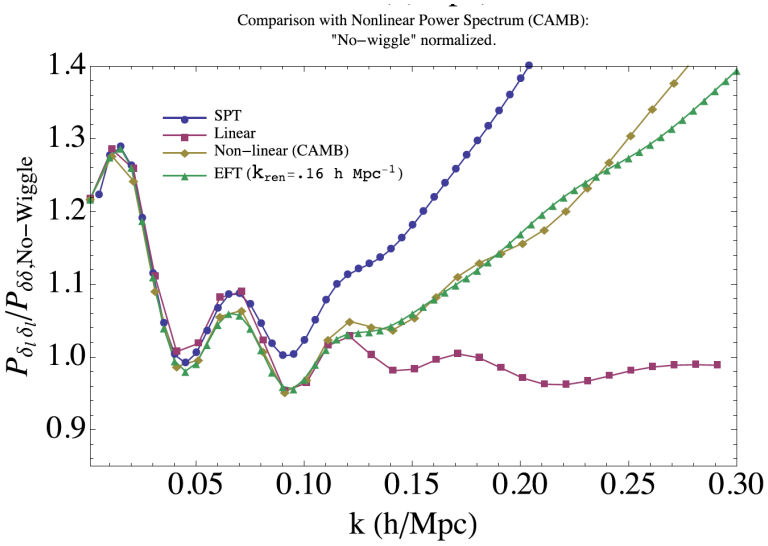

Figure 6.2.1: Comparison of SPT and SPT with counterterms (denoted as EFT here) with a fit to N-body provided in CAMB. From [6].

where $c_0 \equiv -\frac{1}{2}(c_s^2 + c_v^2 f)$. Since this correction increases with k^2, it will be particularly important at small scales; for this reason is also called UV correction. The fact that the correction is negative helps correcting the divergent behavior of the one-loop terms at high k.

To further improve the agreement with N-body simulations, one can add additional semi-empirical terms, all called generically counterterms (see e.g. [7]), of the form (see Fig. 6.4.1)

$$P_{\rm ctr} = -2P_L(k)k^2(c_0 + c_2\beta\mu^2 + c_4\beta^2\mu^4) \tag{6.2.10}$$

Typical values for c_i are around 1 $({\rm Mpc}/h)^2$ but one should leave them as free time-dependent parameters in a real data analysis. The two additional terms depend on μ^2, because they are supposed to improve the modeling of the finger-of-God effect, which smooths the power spectrum by a factor $e^{-k^2\sigma_v^2\mu^2}$ (see Eq. 3.5.21), where σ_v is the velocity dispersion of galaxies inside a halo, proportional to the growth factor f. The Taylor expansion of the smoothing function produces powers of $k^2f^2\mu^2$ which are represented by the $c_{2,4}$ terms. These terms occurs along the line of sight, and vanish for transverse directions $\mu = 0$. So finally the theoretical model for the galaxy power spectrum in redshift space is

$$P_{gg}(k,\mu,z) = Z_1^2 P_L + 2P_{22} + 6Z_1P_{31} - 2P_Lk^2(c_0 + c_2\beta\mu^2 + c_4\beta^2\mu^4) \tag{6.2.11}$$

6.3 Diagrams

The corrections just evaluated are called one-loop following the terminology of quantum field theory. The idea is to associate to each term a diagram. For the m-th loop n-point spectrum, one should draw n points, and connect them in all possible ways with internal lines (the dashed lines in Fig. 6.3.1) such that they describe m loops. Diagram that can be continuously deformed one into another without cutting lines are considered equivalent. Each internal line is labeled by a momentum $\mathbf{q}_i$ associated to a factor of P_L. At zero loop, the diagram is two points joined by a single lines (adding any other line between the two points would create a loop). Two external lines, labeled by $\mathbf{k}$, can also be added or are understood. In this trivial case, the diagram is then just a single continuous line (a *tree* diagram). At one loop, we draw all diagrams that connect two points with internal lines forming only one loop, as in Fig. 6.3.1. Each vertex (i.e. a point with p internal lines) represents a factor $\delta^{(p)}$ and to it we associate a kernel of order p. For instance, the third diagram for P in the figure representes $\delta^{(1)}\delta^{(3)} \sim Z_1Z_3$. To each diagram we associate also a Dirac delta for all the momenta $\delta_D(k - \sum_i q_i)$ that ensures conservation of momenta. Here, k labels the external lines. Each diagram should be

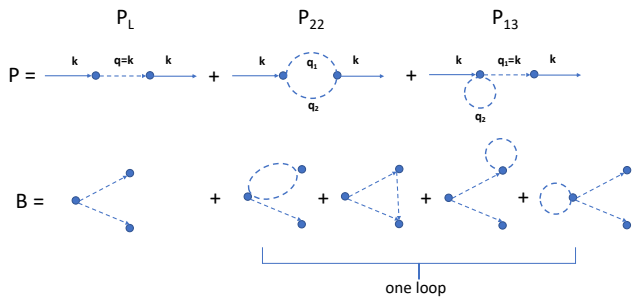

Figure 6.3.1: Diagrammatic expansion of spectrum and bispectrum. For the bispectrum we did not draw the external lines for clarity.

counted according to how many symmetric ways can be built: for instance, the loop in P_{13} can be on the first or second point, and therefore should be counted twice. To each element (vertices, loops, internal and external lines) there is an associated factor that allows to write down at once the final amplitude. More detals in e.g. [9].

6.4 Bispectrum

The power spectum for galaxies in redshift space is defined as

$$(2\pi)^3\delta_D(\mathbf{k}_1+\mathbf{k}_2)P(\mathbf{k}_1,\mathbf{k}_2) \equiv \langle\delta_g(\mathbf{k}_1)\delta_g(\mathbf{k}_2)\rangle \tag{6.4.1}$$

Analogously, the bispectrum is defined as

$$(2\pi)^3\delta_D(\mathbf{k}_1+\mathbf{k}_2+\mathbf{k}_3)B_g(\mathbf{k}_1,\mathbf{k}_2,\mathbf{k}_3) \equiv \langle\delta_g(\mathbf{k}_1)\delta_g(\mathbf{k}_2)\delta_g(\mathbf{k}_3)\rangle \tag{6.4.2}$$

$$= \langle(\delta^{(1)}+\delta^{(2)}+..)_{g\mathbf{k}_1}(\delta^{(1)}+\delta^{(2)}+...)_{g\mathbf{k}_2}(\delta^{(1)}+\delta^{(2)}+...)_{g\mathbf{k}_3}\rangle \tag{6.4.3}$$

Since the linear density contrast is a Gaussian field, the odd moments vanish, so that $\langle\delta_g^{(1)}(\mathbf{k}_1)\delta_g^{(1)}(\mathbf{k}_2)\delta_g^{(1)}(\mathbf{k}_3)\rangle = 0$. The first non-trivial term, called *tree-level* term, is therefore

$$B_g(\mathbf{k}_1,\mathbf{k}_2,\mathbf{k}_3) = \langle\delta_g^{(1)}(\mathbf{k}_1)\delta_g^{(1)}(\mathbf{k}_2)\delta_g^{(2)}(\mathbf{k}_3)\rangle + \text{cyclic} \tag{6.4.4}$$

Here *cyclic* means that we should add the terms $\langle\delta_g^{(1)}(\mathbf{k}_1)\delta_g^{(2)}(\mathbf{k}_2)\delta_g^{(1)}(\mathbf{k}_3)\rangle, \langle\delta_g^{(2)}(\mathbf{k}_1)\delta_g^{(1)}(\mathbf{k}_2)\delta_g^{(1)}(\mathbf{k}_3)\rangle$. Then we obtain

$$B_g(\mathbf{k}_1,\mathbf{k}_2,\mathbf{k}_3) = Z_1(k_1)Z_1(k_2)\langle\delta^{(1)}(\mathbf{k}_1)\delta^{(1)}(\mathbf{k}_2)\delta_g^{(2)}(\mathbf{k}_3)\rangle + \text{cyclic} \tag{6.4.5}$$

with $\sum\mathbf{k}_i = 0$. Since $\mathbf{k}_3 = -\mathbf{k}_1 - \mathbf{k}_2$, we have

$$\langle\delta^{(1)}(\mathbf{k}_1)\delta^{(1)}(\mathbf{k}_2)\delta_g^{(2)}(\mathbf{k}_3)\rangle = \tag{6.4.6}$$

$$\int\frac{d^3q_1}{(2\pi)^3}\frac{d^3q_2}{(2\pi)^3}\langle\delta^{(1)}(\mathbf{k}_1)\delta^{(1)}(\mathbf{k}_2)\delta^{(1)}(\mathbf{q}_1)\delta^{(1)}(\mathbf{q}_2)\rangle \times Z_2(\mathbf{q}_1,\mathbf{q}_2)\delta_D(-\mathbf{k}_1-\mathbf{k}_2-\mathbf{q}_1-\mathbf{q}_2) \tag{6.4.7}$$

$$= \int\frac{d^3q_1}{(2\pi)^3}\frac{d^3q_2}{(2\pi)^3}\{P_L(\mathbf{k}_1)\delta_D(\mathbf{k}_1+\mathbf{k}_2)P_L(\mathbf{q}_1)\delta_D(\mathbf{q}_1+\mathbf{q}_2) \tag{6.4.8}$$

$$+ P_L(\mathbf{k}_1)\delta_D(\mathbf{k}_1+\mathbf{q}_1)P_L(\mathbf{k}_2)\delta_D(\mathbf{k}_2+\mathbf{q}_2) \tag{6.4.9}$$

$$+ P_L(\mathbf{k}_1)\delta_D(\mathbf{k}_1+\mathbf{q}_2)P_L(\mathbf{k}_2)\delta_D(\mathbf{k}_2+\mathbf{q}_1)\} \tag{6.4.10}$$

$$\times (Z_2(\mathbf{q}_1,\mathbf{q}_2)\delta_D(-\mathbf{k}_1-\mathbf{k}_2-\mathbf{q}_1-\mathbf{q}_2) \tag{6.4.11}$$

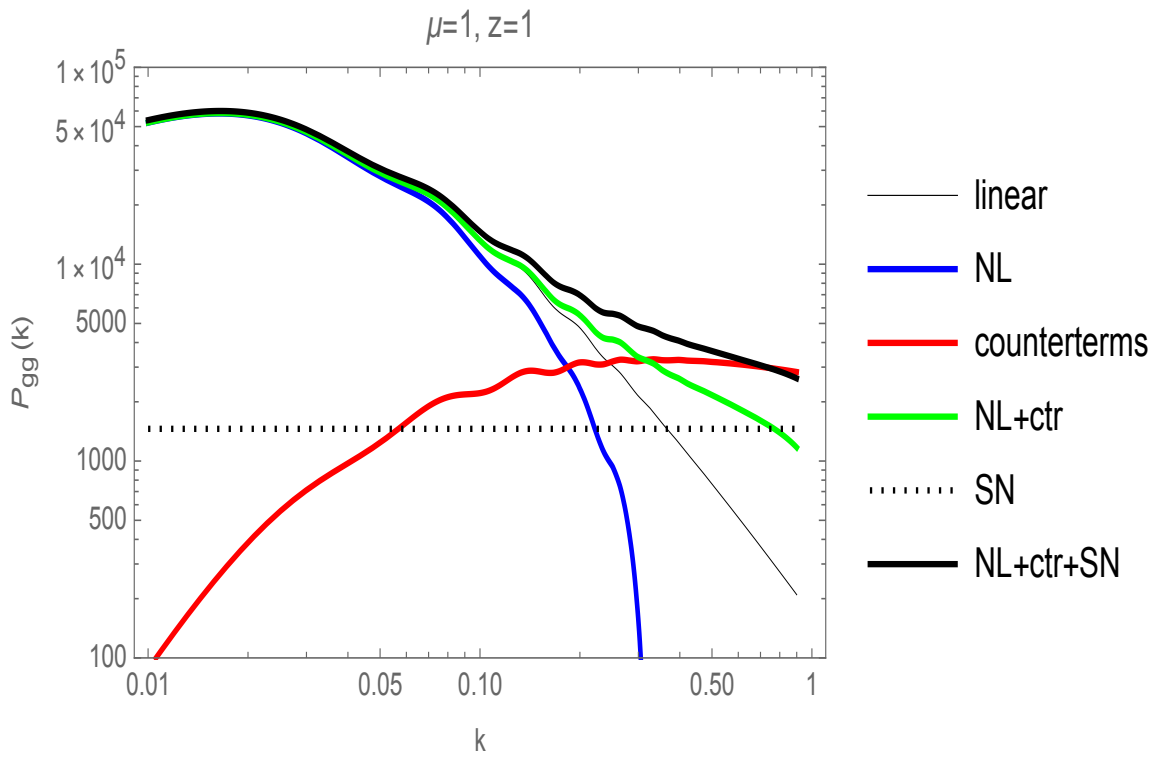

Figure 6.4.1: Linear and non-linear spectra at $z = 1$.

The first term in curly brackets vanishes, since $\delta_D(\mathbf{q}_1 + \mathbf{q}_2)$ implies $\mathbf{q}_2 = -\mathbf{q}_1$, but $Z_2(\mathbf{q}_1, -\mathbf{q}_1) = 0$ due to the property (5.3.52), that is respected also by Z_2. The second and third term are identical under exchange of $\mathbf{q}_1, \mathbf{q}_2$ and therefore

$$B_g(\mathbf{k}_1, \mathbf{k}_2, \mathbf{k}_3) = 2Z_1(\mathbf{k}_1)Z_1(\mathbf{k}_2)\times \tag{6.4.12}$$

$$\int \frac{d^3q_1}{(2\pi)^3}\frac{d^3q_2}{(2\pi)^3} P_L(\mathbf{k}_1)\delta_D(\mathbf{k}_1+\mathbf{q}_1)P_L(\mathbf{k}_2)\delta_D(\mathbf{k}_2+\mathbf{q}_2)Z_2(\mathbf{q}_1,\mathbf{q}_2)\delta_D(-\mathbf{k}_1-\mathbf{k}_2-\mathbf{q}_1-\mathbf{q}_2) + \text{cyclic} \tag{6.4.13}$$

$$= 2Z_1(\mathbf{k}_1)Z_1(\mathbf{k}_2)Z_2(\mathbf{k}_1,\mathbf{k}_2)P_L(\mathbf{k}_1)P_L(\mathbf{k}_2) + \text{cyclic} \tag{6.4.14}$$

where we used the symmetry $Z_2(-\mathbf{k}_1, -\mathbf{k}_2) = Z_2(\mathbf{k}_1, \mathbf{k}_2)$. This is the tree-level bispectrum, that is proportional to the square of the linear spectra and is therefore of the same order as the spectrum 1-loop corrections. The expression for the four one-loop bispectra are given in e.g. [4]**, [11]**.

6.5 Generalized kernels and symmetry conditions

The perturbation theory we have seen so far has been developped for models that obey the standard conservation and Euler equations. This approach can however be generalized to any model that satisfy some general symmetry requirement. We give here only a very sketchy summary following Ref. [8], to which we refer for all the details. We have seen that SPT depends on two crucial "interaction" terms (Eq. 5.3.26), namely

$$\alpha = \frac{(\mathbf{k}_1+\mathbf{k}_2)}{2}\left(\frac{\mathbf{k}_1}{k_1^2}+\frac{\mathbf{k}_2}{k_2^2}\right) = 1 + \frac{1}{2}\mathbf{k}_1\mathbf{k}_2\left(\frac{1}{k_1^2}+\frac{1}{k_2^2}\right) \tag{6.5.1}$$

$$\beta = \frac{(\mathbf{k}_1+\mathbf{k}_2)^2(\mathbf{k}_1\mathbf{k}_2)}{2k_1^2k_2^2} \tag{6.5.2}$$

The main idea is to write down all possible such terms that obey general principles. These requirements can be summarized as

1. Equivalence principle
2. Invariance under a general time-dependent translation, dubbed Extended Galilean Invariance (EGI)

$$\tau \to \tilde{\tau} = \tau; \quad \mathbf{x} \to \tilde{\mathbf{x}} + \mathbf{d}(\tau) \tag{6.5.3}$$

   The standard fluidodynamics equations satisfy this invariance, up to a redefinition of $\mathbf{v}$ and Φ.

3. Mass and momentum invariance

$$\int d^3x\, \delta(x,\tau) = 0 \tag{6.5.4}$$

$$\int d^3x\, \mathbf{x}\delta(x,\tau) = 0 \tag{6.5.5}$$

4. Rotational invariance

Additionally, the symmetry of the multi-dimensional integration can be translated into the symmetry of the kernels under exchange of any pairs of momenta, e.g. $F_2(\mathbf{k}_1,\mathbf{k}_2) = F_2(\mathbf{k}_2,\mathbf{k}_1)$. These symmetries are indeed satisfied by the conservation, Euler, and Poisson equation, as discussed in e.g. [14], once appropriate transformation rules for $\delta, \mathbf{v}$, and Φ are established (see below). The mass and momentum constraints, however, do not apply in general to tracers: galaxies, for instance, can merge and possibly break up, and therefore their number density is not conserved (mass is conserved but we can only *count* the galaxies, not measure their mass).

The equations we are considering here are the same discussed in Sec. 5.1:

$$\dot{\delta} = -\nabla(1+\delta)\mathbf{v} \tag{6.5.6}$$

$$\dot{\mathbf{v}} + \mathcal{H}\mathbf{v} = -\nabla(\mathbf{v}\cdot\nabla\mathbf{v}) + \nabla\phi \tag{6.5.7}$$

$$\nabla^2\phi = \frac{3}{2}\mathcal{H}^2\Omega\delta \tag{6.5.8}$$

Here, the perturbation variables $\delta, \mathbf{v}, \phi$ are all functions of $\mathbf{x}, \tau$ (τ being the conformal time). In the Poisson equation we also included the density fraction $\Omega = 8\pi\rho a^2/3\mathcal{H}^2$. The background variables $a, \mathcal{H}, \rho, \Omega$ are, of course, functions of time alone.

The invariance under EGI can be demonstrated by inserting the following rescalings into Eqs. (5.1.1-5.1.3):

$$\tilde{\tau} = \tau \tag{6.5.9}$$

$$\tilde{\mathbf{x}} = \mathbf{x} + \mathbf{d}(\tau) \tag{6.5.10}$$

$$\tilde{\delta}(\tilde{\mathbf{x}},\tilde{\tau}) = \delta(\mathbf{x},\tau) \tag{6.5.11}$$

$$\tilde{\mathbf{v}}(\tilde{\mathbf{x}},\tilde{\tau}) = \mathbf{v}(\mathbf{x},\tau) + \dot{\mathbf{d}}(\tau) \tag{6.5.12}$$

$$\tilde{\phi}(\tilde{\mathbf{x}},\tilde{\tau}) = \phi(\mathbf{x},\tau) - [\ddot{\mathbf{d}}(\tau) + \mathcal{H}\dot{\mathbf{d}}(\tau)]\cdot\mathbf{x} \tag{6.5.13}$$

The EGI can be seen as a manifestation of general covariance for non-relativistic particles. In fact, it can be employed to settle the observer into an inertial frame. It includes as special cases the ordinary Galileian invariance ($\mathbf{d} = \mathbf{v}_0\tau$) and a constant-acceleration ($\mathbf{d} = \frac{1}{2}\mathbf{a}_0\tau^2$). Since the potential is in general not constant, also the displacement $\mathbf{d}(\tau)$ has to be time-dependent. The possibility of finding an inertial frame depends of course on the validity of the Equivalence Principle for all the particles. The EGI therefore, contrary to the mass and momentum symmetries, also applies to tracers (e.g. galaxies) as long as they obey the Equivalence Principle.

The mass and momentum invariance are obviously satisfied. In fact

$$\int \delta(x)d^3x = \frac{\frac{1}{V}\int \rho(x)d^3x - \frac{1}{V}\int \rho_0 d^3x}{\rho_0/V} = \frac{\rho_0 - \rho_0}{\rho_0/V} = 0 \tag{6.5.14}$$

while the second condition defines a center of mass position $\mathbf{R}$ such that

$$\int \mathbf{x}\delta(x)d^3x = \frac{\frac{1}{M}\int \mathbf{x}(\rho(x)-\rho_0)d^3x}{\frac{1}{M}\rho_0} = \frac{\mathbf{R}}{1/V} \tag{6.5.15}$$

and one can always choose the frame origin so that $\mathbf{R}=0$.

Let us now write the mass and momentum invariance condition in Fourier space and apply them to $\delta^{(2)}$. The mass condition gives

$$\int \delta_k e^{ikx}\frac{d^3k}{(2\pi)^3}d^3x = \int \delta_k \frac{d^3k}{(2\pi)^3}e^{ikx}d^3x = \int \delta_k\delta_D(k)d^3k = \delta_{k=0} = 0 \tag{6.5.16}$$

This implies

$$\delta^{(2)}_{\mathbf{k}=0} = G^2\int \delta_1\delta_2 F_2(\mathbf{k}_1,\mathbf{k}_2)\delta_D(\mathbf{k}_1+\mathbf{k}_2)d^3k_1d^3k_2 \tag{6.5.17}$$

$$= G^2\int \delta_1\delta_2 F_2(\mathbf{k}_1,-\mathbf{k}_1)d^3k_1 = 0 \tag{6.5.18}$$

$$\rightarrow F_2(\mathbf{k}_1,-\mathbf{k}_1) = 0 \tag{6.5.19}$$

which can also be written as

$$\lim_{\sum \mathbf{k_i}\rightarrow 0} F_2(\mathbf{k}_1,\mathbf{k}_2) = 0 \tag{6.5.20}$$

The momentum condition gives

$$\int \mathbf{x}\delta(x)d^3x = \int \mathbf{x}\delta_k e^{i\mathbf{kx}}d^3kd^3x \tag{6.5.21}$$

$$= \int \delta_k \mathbf{x}d^3k e^{i\mathbf{kx}}d^3x = -i\int \delta_k d^3k\frac{d}{d\mathbf{k}}\int e^{i\mathbf{kx}}d^3x \tag{6.5.22}$$

$$= -i\int \delta_k d^3k\frac{d}{d\mathbf{k}}\delta_D(k) = i\int\left(\frac{d}{d\mathbf{k}}\delta_k\right)d^3k\delta_D(k) = i\left(\frac{d}{d\mathbf{k}}\delta_k\right)_{k=0} = 0 \tag{6.5.23}$$

and therefore

$$\lim_{\mathbf{k}\rightarrow 0}\frac{\partial}{\partial\mathbf{k}}\delta^{(2)}_k = 0 \tag{6.5.24}$$

In turn, this condition gives

$$G^2\lim_{\mathbf{k}\rightarrow 0}\frac{\partial}{\partial\mathbf{k}}\int \delta_1\delta_2 F_2(\mathbf{k}_1,\mathbf{k}-\mathbf{k}_1)d^3k_1 = \tag{6.5.25}$$

$$G^2\lim_{\mathbf{k}\rightarrow 0}\int \delta_1\delta_2\frac{\partial}{\partial\mathbf{k}}F_2(\mathbf{k}_1,\mathbf{k}-\mathbf{k}_1)d^3k_1 = 0 \tag{6.5.26}$$

$$\rightarrow \lim_{\mathbf{k}\rightarrow 0}\frac{\partial}{\partial\mathbf{k}}F_2(\mathbf{k}_1,\mathbf{k}-\mathbf{k}_1) = 0 \tag{6.5.27}$$

The last condition can be written as

$$\lim_{\mathbf{k}\rightarrow 0}\frac{\partial}{\partial\mathbf{k}}F_2(\mathbf{k}_1,\mathbf{k}-\mathbf{k}_1) = \lim_{\mathbf{k}\rightarrow 0}\left[\frac{\partial}{\partial\mathbf{k}_2}F_2(\mathbf{k}_1,\mathbf{k}_2)\right]\frac{\partial\mathbf{k}_2}{\partial\mathbf{k}} = -\mathbf{k}_1\lim_{\mathbf{k}\rightarrow 0}\left[\frac{\partial}{\partial\mathbf{k}_2}F_2(\mathbf{k}_1,\mathbf{k}_2)\right] = 0 \tag{6.5.28}$$

and the same by exchanging $\mathbf{k}_1 \leftrightarrow \mathbf{k}_2$. Therefore we obtain

$$\lim_{\sum \mathbf{k}_i\rightarrow 0}\frac{\partial}{\partial\mathbf{k}_1}F_2(\mathbf{k}_1,\mathbf{k}_2) = 0 \tag{6.5.29}$$

$$\lim_{\sum \mathbf{k}_i\rightarrow 0}\frac{\partial}{\partial\mathbf{k}_2}F_2(\mathbf{k}_1,\mathbf{k}_2) = 0 \tag{6.5.30}$$

Together, mass and momentum constraints imply therefore at second order

$$\lim_{\sum \mathbf{k}_i \to 0} F_2(\mathbf{k}_1, \mathbf{k}_2) = 0 \tag{6.5.31}$$

$$\lim_{\sum \mathbf{k}_i \to 0} \frac{\partial}{\partial \mathbf{k}_i} F_2(\mathbf{k}_1, \mathbf{k}_2) = 0 \tag{6.5.32}$$

They are readily generalized to all orders:

$$\lim_{\sum \mathbf{k}_i \to 0} F_n(\mathbf{k}_1, \mathbf{k}_2, ...\mathbf{k}_n) = 0 \tag{6.5.33}$$

$$\lim_{\sum \mathbf{k}_i \to 0} \frac{\partial}{\partial \mathbf{k}_i} F_n(\mathbf{k}_1, \mathbf{k}_2, ...\mathbf{k}_n) = 0 \tag{6.5.34}$$

Same conditions hold for the velocity kernel G_n.

The EGI condition on the kernels is, on the other hand, is more difficult to derive, and we refer to [8]. The main point is that it produces a recursive relation between kernel of different order in the limit of vanishing momenta. At second order, the condition is simply

$$\lim_{\mathbf{k}_2 \to 0} F_2(\mathbf{k}_1, \mathbf{k}_2) = \frac{\mathbf{k}_1 \cdot \mathbf{k}_2}{k_2^2} \tag{6.5.35}$$

and $\mathbf{k}_1 \leftrightarrow \mathbf{k}_2$. This means that the pole for $\mathbf{k}_1, \mathbf{k}_2 \to 0$ is of order 1, i.e. it goes as $1/k_i$. Now, rotational invariance means that the kernel at second order can be built only out of $\mathbf{k}_1 \cdot \mathbf{k}_1 = k_1^2$, $\mathbf{k}_2 \cdot \mathbf{k}_2 = k_2^2$, $\mathbf{k}_1 \cdot \mathbf{k}_2$. Moreover, since the conservation equations contain only quadratic powers of momenta, we also require that each momentum in the kernels appears at most quadratically. There are only four combinations that are dimensionless (as kernels must be), have poles as $1/\mathbf{k}_i$, and contains at most quadratic functions in each momentum:

$$1, \frac{\mathbf{k}_1 \cdot \mathbf{k}_2}{k_1^2}, \frac{\mathbf{k}_1 \cdot \mathbf{k}_2}{k_2^2}, \frac{(\mathbf{k}_1 \cdot \mathbf{k}_2)^2}{k_1^2 k_2^2} \tag{6.5.36}$$

Notice that they are all homogeneous of degree zero, i.e. $f(\lambda \mathbf{k}_1, \lambda \mathbf{k}_2) = f(\mathbf{k}_1, \mathbf{k}_2)$. It turns out convenient to reorganize them into an equivalent set of four basis functions:

$$1, \quad \gamma = 1 - \frac{(\mathbf{k}_1 \cdot \mathbf{k}_2)^2}{k_1^2 k_2^2}, \quad \beta = \frac{(\mathbf{k}_1 + \mathbf{k}_2)^2 \mathbf{k}_1 \cdot \mathbf{k}_2}{2 k_1^2 k_2^2}, \quad \alpha_a = \frac{\mathbf{k}_1 \cdot \mathbf{k}_2}{k_1^2} - \frac{\mathbf{k}_1 \cdot \mathbf{k}_2}{k_2^2} \tag{6.5.37}$$

All the kernels can be expressed in terms of these building blocks. For instance, the previously defined function α is

$$\alpha = \gamma + \beta + \frac{\alpha_a}{2} \tag{6.5.38}$$

At every order n, the kernels are to be built with all possible combinations of $n-1$ basis functions. As an immediate application, we can say that the most general kernel K_2 must have the structure

$$F_2(\mathbf{k}_1, \mathbf{k}_2) = a_0^{(2)} + a_1^{(2)} \gamma(\mathbf{k}_1, \mathbf{k}_2) + a_2^{(2)} \beta(\mathbf{k}_1, \mathbf{k}_2) \tag{6.5.39}$$

where all coefficients depend on time only. The function α_a is absent because it is antisymmetric, and therefore vanishes upon symmetrization. Now, one can immediately show that mass conservation (6.5.27) requires $a_0^{(2)} = 0$, while EGI (6.5.35) implies $a_2^{(2)} = 2$ so that

$$F_2(\mathbf{k}_1, \mathbf{k}_2) = a_1^{(2)} \gamma(\mathbf{k}_1, \mathbf{k}_2) + 2\beta(\mathbf{k}_1, \mathbf{k}_2) \tag{6.5.40}$$

is the most general form. In EdS, we see that $a_{1\mathrm{EdS}}^{(2)} = \frac{10}{7}$. Analogously, for G_2 we find

$$G_2(\mathbf{k}_1, \mathbf{k}_2) = d_1^{(2)} \gamma(\mathbf{k}_1, \mathbf{k}_2) + 2\beta(\mathbf{k}_1, \mathbf{k}_2) \tag{6.5.41}$$

and $d^{(2)}_{1\rm EdS} = \frac{6}{7}$. By analogous arguments, at order $n = 3$ we find

$$F_3(\mathbf{q}_1,\mathbf{q}_2,\mathbf{q}_3) = 2\beta(\mathbf{q}_1,\mathbf{q}_2)\,\beta(\mathbf{q}_{12},\mathbf{q}_3) + a^{(3)}_5\gamma(\mathbf{q}_1,\mathbf{q}_2)\,\gamma(\mathbf{q}_{12},\mathbf{q}_3) - 2\left(a^{(3)}_{10} - h\right)\gamma(\mathbf{q}_1,\mathbf{q}_2)\,\beta(\mathbf{q}_{12},\mathbf{q}_3) \tag{6.5.42}$$

$$+ 2\left(a^{(2)}_1 + 2a^{(3)}_{10} - h\right)\beta(\mathbf{q}_1,\mathbf{q}_2)\,\gamma(\mathbf{q}_{12},\mathbf{q}_3) + a^{(3)}_{10}\gamma(\mathbf{q}_1,\mathbf{q}_2)\,\alpha_a(\mathbf{q}_{12},\mathbf{q}_3) + \text{ cyclic} \tag{6.5.43}$$

$$G_3(\mathbf{q}_1,\mathbf{q}_2,\mathbf{q}_3) = -2\beta(\mathbf{q}_1,\mathbf{q}_2)\,\beta(\mathbf{q}_{12},\mathbf{q}_3) - d^{(3)}_5\gamma(\mathbf{q}_1,\mathbf{q}_2)\,\gamma(\mathbf{q}_{12},\mathbf{q}_3) + 2\left(d^{(3)}_{10} - h\right)\gamma(\mathbf{q}_1,\mathbf{q}_2)\,\beta(\mathbf{q}_{12},\mathbf{q}_3) \tag{6.5.44}$$

$$- 2\left(d^{(2)}_1 + 2d^{(3)}_{10} - h\right)\beta(\mathbf{q}_1,\mathbf{q}_2)\,\gamma(\mathbf{q}_{12},\mathbf{q}_3) - d^{(3)}_{10}\gamma(\mathbf{q}_1,\mathbf{q}_2)\,\alpha_a(\mathbf{q}_{12},\mathbf{q}_3) + \text{ cyclic.} \tag{6.5.45}$$

where h is defined as

$$h(\tau) = \int^\tau d\tau' f(\tau')\left(\frac{G(\tau')}{G(\tau)}\right)^2 d^{(2)}_1(\tau') \tag{6.5.46}$$

There are then overall six free coefficients for $n = 2, 3$: $a^{(2)}_1, d^{(2)}_1, a^{(3)}_5, a^{(3)}_{10}, d^{(3)}_5, d^{(3)}_{10}$. Their EdS values are

$$a^{(2)}_1 = \frac{10}{7}, \quad d^{(2)}_1 = \frac{6}{7}, \quad a^{(3)}_5 = \frac{8}{9}, \quad d^{(3)}_5 = \frac{8}{21}, \quad a^{(3)}_{10} = -\frac{1}{9}, \quad d^{(3)}_{10} = -\frac{1}{21} \tag{6.5.47}$$

Moreover, $h_{\rm EdS} = \frac{3}{7}$. Two combinations are degenerate with the UV correction, so can be discarded (or rather, absorbed away). On top of the remaining four, there are the four bias parameters b_1, b_2, b_G, b_Γ for tracers. Beyond EdS, one can provide differential equations using the same scheme as for Eq. (5.3.69), i.e. by inserting trial forms of the type (5.3.66) for $\delta^{(2)}, \theta^{(2)}, \delta^{(3)}, \theta^{(3)}$... into the conservation equations and matching separately the various components for each basis function. Then one finds

$$a^{(2)\prime}_1 = f(2 - 2a^{(2)}_1 + d^{(2)}_1) \tag{6.5.48}$$

$$d^{(2)\prime}_1 = -fd^{(2)}_1 + \frac{S}{f}\left(a^{(2)}_1 - d^{(2)}_1\right) \tag{6.5.49}$$

$$a^{(3)\prime}_5 = f\left(a^{(2)}_1 + d^{(2)}_1 - 3a^{(3)}_5 + d^{(3)}_5\right) \tag{6.5.50}$$

$$d^{(3)\prime}_5 = -2fd^{(3)}_5 + \frac{S}{f}\left(a^{(3)}_5 - d^{(3)}_5\right) \tag{6.5.51}$$

$$a^{(3)\prime}_{10} = -f\frac{1}{2}\left(a^{(2)}_1 - d^{(2)}_1 + 6a^{(3)}_{10} - 2d^{(3)}_{10}\right) \tag{6.5.52}$$

$$d^{(3)\prime}_{10} = -2fd^{(3)}_{10} + \frac{S}{f}\left(a^{(3)}_{10} - d^{(3)}_{10}\right) \tag{6.5.53}$$

The initial conditions at early times can be taken to be EdS. These equations have to be complemented by the equation for f, ie.

$$f' + f^2 + Ff - S = 0 \tag{6.5.54}$$

The numerical or analytical solutions then provide the general forms of the time-dependent kernels in all the cosmologies that respect the equivalence principle and allow for $\mathbf{k}$-independent f and S. In most cases, the deviation from the EdS values are at most a few percent.

The equations for $a^{(2)}_1, d^{(2)}_1$ can be combined to get a single equation for $a \equiv a^{(2)}_1$

$$a'' + a'(4f + F) + a\left(2f^2 + S\right) = 2\left(f^2 + S\right) \tag{6.5.55}$$

Replacing a with $g_A/2$, we see that this equation coincides with the first of Eq. (5.3.69). Repeating the same argument that leads to the kernel F_2 in Eq. (5.3.71) we see it coincides with Eq. (6.5.40) above.

6.6 Comparing to real data

Let's be assigned a number of observational estimates of the power spectrum $P_i = P(\mathbf{k}_i)$ for a given tracer, eg galaxies, and let's approximate their distribution as a Gaussian (even if actually the Gaussian variables are the δ's). We have then the likelihood (implicit sum over the $\mathbf{k}$-vectors labelled by i, j)

$$L = \frac{1}{(2\pi)^{N/2}|C|} \exp -\frac{1}{2}(P_i - \hat{P}_i)C_{ij}^{-1}(P_j - \hat{P}_j) \tag{6.6.1}$$

where $\hat{P}$ is our theoretical model. Spectra at different $\mathbf{k}$ are assumed to be uncorrelated.

The power spectrum we extract from data is $P(k) = \delta_k \delta_k^*$. Its variance is therefore

$$\langle \delta_k \delta_k^* \delta_k \delta_k^* \rangle = \langle \delta_k \delta_k^* \rangle \langle \delta_k \delta_k^* \rangle + \langle \delta_k \delta_k^* \rangle \langle \delta_k^* \delta_k \rangle + \langle \delta_k \delta_k \rangle \langle \delta_k^* \delta_k^* \rangle = 2P(\mathbf{k})P(\mathbf{k}) \tag{6.6.2}$$

since $(2\pi)^3 P(k)\delta_D(\mathbf{k} - \mathbf{k}') = \langle \delta_k \delta_k^* \rangle = \langle \delta_k \delta_{-k} \rangle$ and therefore $\langle \delta_k \delta_k \rangle = \langle \delta_k^* \delta_k^* \rangle = 0$. Data are collected into bins of size $k^2 \Delta k \Delta\mu \Delta\phi = 2\pi k^2 \Delta k \Delta\mu$, where ϕ is the azimuthal angle. The choice of the bins is relatively arbitrary, but they should not be too small to contain too few modes, and not too large that possible interesting features in the k-trend are smoothed out. All the modes $\mathbf{k}$ that fall into a bin are lumped together. If there are $N_P(\mathbf{k})$ modes into a given bin around $\mathbf{k}$, the sum over i, j becomes a sum over bins of the multiplicities $N_P(\mathbf{k})$

$$\sum_{ij} \to \sum_{\text{bins}} N_P(\mathbf{k}) \tag{6.6.3}$$

and the likelihood becomes then

$$L(P) = \frac{1}{(2\pi)^{N/2}|C^{(P)}|^{1/2}} \exp -\frac{1}{2} \sum_{\text{i,j}} (P_i - \hat{P}_i)[C_{ij}^{(P)}]^{-1}(P_j - \hat{P}_j) \tag{6.6.4}$$

$$= \frac{1}{(2\pi)^{N/2}|C^{(P)}|} \exp -\frac{1}{2} \sum_{\text{a,b}\in\text{bins}} N_P(P_a - \hat{P}_a)[C_{ab}^{(P)}]^{-1}(P_b - \hat{P}_b) \tag{6.6.5}$$

$$= \frac{1}{(2\pi)^{N/2}|\bar{C}^{(P)}|} \exp -\frac{1}{2} \sum_{\text{a,b}\in\text{bins}} (P_a - \hat{P}_a)[\bar{C}_{ab}^{(P)}]^{-1}(P_b - \hat{P}_b) \tag{6.6.6}$$

where now a, b run over the bins and $\bar{C}_{ab}^{(P)} \equiv \frac{C_{ab}^{(P)}}{N_P}$. We need then to count how many vectors $\mathbf{k}$ fit into such bins in a survey of size V. In a 1D discrete Fourier transform over a length L, the k coefficients are spaced by $2\pi/L$. In 3D this becomes $(2\pi)^3/V$, which is therefore the size of the elementary $\mathbf{k}$ cell. Therefore there are

$$N_P(k, \mu) = \frac{2\pi k^2 \Delta k \Delta\mu}{(2\pi)^3/V} = \frac{V}{(2\pi)^2} k^2 \Delta k \Delta\mu \tag{6.6.7}$$

modes per data bin. Since we assumed uncorrelated spectra, the covariance for the galaxy spectrum P_{gg} can be written as a diagonal matrix

$$\bar{C}_{ab}^{(P)} \equiv \frac{C_{ab}^{(P)}}{N_P} = \frac{2}{N_P} P(\mathbf{k}_a)P(\mathbf{k}_b)\delta_{ab}\,, \tag{6.6.8}$$

An analogous calculation for the bispectrum shows that the covariance matrix between triangles a, b (see Fig. 6.6.1) can be written as

$$\bar{C}_{ab}^{(B)} = s_B \frac{V}{N_B} G^6 P(k_1)P(k_2)P(k_3)\delta_{ab} L_i\,, \tag{6.6.9}$$

where $s_B = 6, 2, 1$ for equilateral, isosceles, and scalene triangles, respectively, to avoid overcounting of identical triangles. Also, $L_i = 2$ for co-linear triangles (i.e. such that $\mathbf{k}_3 = \mathbf{k}_1 + \mathbf{k}_2$ or $\mathbf{k}_3 = |\mathbf{k}_2 - \mathbf{k}_1|$) and 1 otherwise. The number of triangles per bin is given by

$$N_B = 2\frac{V^2}{8\pi^4} k_{a_1} k_{a_2} k_{a_3} (\Delta k)^3 \Sigma(\Omega) \Delta\Omega\,, \tag{6.6.10}$$

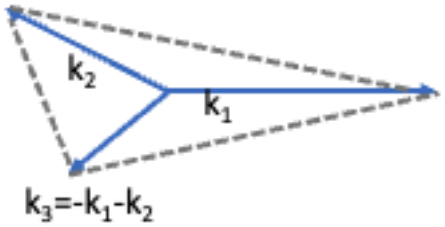

Figure 6.6.1: Triangle configuration in **k**-space.

where $k_{a_{1,2,3}}$ are the central value of the k-bins, and $\Sigma(\Omega)\Delta\Omega$ is the number of triangles within the angle orientation $\Delta\Omega = (\Delta\mu)^2$, that depends on which coordinate system is used. The bispectrum likelihood is then

$$L(B) = \frac{1}{(2\pi)^{N/2}|C^{(B)}|^{1/2}} \exp -\frac{1}{2} \sum_{\mathrm{a,b}\in\mathrm{bins}} N_P(B_a - \hat{B}_a)[C^{(B)}_{ab}]^{-1}(B_b - \hat{B}_b) \tag{6.6.11}$$

One should also consider the correlation between spectra and bispectra, but this is usually negligible. Then one can simply multiply the two likelihoods.

The comparison to data consists then in sampling the P, B likelihoods over the parameter space, building therefore the corresponding posterior. The parameters are those that characterize the cosmology (e.g. $\Omega_m, \Omega_b, n_s, h$ etc) plus those that characterize the bias, one-loop, and UV corrections.

6.7 Surveys

A galaxy survey that has been studied a lot with non-linear correction is the Baryon Oscillation Spectroscopic Survey (BOSS). BOSS is a key component of the Sloan Digital Sky Survey III (SDSS-III), which ran from 2009 to 2014. The primary goal of BOSS was to create a highly detailed three-dimensional map of the large-scale structure of the universe, focusing on the detection of baryon acoustic oscillations (BAOs). The power spectra and bispectra of BOSS are publicly available.

The BOSS survey used the 2.5-meter Sloan Foundation Telescope at Apache Point Observatory in New Mexico, USA, as well as the 4.1-meter Southern Astrophysical Research (SOAR) telescope in Chile, for spectroscopic observations. The survey targeted a large sample of galaxies and quasars, specifically focusing on a volume of space that spanned about 10 billion light-years. In total, BOSS measured the redshifts of over 1.5 million galaxies, producing a high-precision catalog that covers approximately one-third of the entire sky.

Two much larger surveys that are under production now are DESI and Euclid. The Dark Energy Spectroscopic Instrument (DESI) is hosted on the 4-meter Mayall Telescope at Kitt Peak National Observatory in Arizona. DESI began full science operations in 2021 and is slated to run for five years. DESI's spectroscopic system features 5,000 robotic fiber-optic positioners, enabling it to simultaneously capture light from 5,000 galaxies or quasars in a single exposure. It targets over 30 million galaxies and quasars. Key Features are a Survey Area of about 14,000 square degrees, roughly one-third of the entire celestial sphere, reaching redshifts $z \approx 3$.

The Euclid mission is a major space-based observatory dedicated to understanding the nature of dark energy and dark matter, and to mapping the large-scale structure of the universe. Launched by the European Space Agency (ESA) in July 2023, Euclid is equipped with two main instruments:

1. Visible Imaging Channel (VIS): A large visible-light camera that will capture high-resolution images of galaxies across a wide range of wavelengths (from 550 to 900 nm). This allows it to trace the geometry of the universe through galaxy clustering and the patterns of weak gravitational lensing.

2. Near-Infrared Imaging Channel (NISP): An infrared camera that will observe galaxies at longer wavelengths (from 1 to 2 microns). This provides crucial information on galaxy evolution, especially for distant, faint galaxies that are redshifted to longer wavelengths due to the expansion of the universe.

Euclid's observations will focus on a large section of the sky spanning approximately 15,000 square degrees, up to redshift 3, including about 30 million galaxy spectra and imaging of up to two billions galaxies. This vast survey area will provide a statistically significant sample of galaxies to investigate cosmic structures at various scales.

Bibliography

[1] C. Alcock and B. Paczynski. An evolution free test for non-zero cosmological constant. *Nature* , 281:358, October 1979.

[2] W. E. Ballinger, J. A. Peacock, and A. F. Heavens. Measuring the cosmological constant with redshift surveys. *Mon. Not. R. Ast. Soc.* , 282:877, October 1996.

[3] Daniel Baumann, Alberto Nicolis, Leonardo Senatore, and Matias Zaldarriaga. Cosmological non-linearities as an effective fluid. *Journal of Cosmology and Astroparticle Physics*, 2012(07):051–051, July 2012.

[4] F. Bernardeau, S. Colombi, E. Gaztañaga, and R. Scoccimarro. Large-scale structure of the universe and cosmological perturbation theory. *Physics Reports*, 367(1–3):1–248, September 2002.

[5] Edmund Bertschinger. Cosmological dynamics, 1995.

[6] John Joseph M. Carrasco, Mark P. Hertzberg, and Leonardo Senatore. The Effective Field Theory of Cosmological Large Scale Structures. *JHEP*, 09:082, 2012.

[7] Anton Chudaykin, Mikhail M. Ivanov, Oliver H. E. Philcox, and Marko Simonović. Nonlinear perturbation theory extension of the Boltzmann code CLASS. *Phys. Rev.* **D**, 102(6):063533, September 2020.

[8] G. D'Amico, M. Marinucci, M. Pietroni, and F. Vernizzi. The large scale structure bootstrap: perturbation theory and bias expansion from symmetries. *Journal of Cosmology and Astroparticle Physics*, 2021(10):069, October 2021.

[9] Vincent Desjacques, Donghui Jeong, and Fabian Schmidt. Large-Scale Galaxy Bias. *Phys. Rept.*, 733:1–193, 2018.

[10] Daniel J. Eisenstein, Hee-Jong Seo, Edwin Sirko, and David N. Spergel. Improving Cosmological Distance Measurements by Reconstruction of the Baryon Acoustic Peak. *Ap. J.* , 664(2):675–679, August 2007.

[11] Ichihiko Hashimoto, Yann Rasera, and Atsushi Taruya. Precision cosmology with redshift-space bispectrum: A perturbation theory based model at one-loop order. *Phys. Rev. D*, 96:043526, Aug 2017.

[12] Johannes Hendrik Hidding, Sergei F. Shandarin, and Rien van de Weygaert. The zel'dovich approximation: key to understanding cosmic web complexity. *Monthly Notices of the Royal Astronomical Society*, 437:3442–3472, 2013.

[13] Mikhail M. Ivanov and Sergey Sibiryakov. Infrared resummation for biased tracers in redshift space. , 2018(7):053, July 2018.

[14] A. Kehagias and A. Riotto. Symmetries and consistency relations in the large scale structure of the universe. *Nuclear Physics B*, 873(3):514–529, August 2013.

[15] Robert Lilow, Felix Fabis, Elena Kozlikin, Celia Viermann, and Matthias Bartelmann. Resummed Kinetic Field Theory: general formalism and linear structure growth from Newtonian particle dynamics. *JCAP*, 04:001, 2019.

[16] J. A. Peacock and R. E. Smith. Halo occupation numbers and galaxy bias. *Mon. Not. Roy. Astron. Soc.*, 318:1144, 2000.

[17] Lado Samushia et al. Effects of cosmological model assumptions on galaxy redshift survey measurements. *Mon. Not. Roy. Astron. Soc.*, 410:1993–2002, 2011.

[18] Román Scoccimarro, H. M. P. Couchman, and Joshua A. Frieman. The Bispectrum as a Signature of Gravitational Instability in Redshift Space. *Ap. J.* , 517(2):531–540, June 1999.

[19] R. E. Smith, J. A. Peacock, A. Jenkins, S. D. M. White, C. S. Frenk, F. R. Pearce, P. A. Thomas, G. Efstathiou, and H. M. P. Couchmann. Stable clustering, the halo model and nonlinear cosmological power spectra. *Mon. Not. Roy. Astron. Soc.*, 341:1311, 2003.

[20] R. Takahashi. Third-order density perturbation and one-loop power spectrum in dark-energy-dominated universe. *Progress of Theoretical Physics*, 120(3):549?559, September 2008.